MASTERARBEIT | MASTER'S THESIS

Titel | Title

Detection of (R)- and (S)-aerugine in human pathogenic bacteria and development of a LC-MS/MS quantification method

verfasst von | submitted by

Alexandra Katholnig BSc

angestrebter akademischer Grad | in partial fulfilment of the requirements for the degree of

Master of Science (MSc)

Wien | Vienna, 2024

Studienkennzahl lt. Studienblatt | Degree programme code as it appears on the student record sheet:	UA 066 863
Studienrichtung lt. Studienblatt | Degree programme as it appears on the student record sheet:	Masterstudium Biologische Chemie
Betreut von | Supervisor:	Univ.-Prof. Dr. Thomas Böttcher

I. Summary

Recently, the identification of small bacterial molecules has been of great interest. They act, for example, as virulence factors or toxins of pathogenic bacteria and in some cases have harmful effects on the physiology of their hosts. In this context, neurodegenerative effects of the bacterial metabolite aerugine on dopaminergic neurons have been identified.[1]

This thesis work aimed at detection and quantification of the production of aerugine in human pathogenic bacteria. To achieve this, an LC-MS/MS method enabling the detection and quantification of aerugine from liquid cultures was developed. (*R*)-aerugine was synthesized *via* an already established stereospecific synthesis pathway for usage as reference material for LC-MS/MS method development. In addition, deuterated aerugine was synthesized as an internal standard for the use as extraction control. The LC-MS/MS method for detection and quantification of aerugine from liquid cultures was established using *Pseudomonas aeruginosa*. Neurotoxic effects of aerugine have been observed at exposure of 3-4 µM.[1] By means of this successfully established quantification method, it could be shown that *P. aeruginosa* produces aerugine in a concentration of 6.43 ± 1.09 µM within 24 h. This finding can be emphasized with regard to the discovery of the effects of neurotoxic metabolites from human pathogenic bacteria on the development of neurodegenerative diseases, such as Parkinson's disease.

Furthermore, a screening for culturing conditions to induce aerugine production in the human pathogenic bacteria *Yersinia enterocolitica* (DSM 4780) and *Klebsiella pneumoniae* (DSM 30104) was performed. By this the chemically defined minimal medium PMH, after feeding of salicylic acid and L-cysteine, was identified to possibly induce aerugine production in *Y. enterocolitica.* Furthermore, the screening identified deferrated PGM to be a growth medium for further investigations of aerugine production by *K. pneumoniae*. Initial experiments on the inhibition of aerugine production by *P. aeruginosa* and *Y. enterocolitica* did not yield statistically significant results due to incompleteness and insufficient quality of the data. It is suggested to repeat these experiments in the future.

Finally, four aerugine derivatives were synthesized for a small structure activity relationship study, by condensation reaction of various benzonitriles and L-cysteine. Despite best efforts, results of biological testing, which is performed by the Leist Group at University of Konstanz, were not available within the timeframe of this thesis.

Overall, the results of this work could make a small contribution to understanding the role of human pathogenic bacteria in the development of neurodegenerative diseases, in particular Parkinson's disease.

II. Zusammenfassung

In letzter Zeit ist die Identifizierung kleiner bakterieller Moleküle von großem Interesse. Sie wirken zum Beispiel als Virulenzfaktoren oder Toxine pathogener Bakterien und haben in einigen Fällen schädliche Auswirkungen auf die Physiologie ihrer Wirte. In diesem Zusammenhang wurden neurodegenerative Auswirkungen des bakteriellen Metaboliten Aerugin auf dopaminerge Neuronen festgestellt.[1]

Ziel dieser Arbeit war der Nachweis und die Quantifizierung der Produktion des neurotoxischen Metaboliten Aerugin in humanpathogenen Bakterien. Zu diesem Zweck wurde eine LC-MS/MS-Methode entwickelt, die den Nachweis und die Quantifizierung von Aerugin aus Flüssigkulturen ermöglicht. (*R*)-Aerugin wurde über einen bereits etablierten stereospezifischen Syntheseweg synthetisiert und diente als Referenzmaterial für die Entwicklung der LC-MS/MS-Methode. Darüber hinaus wurde deuteriertes Aerugin als interner Standard für die Verwendung als Extraktionskontrolle synthetisiert. Die LC-MS/MS-Methode zum Nachweis und zur Quantifizierung von Aerugin aus Flüssigkulturen wurde mit *Pseudomonas aeruginosa* etabliert. Neurotoxische Wirkungen von Aerugin wurden zuvor bei einer Exposition von 3-4 µM beobachtet.[1] Mit Hilfe dieser erfolgreich etablierten Quantifizierungsmethode konnte gezeigt werden, dass *P. aeruginosa* innerhalb von 24 h Aerugin in einer Konzentration von 6,43 ± 1:09 µM produziert. Dieses Ergebnis kann im Hinblick auf die Erforschung der Auswirkungen neurotoxischer Metabolite humanpathogener Bakterien auf die Entwicklung neurodegenerativer Erkrankungen, wie der Parkinson-Krankheit, hervorgehoben werden.

Des Weiteren wurde ein Screening nach Kultivierungsbedingungen zur Induktion der Aeruginproduktion in den humanpathogenen Bakterien *Yersinia enterocolitica* (DSM 4780) und *Klebsiella pneumoniae* (DSM 30104) durchgeführt. Dabei wurde festgestellt, dass das chemisch definierte Minimalmedium PMH nach Zuführung von Salicylsäure und L-Cystein möglicherweise die Aeruginproduktion in *Y. enterocolitica* induziert.[4] Darüber hinaus erwies sich deferriertes PGM als ein Wachstumsmedium für weitere Untersuchungen der Aeruginproduktion durch *K. pneumoniae*. Erste Tests zur Hemmung der Aeruginproduktion von *P. aeruginosa* und *Y. enterocolitica* ergaben aufgrund von Unvollständigkeit und

unzureichender Qualität der Daten keine statistisch signifikanten Ergebnisse. Es wird vorgeschlagen, diese Versuche in Zukunft zu wiederholen.

Schließlich wurden vier Aeruginderivate für Studien zur Struktur-Aktivitäts-Beziehung durch Kondensationsreaktion verschiedener Benzonitrile und L-Cystein synthetisiert. Die Ergebnisse dieser Studie, die durch die Arbeitsgruppe Leist an der Universität Konstanz durchgeführt wird, lagen zum Zeitpunkt der Fertigstellung dieser Arbeit noch nicht vor.

Die Ergebnisse dieser Arbeit könnten einen kleinen Beitrag zum Verständnis der Rolle humanpathogener Bakterien bei der Entstehung neurodegenerativer Erkrankungen, insbesondere der Parkinson-Krankheit, leisten.

III. Acknowledgements

First, I want to thank Univ.-Prof. Dr. Thomas Böttcher for being the supervisor of this master thesis and for inducing my interest in this field of research with his lecture, *the chemistry of microbial interactions*. I also want to thank my co-supervisor Nathalie Wörz for her excellent support. She gave me some valuable input on thorough scientific work and the opportunity to work independently on parts of her research project.

Furthermore, I want to thank Viktoriia Savchenko who introduced me to the LC-MS/MS instrument of the Böttcher Lab and who helped me out, whenever I had issues with the instruments or the software. And, Shubham Joge, who very often gave me advice for the work in the S2-Lab, which I appreciated a lot. I also want to thank Dr. Felix Anderl for an intense one-month course on organic synthesis for a more bio analytics-oriented student like me. The synthesis part was an interesting insight that really broadened my scientific understanding. Of course, I also appreciate the help of everyone else in the lab who was there and took time when I needed help.

Furthermore, I want to thank Dr. Martin Zehl, head of the mass spectrometry facility at the department of chemistry, Vienna, for giving me advice on the interpretation and peak assignment of mass spectrums. And not to forget my friend Tamara, for her proofreading work.

Finally, I want to thank my family and friends for their support, which guided me through some frustrating and uncertain times when finishing my master studies. Especially Lana, who was the best company when staying in the library with me until closing hour. And not to forget, my bicycle, which brought me to the lab safely every single day and ensured that I got at least some fresh air and sunbeams, also after long days in the lab.

IV. Contents

Abstract

English: Bacterial small molecules can act as virulence factors or toxins of pathogenic bacteria and in some cases have harmful effects on the physiology of their hosts. This work aimed at detection and quantification of the production of the neurotoxic metabolite aerugine in human pathogenic bacteria. To achieve this, an LC-MS/MS method enabling the detection and quantification of aerugine from liquid cultures was developed. Deuterated aerugine was synthesized as an internal standard for the use as extraction control. A method for the in-house deuteration of salicylic amide was successfully established for this purpose. By means of the LC-MS/MS quantification method, it could be shown that Pseudomonas aeruginosa (DSM 22644) produces aerugine in a concentration of 6.43 ± 1.09 µM within 24 h. This finding can be emphasized with regard to the discovery of the effects of neurotoxic bacterial metabolites on the development of neurodegenerative diseases, such as Parkinson's disease. Finally, four aerugine derivatives were synthesized for a small structure activity relationship study.

Deutsch: Bakterielle kleine Moleküle können als Virulenzfaktoren oder Toxine von pathogenen Bakterien wirken und in einigen Fällen schädliche Auswirkungen auf die Physiologie ihrer Wirte haben. Ziel dieser Arbeit war der Nachweis und die Quantifizierung der Produktion des neurotoxischen Metaboliten Aerugin in humanpathogenen Bakterien. Zu diesem Zweck wurde eine LC-MS/MS Methode entwickelt, die den Nachweis und die Quantifizierung von Aerugin aus Flüssigkulturen ermöglicht. Deuteriertes Aerugin wurde als interner Standard für die Verwendung als Extraktionskontrolle synthetisiert. Dazu wurde erfolgreich eine Methode zur in-house Deuterierung von Salicylamid etabliert. Mit Hilfe der LC-MS/MS Quantifizierungsmethode konnte gezeigt werden, dass Pseudomonas aeruginosa (DSM 22644) innerhalb von 24 h Aerugin in einer Konzentration von 6,43 ± 1,09 µM produziert. Dieses Ergebnis ist im Hinblick auf die Entdeckung der Auswirkungen neurotoxischer bakterieller Metabolite auf die Entstehung neurodegenerativer Erkrankungen, wie Zum Beispiel der Parkinson-Krankheit, hervorzuheben. Schließlich wurden vier Aeruginderivate für eine kleine Struktur-Aktivitäts-Beziehungsstudie synthetisiert.

1. Introduction

1.1. Bacterial small molecules

Very often, an individual is no longer considered as a single human being, but as a *holobiont* - the ensemble of cells, tissues, organs, and microbes that colonize niches in the human body.[5] Interactions between microbes and their hosts can be facilitated *via* small molecules.[6–9] In this way, microbial metabolites enable reciprocal or harmful interactions with their hosts. Small molecules are also an important element of communication within microbial populations.[10,11] Bacteria, as well as other microbes, also secrete small molecules as a weapon in the competition for the uptake of limited nutritional components.[12,13] In many cases, small molecules act as virulence factors or toxins of pathogenic bacteria and have harmful effects on the hosts physiology.[14] For these reasons, the identification of small bacterial molecules has recently been of great interest.

The gut-microbiome-brain axis

An important example of interactions between bacteria and their hosts is the influence of the gut microbiome on the health of the entire organism, with the gastrointestinal tract being the area of the human body most colonized by microorganisms.[15] The gut microbiome is not only associated to gastro-intestinal disease, but also neurodegenerative and central nervous system (CNS) disorders. This has led to the assumption of the gut microbiome being linked to the nervous system by the gut-microbiome-brain axis.[16–18] After passing through the intestinal barrier, microbial metabolites are involved in neurotransmission, act as immune mediators or microbe-associated molecular patterns.[19–21] Furthermore, they seem to have effects on the CNS, by means of the circulatory, immune and enteric nervous system or the vagal nerve.[22–24] For example, a reduced diversity of gut microbiomes in patients suffering from the most common neurodegenerative disorder, which is Alzheimer's disease, has been shown.[25] And also Major Depressive Disorder can be associated to changes in the gut microbiome and is linked to an increased abundance of *Bacteroides* and certain metabolic alterations.[26]

Siderophores – bacterial iron chelators

Communities of microorganisms often live in biological niches with limited amounts of nutrients. Competing for limited resources, they produce molecules that are useful for the uptake of rare nutrients such as iron.[27] Although iron is one of the most abundant elements in the earth's crust, its availability to living organisms is limited. When iron is sequestered to oxidizing environments, water soluble ferrous iron is oxidized to water insoluble ferric iron.

Ferric iron precipitates as hydroxide at physiological pH and is no longer biologically available.[28]

Bound to heme proteins or as iron sulfur clusters, iron is part of redox reactive enzymes.[29] For this crucial part in electron transport chains and its role in redox reactive reactions of many organisms, iron is essential for growth and survival of not only humans, but also bacteria.[27] In vertebrates ferric iron is bound to transferrin and lactoferrin to be transported *via* blood plasma.[30] By this means, ferric iron is sequestered by the host itself, for example during an infection. In competition for the limited amount of bioavailable iron, microorganisms also produce small molecules acting as iron chelators.[27] The secreted iron chelators, also considered as siderophores, facilitate the uptake of iron-siderophore complexes through receptors and uptake systems that are specific for certain siderophores. As iron is also essential for bacterial growth during an infection, siderophores may act as virulence factors.[14] For example, it has been shown that deletions in genes required for synthesis of yersiniabactin, a siderophore of *Klebsiella pneumoniae*, caused a decrease in virulence of these mutant strains using a *in vivo* intranasal infection model.[14]

Bacterial toxins

Pathogenic bacteria affect human health particularly by the production of various toxins. Well-known examples for toxin producing bacteria constitute of *Corynebacterium diphtheriae*, *Bordetella pertussis* or *Vibrio cholerae.*[31–33] *Clostridium* species like *C. tetani* and *C. botulinum* are known to produce various neurotoxins interfering with acetylcholine receptors of neuromuscular junctions.[34] Furthermore, it has been shown that various pulicatins, produced by *Streptomyces sp.*, selectively bind human serotonin receptor 5-HT_{2b} or show *in vitro* effects on mouse dorsal root ganglion neurons.[35] And also neurotoxic effects of a microbial metabolite produced by the common soil bacterium *Streptomyces venezuelae* were previously described by Caldwell and coworkers as further discussed in the following paragraph.[36]

Aerugine – a bacterial metabolite with neurotoxic effects

As already mentioned above, Caldwell and coworkers unveiled the neurotoxic role of a metabolite from the commensal soil bacterium *S. venezuelae.*[36] They describe damaging effects of the molecule on dopaminergic nerve cells as possible risk factor for developing Parkinson's disease (PD). PD is a widespread neurodegenerative disease, but its pathogenesis is still not fully understood. Probably, beside genetic factors, also environmental factors such as certain pesticides play a role.[37] Recently, Ückert and coworkers identified the neurotoxic metabolite from *S. venezuelae* as the iron chelator aerugine.[1]

Ückert and coworkers demonstrated that the neurotoxicity of aerugine is specific to human dompaminergic neurones and that the toxicity is caused by its specific structure and is not due to general toxic effects of phenolic compounds. Knowledge about the molecular mechanisms of aerugines neurotoxicty is limited. However, some results from Ückert and coworkers suggest that apoptosis and possibly ferroptosis or dopaminergic autooxidation may play a role. Aeruginol, a structurally highly related metabolite that was also isolated from *S. venezuelae* appeared to be a less potent neurotoxicant than aerugine. In comparison to structural analogues of aerugine, Ückert and coworkers could show that its aliphatic hydroxy group seems to be important for neurotoxicity.[1] It is not known, whether aerugine is naturally produced by *S. venezuelae* as *(R)*- or *(S)*-enantiomer and if there are any differences in the toxicity of the stereoisomers.

1.2. Parkinson´s disease

PD is a chronic neurodegenerative disease that affects motility and causes problems with body movements. Symptoms include tremors of body parts, rigidity, slowed movements or difficulties with walking.[38] Besides these main symptoms, PD can also be followed by gastrointestinal dysfunctions, such as constipation.[18] The death of dopaminergic neurons in the *substancia nigra* results in the development of PD. The *substantia nigra* is a region in the midbrain where a high number of dopamine producing nerve cells is located.[39] Therefore, it plays an important role for dopamine messaging pathways that are involved in the control of body movements.

In the following, genetic and environmental risk factors are discussed. Furthermore, the influence of the human microbiome and microbial metabolites is pointed out.

Genetic risk factors

In PD, neurodegeneration can be caused by aggregation of the protein alpha-synuclein, followed by the formation of intransient fibrils. As previously published, the synuclein gene seems to be exclusively expressed in nervous system tissue.[40] Aggregation within dopaminergic neurons seems to especially impair the function of these cells.[16] This formation of alpha-synuclein aggregates seem to be correlated to mutation in the alpha-synuclein gene SNCA, which is also designated as PARK1 and 4.[41,42] There are further PARK-designated genes that are involved in family associated PD cases. For example, the E3 ubiquitin ligase parkin encoded by PARK2, or leucine-rich repeat kinase 2 (LRRK2) designated as PARK8 and others. [43,44]

Environmental risk factors

Furthermore, environmental risk factors seem to play an important role in the development of PD. The herbicide Paraquat, the pesticide Rotenone and the fungicide Maneb correlate with the development of PD, to name just a few examples.[37,45,46]

Influence of the microbiome

Scheperjans *et al.* argue for an influence of environmental factors due to the early involvement of gastrointestinal symptoms such as constipation. To add on this, they observed an altered gut microbiome in Parkinson's patients, showing an increased abundance of *Enterobacteriaceae* in patients affected by an impaired motor phenotype.[18] In line with these findings, the involvement of the human microbiome intrudes to play an important role for Parkinson´s pathogenesis. In addition, it was shown that peripheral inflammation enhances LPS-induced neuroinflammation. They observed increased inflammatory markers in the *substantia nigra* of rats, after inducing ulcerative colitis by ingestion of dextran sulfate sodium.[17] Furthermore, it has been observed in a mouse model, that alterations of intestinal microbiota influence alpha-synuclein pathogenesis, promoted *via* microbial short chain fatty acid production.[16]

Bacterial metabolites as environmental risk factors

It was hypothesized by Caldwell and Watkins *et al.* that also metabolites from soil bacteria might contribute to PD, which is in accordance with the often-stated higher prevalence of the disease in rural areas.[36,47] Ückert and coworkers state that the influence of soil bacteria derived metabolites might be limited. They argue that the same compounds might be produced by human pathogenic bacteria, due to the horizontal gene transfer (HGT) of relevant biosynthetic gene clusters.[1]

1.3. Homologous biosynthetic gene clusters

Many bacterial secondary metabolites are produced *via* non-ribosome peptide synthetase (NRPS) modules that are encoded in biosynthetic gene clusters and form assembly lines of enzymatic units.[52] As for example, many siderophores and thiazoline- or thiazole-related metabolites. Various thiazoline- and thiazole-related bacterial secondary metabolites are formed *via* highly homologous biosynthetic pathways and therefore, highly homologous genes are involved in their biosynthesis.[1] For instance, homologues of biosynthetic genes that are involved in the biosynthesis of watasemycin by *S. venezuelae* are involved in the biosynthesis of pyochelin by *Pseudomonas aeruginosa*.[12] Especially biosynthesis of pyochelin is very well described in the literature.[53]

It can be assumed that aerugine is also formed by a NRPS module. Ückert and coworkers hypothesize that pathogenesis associated biosynthetic gene clusters might be spread across soil and human pathogenic bacteria, due to HGT of relevant gene clusters.[1] Aerugine was first isolated in 1987 from *Pseudomonas aeruginosa*.[48] Its structure contains a thiazoline ring and it belongs to the family of 2- hydroxyphenylthiazolines (figure **1-1**). These metabolites are non-ribosomal peptide products mainly produced by Gram negative bacteria.

Other members of the 2-hydroxyphenylthiazoline family are shown in Figure **1-1** as well. Many of these thiazoline- and thiazole-related small molecules are considered as siderophores of bacterial pathogens. For example, yersiniabactin **4** is produced by highly virulent *Yersinia* species such as *Yersinia pseudotuberculosis*, *Yersinia pestis* and *Yersinia enterocolitica*. Pyochelin **2** and aerugine **1** are both produced by the ubiquitous and potentially pathogenic bacterium *Pseudomonas aeruginosa*.[48–50] But some members of the 2-hydroxyphenylthiazoline family also have antibiotic or neuroactive effects. Watasemycin **5,** isolated from marine *S. venezuelae* showed antimicrobial activity against bacteria and yeasts.[51] Lin *et al.* detected binding of pulicatins (**6-10**) and aerugine **1** to serotonin 5-HT receptors, which are involved in the gut-brain axis and have central roles in human physiology.[35]

Watasemycin, pyochelin and aerugine are 2-hydroxyphenylthiazolines and therefore, it can be suggested that aerugine may be produced for example as a shunt product of the same biosynthetic pathways.

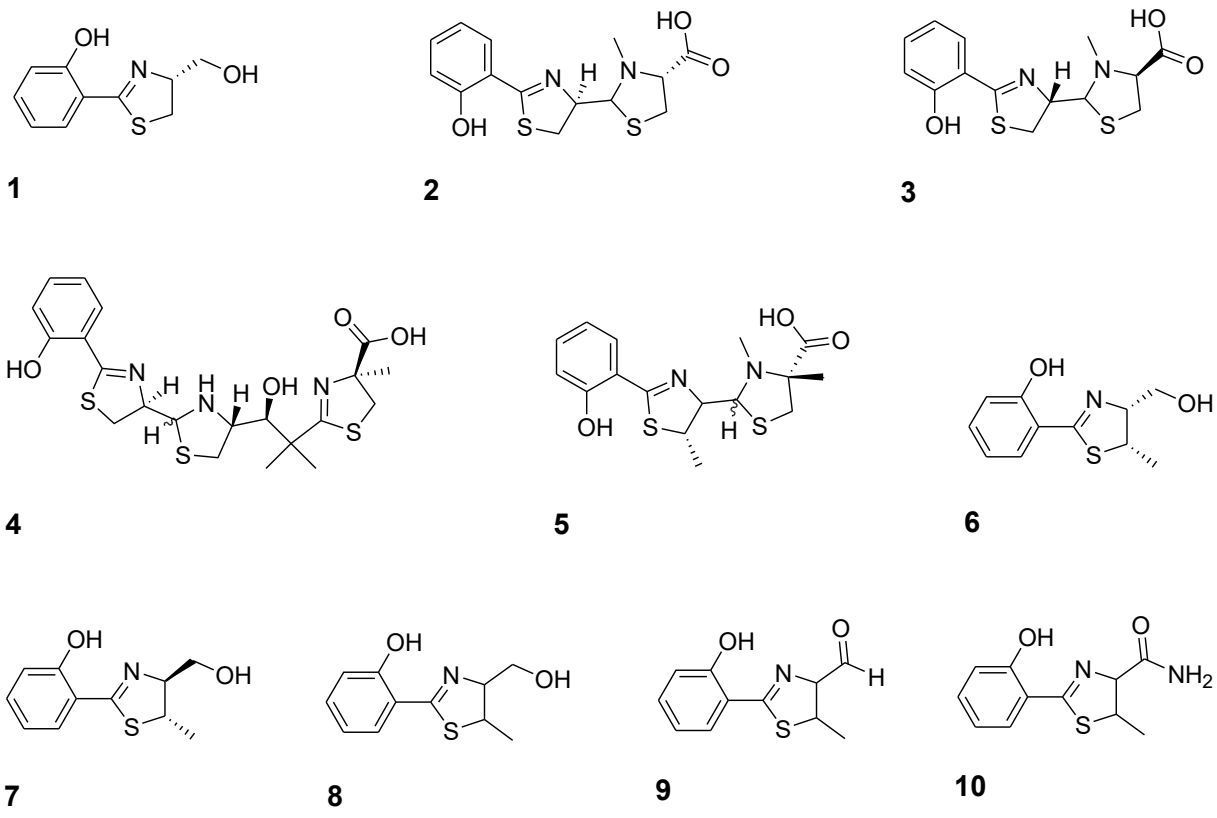

Figure 1-1 Members of the 2-hydroxyphenylthiazoline family (1: aerugine, 2: Pyochelin, 3: Enantiopyochlein, 4: Yersiniabactin, 5: Watasemycin, 6: Pulicatin A, 7: Pulicatin B, 8: Pulicatin C, 9: Pulicatin D,10: Pulicatin E).

Biosynthetic gene cluster analysis

By using the bioinformatic portal AntiSMASH, aerugine biosynthesis by other human pathogenic bacteria can be suggested. AntiSMASH is a bioinformatic tool, which allows identification, annotation, and analysis of secondary metabolite biosynthesis gene clusters. Ückert and coworkers carried out a biosynthetic gene cluster analysis and identified *K. pneumoniae* and *Y. enterocolitica* as further possible aerugine producing organisms. The biosynthetic pathway of aerugine synthesis by *S. venezuelae* was investigated based on the work of Inahashi and coworkers, who propose biosynthetic pathways for various 2-hydroxyphenylthiazolines in *P. aeruginosa* and *S.venezuelae*.[12] The biosynthetic pathway of aerugine synthesis by *S. venezuelae* that is proposed by Ückert and coworkers is depicted in Figure **1-2**.

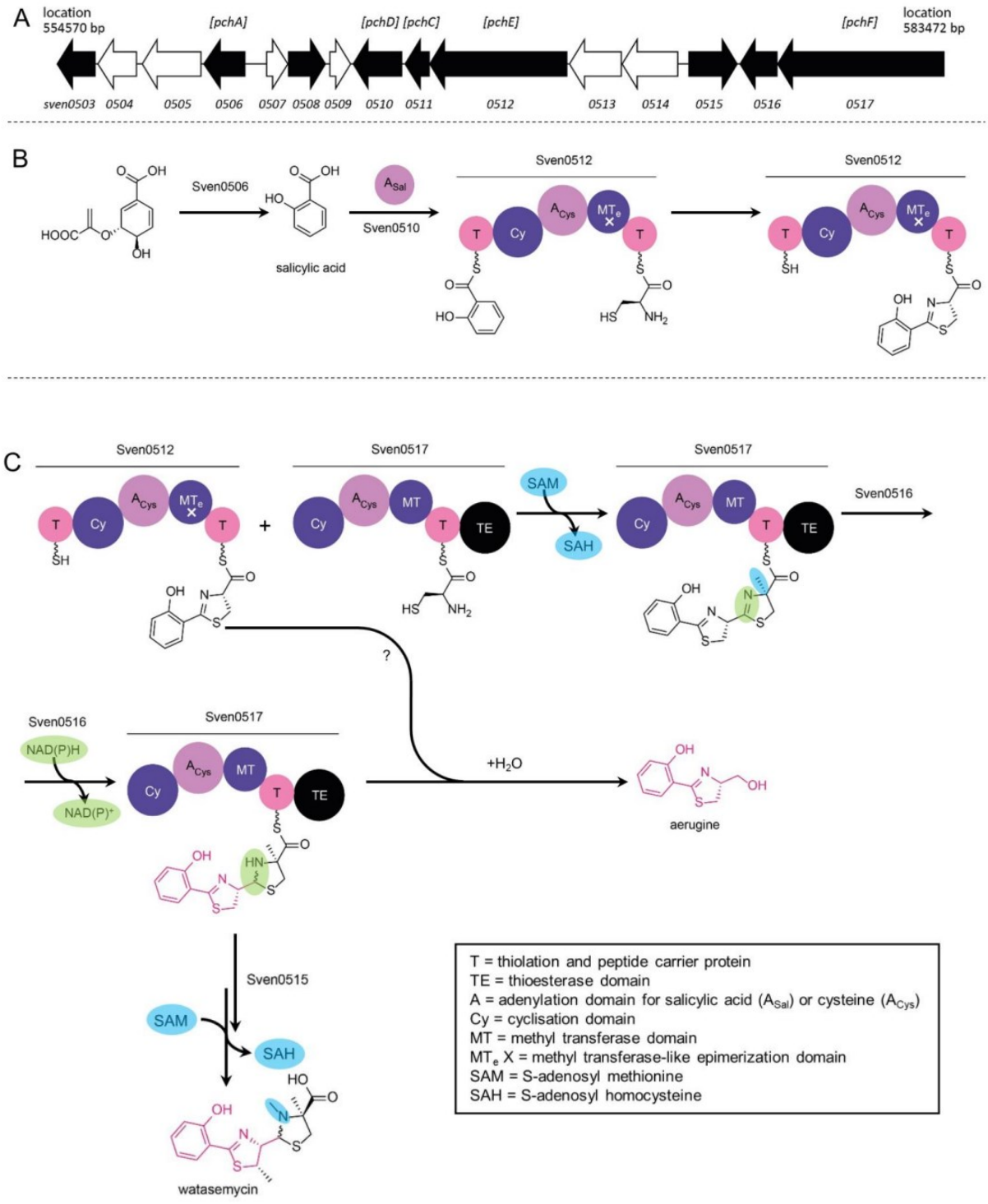

Figure 1-2 Biosynthetic gene cluster of watasemycin of *Streptomyces venezuelae* ATCC 10712 investigated via antiSMASH and proposed biosynthesis of watasemycin and aerugine. Homologs of the pyochelin gene cluster of Pseudomonas aeruginosa are indicated in brackets; black arrows: genes encoding biosynthetic enzymes, white arrows: genes with transport and regulatory functions. Figure taken from Ückert *et al.*[1]

In this mechanism proposed by Ückert *et al*., salicylic acid is formed in a first step, followed by condensation to cysteine and finally the hydrolysis of aerugine. Salicylic acid is produced *via* salicylate synthase Sven0506. Salicylic acid is then activated by adenylation domain Sven0510 and loaded on the peptide carrier domain of NRPS module Sven0512, *via* reaction

with the thiol group of phosphopantetheine. Cysteine is also activated with the help of the cysteine adenylation domain and loaded on the Sven0512 module. The methyl transferase-like epimerization domain of Sven0512 is nonfunctional. The heterocyclisation domain catalyzes condensation of the salicyl thioester with the cysteinyl thioester, both bound to the NRPS module, to form a thiazoline ring. Finally, aerugine might be produced by hydrolysis of the thiazoline ring.[1]

1.4. Bacterial strains

The bacterial strains investigated for aerugine production in this thesis research include the human pathogenic bacteria *P. aeruginosa* (DSM 22644), *Y. enterocolitica* (DSM 4780) and *K. pneumoniae* (DSM 30104), which belong to the phylum Proteobacteria. The HGT of biosynthetic gene clusters involved in the production of aerugine between these human pathogenic bacteria and the soil bacterium *S. venezuelae* seems plausible, as biofilms and aquatic environments have been observed to be hotspots of HGT. [54] HGT of antibiotic resistance genes from antibiotic producing Actinobacteria to Proteobacteria has been shown and HGT of genes involved in siderophore acquisition has also been observed. [55,56]

Streptomyces venezuelae belongs to the class of Actinomycetes, a group of Gram positive, spore forming soil bacteria. Many of these filamentous and aerobe bacteria are known to produce a variety of antibiotics that are active against other bacteria.[57] For example, *S venezuelae* produces the broad band antibiotic chloramphenicol, which is used against typhus with high efficacy.[58] The production of antibiotics might play a role for mediating the nutrient uptake and competition of cohabitating Streptomyces species in soils.[59] In addition, Streptomyces species including *S. venezuelae* have been shown to produce siderophores, as for example desferrioxamine or watasemycin, in low iron-environments.[12,57] Furthermore, aerugine was identified as metabolite of *S. venezuelae*.[1]

Pseudomonas aeruginosa are Gram negative, polar flagellated bacteria that can grow under anoxic conditions and with very simple nutritional requirements. These ubiquitous bacteria are also opportunistic pathogens causing urogenital tract and systemic infections especially in immunocompromised patients. In cystic fibrosis, the presence of *P. aeruginosa* plays a major role in disease development.[60] Under iron-limited conditions, *P. aeruginosa* produces the siderophores pyochelin, pyoverdine and the metabolite aerugine.[12,13]

Yersinia enterocolitica are facultative anaerobic, non- spore-forming, Gram-negative Enterobacteria that are widespread in nature. The bacteria are distributed in water, food and especially swine as a host for human pathogenic strains. The pathogenicity of *Y. enterocolitica* mainly includes Yersiniosis, which is a disease of the intestinal tract. Infection with *Y. enterocolitica* is obtained mainly from food borne origins and rarely from blood transfusions.[61] Lassen *et al.* found the involvement of acute or chronic neurological disorders in 14 of 458 with Yersiniosis hospitalized patients.[62] Followingly, they hypothesize that infection with *Y. enterocolitica* might be connected to the development of neurologic disorders. Under iron-limited conditions *Y. enterocolitica* produces the siderophores yersiniabactin and yersiniophore.[63,64]

Klebsiella pneumoniae are facultative anaerobic, encapsulated, non-spore forming and non-motile gram-negative Enterobacteria. They inhabit the environment in soil or surface water and can colonize the human intestinal mucosa or oropharynx without harmful effects. From there, they can invade other tissues and cause a variety of diseases such as pneumonia, urinary tract infections or bacteremia, not only in immunocompromised individuals. Recently, the occurrence of hypervirulent strains and antibiotic resistances make the bacterium an increasing threat as a cause of nosocomial infections.[65] The factors that play a role for the virulence of *K. pneumoniae* partially include its siderophores enterobactin, yersiniabactin, salmochelin and aerobactin.[66,67]

1.5. Conditions for the biosynthesis of bacterial siderophores

As the secretion of siderophores mainly occurs under limited availability of iron, growth conditions are of essential importance for their biosynthesis and consequentially for their detection.

For example, it was stated in the literature that incubation temperature may have influence on siderophore production. Piscibactin production by *Vibrio aguillarum* and pyoverdine production in *Pseudomonas fluorescens* seem to be favored at low temperatures.[68,69] Furthermore, adding substrates that are used in biosynthesis to growth media could also be beneficial for siderophore production. It has been shown that it is possible to increase the siderophore production of desferroxamine E in *Streptomyces olivaceus* by adding L-lysine.[70] In *Microbacterium spp*. siderophore production was increased by adding glutamic acid or asparagine.[71] And siderophore production of staphyloferrin A in *staphylococci* by adding D- or L-ornithine.[72]

In the following various growth media are discussed that have been used for cultivation and siderophore production in *Yersinia* and *Klebsiella*.

Siderophore production of *Yersinia*

Perry *et al*. published a method to prepare a chemically defined minimal medium for the investigation of iron accumulation by *Yersiniae*.[4] This culture medium should prevent the supply of external iron, as it reduces the use of chelating components. For example, the usage of buffer systems like morpholinopropanesulfonic acid (MOPS), which is a poor iron chelator, should reduce the introduction of external iron.[73] Furthermore, an iron chelation step is performed to remove iron from the medium. Later, Staggs *et al.* published a very similar chemically defined minimal medium, and named it PMH, to study the iron acquisition system of *Y. pestis*.[74] PMH differs in that MOPS is exchanged for *N*-2-hydroxyethylpiperazine-*N*'-2-ethanesulfonic acid (HEPES) as a buffering agent. It is not stated what PMH stands for. Yfu ABC iron transport system of *Y. pestis* was investigated by culturing in PMH2, where piperazine-*N*,*N*'bis[2-ethanesulfonic acid] (PIPES) is used instead of the HEPES buffer system.[75] PMH2 was also used for the extraction, purifaction and identification of yersiniabactin of *Y. pestis*.[76] Yersiniabactin biosynthetic gene cluster was investigated in *Y. enterocolitica* using nutrient broth (NB) after iron chelation using 2,2´-dipyridyl.[63]

Siderophore production of *Klebsiella*

The production of siderophores in *K. pneumoniae* has been carried out using various culture media, often after an iron chelation step. Excretion of enterochelin by *K. pneumoniae* was detected in a chrome azurol S (CAS) agar plate assay using M9 minimal medium plus casamino acids.[77] Siderophore production in *K. pneumoniae* was assessed in iron-chelated M9 minimal medium plus casamino acids.[78] And interaction of lipocalin, transferrin and the siderophores enterobactin and yersiniabactin during pneumonia was investigated *in vitro* by cultivating *K. pneumoniae* in Luria-Bertani broth (LB) after iron-chelation with 2,2´-dipyridyl.[79] Furthermore, production of enterochelin by *K. pneumoniae* cultured in a chemically defined medium for siderophore production in *Yersiniae* was reported.[80]

1.6. Detection of bacterial small molecule metabolites *via* LC-MS/MS

Recently, liquid chromatography coupled with tandem mass spectrometry (LC-MS/MS) is a technology on the advance. The coupling of a separation technique to a highly sensitive detector enables the identification and quantification of analytes in complex matrices in the parts per

million (ppm) range, or ng/mL scale.[81] Therefore, this combination enabled commercialization and routine use of mass spectrometry in clinical diagnostics.[82,83]

In LC-MS/MS, analytes are ionized and injected into the vacuum of a mass spectrometer, after separation by high pressure liquid chromatography (HPLC). Ionization produces charged fragments of analytes. The detection of these fragments, which have a specific mass-to-charge ratio (m/z), is then used to identify the corresponding analytes.[81,84,85] In tandem mass spectrometry, selectivity is increased by a second fragmentation step for selected fragments. These sequential fragmentation steps are often realized by the spatial arrangement of three quadrupoles in a mass spectrometer. A quadrupole consists of four metal rods, to which an oscillating electric field is applied. In this way a quadrupole acts as a bandpass filter that only lets through ions of a certain m/z ratio. [86,87]

One widespread realization of a LC-MS/MS instrument is a (Ultra-)High Performance Liquid Chromatography [(U-)HPLC] system connected to a triple quadrupole mass spectrometer, as depicted in Figure **1-3**. The analytes are ionized and isolated from the chromatography solvent by Electrospray Ionization (ESI). ESI applies high voltages to create an electrically charged spray or aerosol. During this process the analytes are solvated in tiny droplets after being nebulized. In the gas phase, isolated ions then enter the mass spectrometer where a vacuum is created step by step. Quadrupoles 1 and 3 act as bandpass filters that select ions by specific m/z ratios. After ionization, certain Precursor Ions are selected to be further fragmented into Product Ions in the collision cell. Product Ions of a certain m/z value are then passed through to the detector. The m/z values can be determined *via* electric voltage that is applied to the quadrupoles. Quadrupole 2 acts as a collision cell where Precursor Ions are fragmented into Product Ions with the help of an inert collision gas. The fragmentation of a Precursor Ion into a specific Product Ion is called a transition. If a specific transition is selected for an MS/MS experiment, this method is called Selected Reaction Mode (SRM). SRM experiments enable the detection and quantification of analytes in a complex matrix with high sensitivity, as the signal-to-noise ratio is increased when only certain fragments are detected.[81,86,87]

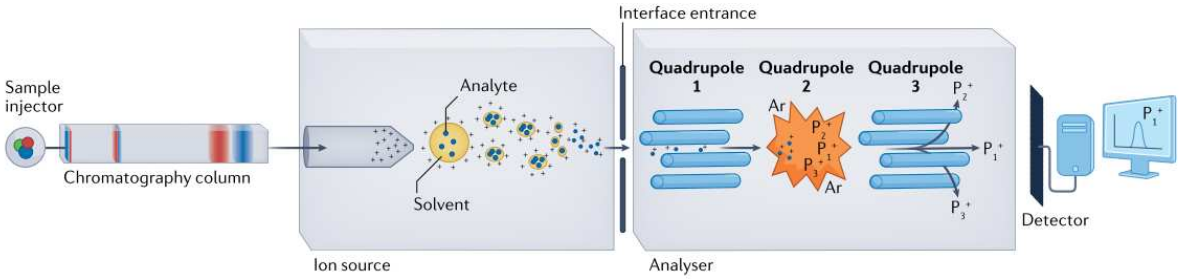

Figure 1-3 Depiction of a liquid chromatography–tandem mass spectrometry system. Fragmentation via electrospray ionization (ESI) followed by triple quadrupole fragmentation. (figure taken from Thomas *et al.*[86])

LC-MS/MS offers interesting applications for the detection and quantification of siderophores, and several examples have recently been published in this area. For example, a validated method for LC-MS/MS quantification of pyochelin and pyoverdin as possible cystic fibrosis biomarker, using a ^{13}C labeled internal standard, was published.[88] Another LC-MS/MS quantification method for pyochelin of *P. aeruginosa* was presented using caffeine as internal standard.[89] Also quantification of yersiniabactin and colibactin in *E. coli* and *K. pneuimoniae* by LC-MS/MS using 5,6,7,8-tetradeutero-3,4-dihydroxy-2-heptylquinoline as internal standard has been reported.[90,91] Siderophores influence on virulence of pathogenic *E. coli* was investigated by LC-MS/MS quantification of secreted siderophores in a chicken model, after deletions of export and synthesis genes in *E. coli*.[92] Szamosvári *et al.* suggest a procedure to quantify saturated and unsaturated 2-alkyl-4(1H)-quinolone N-oxides from *Pseudomonas* and *Burkholderia* via LC-MS/MS using NQNO-2-^{13}C internal standard as extraction control.[93]

Furthermore, attempts have been made to detect and quantify siderophores in soil samples. Ferrichrome and ferricrocin was identified in soil samples from Sweden by LC-MS/MS. Siderophores in soil samples were quantified *via* LC-MS (single quadrupole) experiments and an untargeted approach using ultra-high resolution mass spectrometry was reported.[94–96]

1.7. Quantification *via* LC-MS/MS

LC-MS/MS is a powerful tool for the detection and quantification of small bacterial molecules. Nevertheless, some characteristics of this method must be considered. In addition to the essential importance of calibration for quantification, the problem of matrix effects can be significant for quantification. Furthermore, sample preparation influences can affect the quality of the measurements.

Calibration

Calibration can be performed *via* external calibration of the analyte or a surrogate in the working solvent. Quantification methods of bacterial small molecules for research purposes are

frequently performed in this way.[89,90] External calibration can also be performed by mimicking the matrix of the samples to be analyzed. Szamosvári *et al.,* for example, dissolve and subsequently extract the analyte from the growth medium used and then carry out an external calibration.[93] Ji *et al*. perform the calibration by dilutions of the analyte in homogenized serum to develop a validated quantification method for clinical purposes.[88]

Matrix effects

During ionization, coeluting matrix components can suppress or enhance the ionization of the analyte itself and therefore, have impact on sensitivity of measurements. This problem is known as ion suppression or ion enhancement and is an especially difficult problem when dealing with biological matrices like blood, saliva, or urine. A very important factor in reducing effects and complexity of the matrix is the preparation of the samples. Sample preparation can consist of centrifugation and filtration steps to pellet cells and collect supernatants and extraction to avoid ions such as potassium, sodium, chloride, etc. The reproducibility of sample preparation steps, *e.g*. during extraction, can be monitored by using an internal standard as extraction control.[97–100]

Internal standards

Very often stable isotopologues such as ^{13}C containing or deuterated compounds are used as internal standards. When used as an extraction control, the internal standard is added to the sample prior to extraction and undergoes the same preparation steps as the analyte, which was also performed by Szamosvári and coworkers.[93] In this way, it can be monitored whether negative measurements, where no analyte is found, are due to insufficient extraction.

Deuterium is a stable hydrogen isotope. The bond dissociation energy of C-D bonds is higher compared to the corresponding C-H bonds.[2] This opens a highly interesting space of potential applications, for example labelling of internal standard compounds for LC-MS/MS. In mass spectra, deuterium-labelled compounds differ from their corresponding unlabeled versions by their m/z ratio.[101] In addition, it is described in the literature that deuterated compounds elute somewhat earlier than the same non-deuterated compounds.[101] Deuterium-containing compounds hardly differ in their chemical properties from their hydrogen-containing versions, so that a similar behavior can be assumed during extraction.[102]

2. Aims of this thesis

The aim of this thesis is to detect and quantify the production of the neurotoxic metabolite aerugine in human pathogenic bacteria and to determine whether its (*R*)- or (*S*)-enantiomer is produced. To achieve this, an LC-MS/MS method enabling the detection and quantification of aerugine from liquid cultures will be developed. This includes the synthesis of an internal deuterated standard as extraction control.

For method development, extracts of *Pseudomonas aeruginosa* cultures, which are known to produce aerugine, will be used. In parallel to aerugine quantification, it will be investigated whether quantification of pyochelin in *P. aeruginosa* is possible from the same samples. Once the LC-MS/MS quantification method is established in the *P. aeruginosa* system, it will be used to find growing conditions for *Klebsiella pneumoniae* (DSM 30104) and *Yersinia enterocolitica* (DSM 4780) under which the production of aerugine is induced. Once the growth conditions that induce the production of aerugine have been identified for the above-mentioned human pathogenic bacteria, it will be shown whether these organisms produce (*R*)- or (*S*)-aerugine *via* chiral HPLC. Furthermore, effects of increasing iron concentrations in the culture media will be investigated *via* LC-MS/MS quantification. Another aim of the thesis is the synthesis of several aerugine derivatives. These derivatives will enable a small structure-activity relationship study to further investigate the mode of action of aerugine.

Altogether, this work aims to contribute to the understanding of the role of human pathogenic bacteria in the development of neurodegenerative diseases, particularly Parkinson's disease.

3. Results and Discussion

3.1. Stereospecific synthesis of *(R)*-aerugine

The stereospecific synthesis of (*R*)-aerugine **1** was carried out as established by Dr. Felix Anderl, employed as a senior scientist of the Böttcher group. The first step of this synthesis consists of the reduction of L-cysteine to L-cysteinol, which was adapted from Rodrigues et al.[103] The conditions for the reduction are shown in Figure **3-1** (reaction **a**).

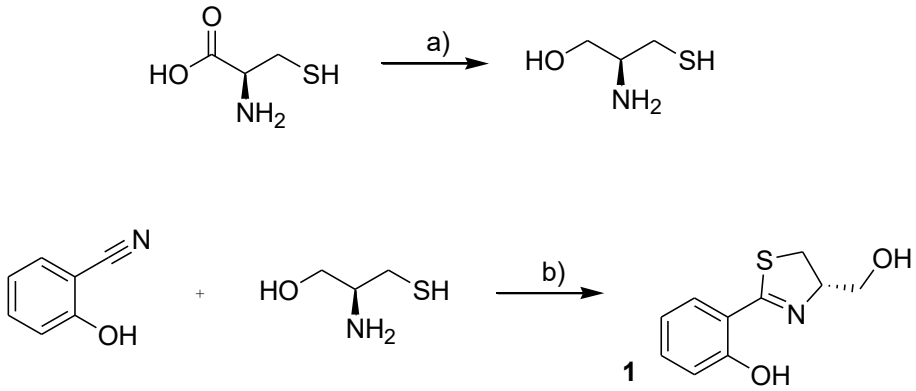

Figure 3-1: Synthesis of (*R*)-aerugine (compound 1) by reduction of L-cysteine to L-cysteinol and condensation of 2-hydroxybenzonitrile and L-cysteinol. Conditions: a) BH_3SMe_2, THF, 0 °C to rt, 16 h, sealed under N_2. b) 0.1 M phosphate buffer pH = 6.4, 16 h at 65 °C, sealed under N_2, 25% yield (reaction **b**).

By performing the reduction prior to the condensation reaction, pure enantiomers of the final compound can be obtained from L- or D-cysteine.[103] Furthermore, the formation of disulfide byproducts, which would reduce yields and complicate purification of the final product, can be avoided in this way.[103] Following the reduction step, a condensation reaction of L-cysteinol to 2-hydroxybenzonitrile was performed as shown in Figure **3-1** (reaction **b**). Reactions **a** and **b** were performed as one-pot reaction, without purification in between. In this condensation reaction, carried out under aqueous buffered conditions, a thiazoline ring is formed.

In this work the condensation reaction was carried out successfully with a yield of 25% using 2-hydroxybenzontrile as the limiting starting compound.

3.2. Synthesis of a deuterated internal standard for LC-MS/MS

Based on the established stereospecific synthetic pathway for (*R*)-aerugine, this work aims at the synthesis of deuterated aerugine as an internal standard for LC-MS/MS analysis. In general, deuterated starting compounds are expensive and only small amounts are required for LC-MS/MS analysis. Instead of purchasing deuterated starting compounds such as deuterated L-cysteine or 2-hydroxybenzonitrile, this work presents a cost-saving alternative. The approach pursued involves the deuteration of 2-hydroxybenzonitrile and subsequent condensation to L-

cysteinol. Therefore, deuteration of arenes was investigated to establish an in-house deuteration procedure of the starting material for the further synthesis of the internal standard itself.

Deuteration of arenes by Pt/C catalyzed H-D exchange

To develop a suitable deuteration procedure for synthesis of the internal standard, Pt/C catalyzed H-D exchange was performed according to the work of Sawama and coworkers.[2] In a first step, deuteration of salicylic acid (compound **2-d**) was reproduced. The reaction was carried out in the conditions shown in Figure **3-2**.

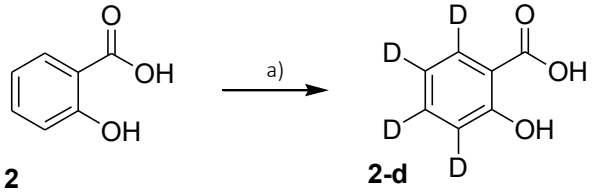

Figure 3-2: Deuteration of salicylic acid (compound 2). Conditions: a) 10% Pt/C (6 mol%), D_2O (2 mL)/2-PrOH (1 mL), rt, 23 h; then 90 °C, 21 h, sealed under N_2, 42% yield.

Proceeding of H-D exchange was determined by the decrease in intensity of signals corresponding to aromatic hydrogens in the ^{1}H-NMR spectra. This decrease was determined relative to the solvent peak or a reference compound that was added prior to recording the NMR spectrum. However, the reaction showed very slow proceeding and complete H-D exchange was not reached. Therefore, an attempt was made to improve the reactions efficiency by increased temperature. The dependency of the H-D exchange on temperature was already examined by Ito *et al*.[3] According to their work, especially in Pd/C catalyzed H-D exchange reactions, but also in Pt/C catalyzed H-D exchange of phenol, deuteration efficiency can be improved by heating. In line with these findings, the H-D exchange reaction that was performed in this thesis work using salicylic acid as a substrate, proceeded significantly faster, after heating to 90 °C. After increasing the reaction temperature, almost full exchange of aromatic hydrogens by deuterium atoms could be observed.

Based on the conditions that enabled reproducing deuteration of salicylic acid in this work, deuteration of 2-hydroxybenzonitrile as an educt for aerugine synthesis, several aerugine derivatives and salicylic amide were investigated. The results are shown in Figure **3-3** and Table **3-1**.

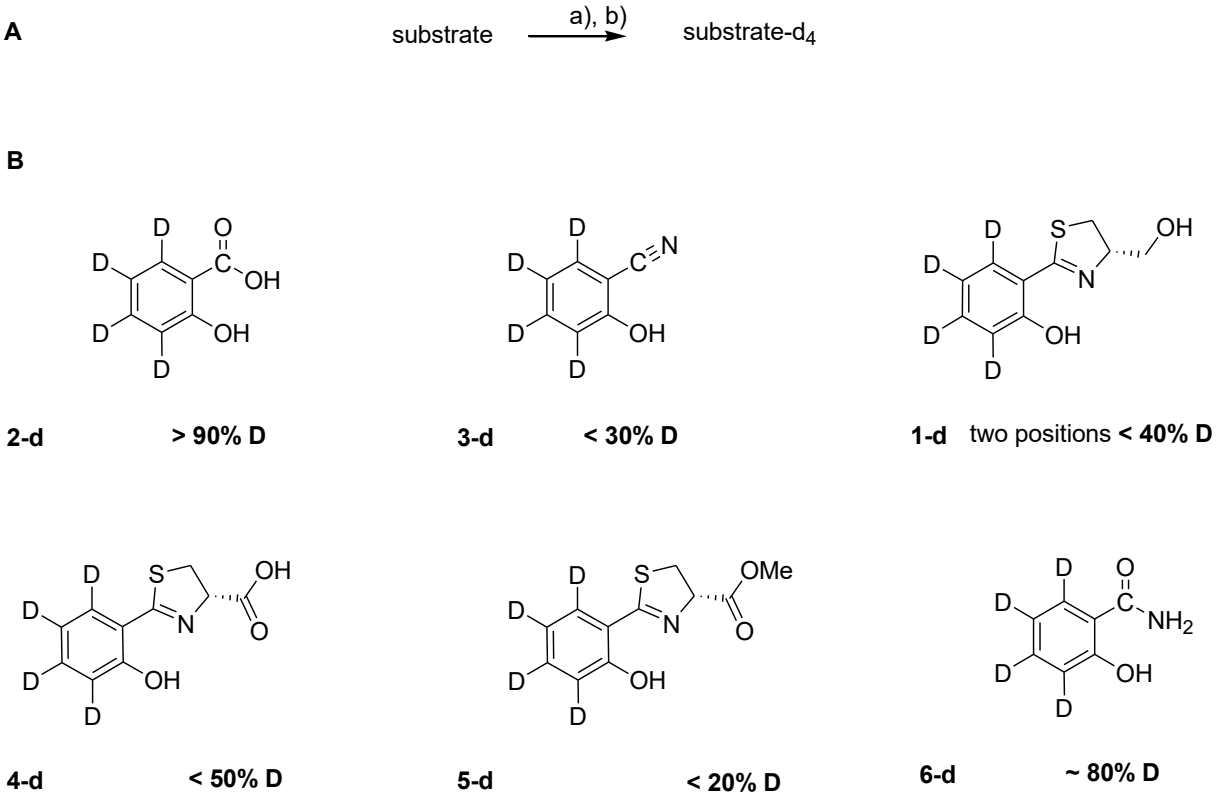

Figure 3-3: Deuteration of 2-hydroxybenzonitrile and aerugine derivatives. A: Deuteration conditions: a) 10% Pt/C (6 mol%), D_2O (2 mL)/2-PrOH (1 mL) 90 °C, 16 h, sealed under N2. b) 10% Pt/C [3 mol%), D_2O (8 mL)/2-PrOH (4 mL), 90 °C, 16 h, sealed under N_2, 64% yield. B: Compounds **2-d** - salicylic acid, **3-d** - 2-hydroxybenzonitrile, **1-d** - (R)-aerugine, **4-d** - (R)-dihydroaeruginoic acid, **5-d** - (R)-2-(2'-hydroxyphenyl)-4-methoxycarbonyl-4,5-dihydrothiazole, **6-d** - salicylic amide. Grade of deuteration is indicated with % D.

Deuteration of 2-hydroxybenzonitrile was not successful, which could be due to the presence of the strongly electron withdrawing nitrile group. Low H-D exchange efficiencies for neighboring aromatic carbons of nitrile groups have been observed already.[3] Furthermore, deuteration of aerugine derivatives was not successful, which might be caused by the presence of a sulfur atom in these compounds acting as a catalytic poison for Pt/C. This was also observed by Ito and coworkers, where H-D exchange of thiophenol showed deuteration efficiency of less than 10%.[3]

Considering results of previous publications by Sawama and Ito *et.al.*, it could be hypothesized that salicylic amide itself could be successfully deuterated by Pt/C catalyzed H-D exchange.[2,3] It has been shown that introducing amines to hydroxylated arenes does not affect H-D exchange. Furthermore, replacement of carboxylic groups by amide groups seems to have only a minor effect on deuteration of aromatic carbons located in immediate vicinity of the amide group.[3]

Table 3-1 Deuteration efficiency of compounds: 2-d - salicylic acid, **3-d** - 2-hydroxybenzonitrile, **1-d** - (R)-aerugine, **4-d** - (R)-dihydroaeruginoic acid, **5-d** - (R)-2-(2'-hydroxyphenyl)-4-methoxycarbonyl-4,5-dihydrothiazole, **6-d** - salicylic amide.

Compound	Chemical shift [ppm]	Integrated area	Deuteration [%D]
2-d	7.68	0.09	95
	7.34	0.04	98
	6.78; 2H	0.08	98
1-d	7.38, 2H	1.68	13
	6.97	0.75	25
	6.87	0.74	26
3-d	7.82	0.12	88
	7.38	0.65	35
	6.91	0.72	28
	6.87	0.18	82
4-d	7.88	0.51	49
	7.49	0.54	46
	6.97, 2H	1.51	25
5-d	7.29, 2H	1.77	12
	6.87	0.82	18
	6.79	0.82	18
6-d	7.74	0.31	76
	7.34	0.21	84
	6.84, 2H	0.32	88
6-d upscale	7.62	0.16	88
	7.27	0.17	87
	6.79, 2H	0.34	87

In line with the findings of Sawama and Ito *et al*., H-D exchange was carried out successfully with salicylic amide. And, for eight times upscale, D_2O amounts could be reduced by 50% without impairment of H-D exchange efficiency. This observation is in accordance with previous findings about the effects of reduced D_2O usage on the deuteration efficiency of benzoic acid.[2]

Concerning the hypothetical reaction mechanism, proceeding of the H-D exchange is highly dependent on the absence of oxygen withdrawing hydrogen from the Pt/C–D_2O–H_2 complex that has been discussed by Ito and coworkers as mechanism for the exchange reaction.[3] Hydrogen is crucial for formation of this complex and in the reaction mixture isopropanol is used as a hydrogen donor. Platinum catalyzes the dehydrogenation of isopropanol to acetone leading to the generation of hydrogen, which is needed for the activation of platinum prior to complex formation.

Synthesis of 2-hydroxybenzonitrile

Following successful deuteration of salicylic acid, a synthesis pathway for the deuterated starting material of aerugine was established. In this work, the approach of introducing the amino group by generating salicylic amide and subsequent dehydration to 2-hydroxybenzonitrile was followed. Prior to synthesis of deuterated 2-hydroxybenzonitrile, synthesis conditions were optimized using non-deuterated starting materials.

First, salicylic acid **2** was transformed into the more reactive corresponding methyl ester as shown in Figure **3-4**. For this, hydrogen chloride was generated *in situ* by the addition of acetylic chloride to methanol (MeOH) and was used as a reagent for the acidic catalysis of carboxylic acid esterification, as described in the literature.[2] After successful esterification with yields of up to 95%, salicylic methyl ester **7** was transformed to salicylic amide **6** *via* ammonolysis (reaction **b**).

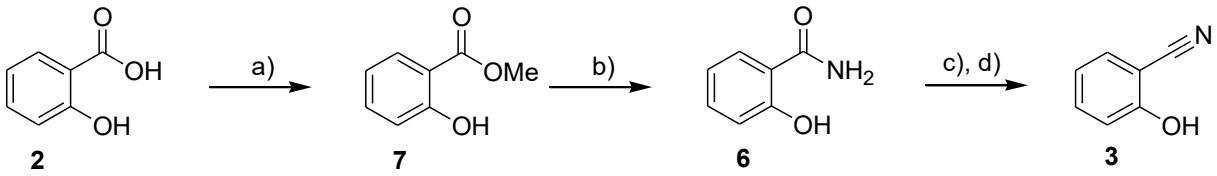

2 **7** **6** **3**

Figure 3-4: Esterification of salicylic acid **2**, followed by ammonolysis of salicylic methyl ester **7** to salicylic amide **6** and reduction to 2-hydroxybenzonitrile **3**. Conditions: a) AcCl, MeOH, heated to reflux, 16 h, 95% yield. b) ammonia in pressure vial, 85 °C, 16 h, 89% yield. Dehydration. Conditions: c) triphosgen, pyridine, 0 °C – rt, 16 h, sealed under N_2, 41% yield. d) Burgess reagent, THF, rt, 1.5 h, sealed under N_2.

To obtain deuterated 2-hydroxybenzonitrile, dehydration of acidic amide **6** to the corresponding nitrile **3** was performed. In this thesis two possible dehydration reactions are compared. First, Einhorn *et al*. described a phosgene pyridine dehydrating agent that converts acidic amides into nitriles.[104] Due to the toxic properties of phosgene, triphosgene is used as a substituent in organic synthesis and for industrial purposes.[105] As a solid, triphosgene is more practical and safer to handle than poisonous phosgene gas. To prevent handling of the extremely poisonous phosgene gas, in this work the dehydration reaction using phosgene in pyridine was adapted by the usage of triphosgene in pyridine as dehydrating agent (reaction **c**). Second, Burgess reagent has been suggested as a mild and chemo-selective dehydrating agent of amides to nitriles.[106] By using Burgess reagent, dehydration of salicylic amide was performed within less than 2 h (hours) yielding 52% 2-hydroxybenzonitrile without the usage of any toxicants (reaction **d**). Consequently, amide dehydration by Burgess reagent was used for all further experiments.

Synthesis of aerugine-d4

Finally, synthesis of the deuterated internal standard was performed by condensation reaction of 2-hydroxybenzonitrile-d4 and L-cysteinol (see Figure **3-5**). Deuterated salicylic amide was generated by deuteration of salicylic amide, and dehydration was performed using Burgess reagent as described in Figure **3-4**. The synthesis pathway is shown in Figure **3-5**.

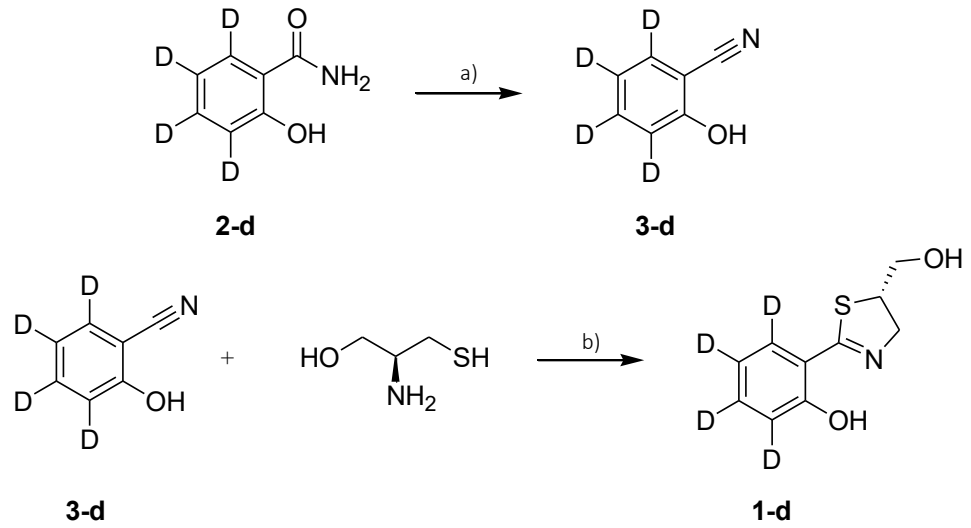

Figure 3-5: Dehydration of deuterated salicylic amide. Conditions: a) Burgess reagent, dry THF, rt, 1.5 h, sealed under N_2, 52% yield. Condensation of deuterated 2-hydroxybenzonitrile and L-cysteinol to form deuterated aerugine. Conditions: b) 0.1 M phosphate buffer pH = 6.4, 16 h at 65 °C, sealed under N_2, 12% yield.

In conclusion, synthesis of the deuterated internal standard was performed successfully. In this work, two pathways to obtain deuterated 2-hydroxybenzonitrile as starting material for its synthesis, starting with deuteration of salicylic acid or deuteration of salicylic amide, were investigated in parallel. Especially, in-house deuteration of salicylic amide, using deuterium oxide (D_2O) as inexpensive deuterium source, presents an interesting reaction for synthesis of further deuterated thiazoline compounds. One example is the 2-hydroxyphenylthiazoline family which includes antibiotic and neurotoxic bacterial metabolites. Deuterated standards of these metabolites may be of interest in analytical applications as well as in applications studying drug metabolism, kinetics, or reaction mechanism.[3]

3.3. Development of a LC-MS/MS quantification method

For detection and quantification of aerugine in human pathogenic bacteria, an LC-MS/MS quantification method was developed. An attempt was made to quantify pyochelin in parallel. Extraction of bacterial supernatants and conditions for LC-MS/MS measurements were based on the work of Szamosvári *et al.* and Savchenko *et al.*[9,93] Sufficient extraction was controlled using deuterated aerugine as internal standard. Detection was performed in SRM mode and

fragments for detection were identified in Product Ion Scans of synthetic aerugine, pyochelin and of the internal standard aerugine-d_4. Hypothetical fragmentation patterns and probable structures of the most abundant fragments are discussed in the following paragraphs.

Reference spectra and Peak assignment

Mass spectra of aerugine, aerugine-d_4 and pyochelin were obtained in Product Ion Scan mode and are shown in the following chapter. Fragmentation pathways are discussed, and possible structures of the most abundant peaks are proposed. The most abundant peaks were selected for quantification of the molecules in SRM mode. Figure **3-6** shows the ms^2 spectrum of aerugine and proposed structures of the most abundant fragments in the spectrum and a probable fragmentation pattern. Chromatograms and ms^2 spectra without annotations can be found in the appendix.

It should be mentioned that the proposed structures are plausible, but hypothetical structures. The rearrangement reactions during dissociation inside the collision cell of the mass spectrometer are complex and there is a lack of knowledge about fragmentation patterns in tandem MS.[84]

A

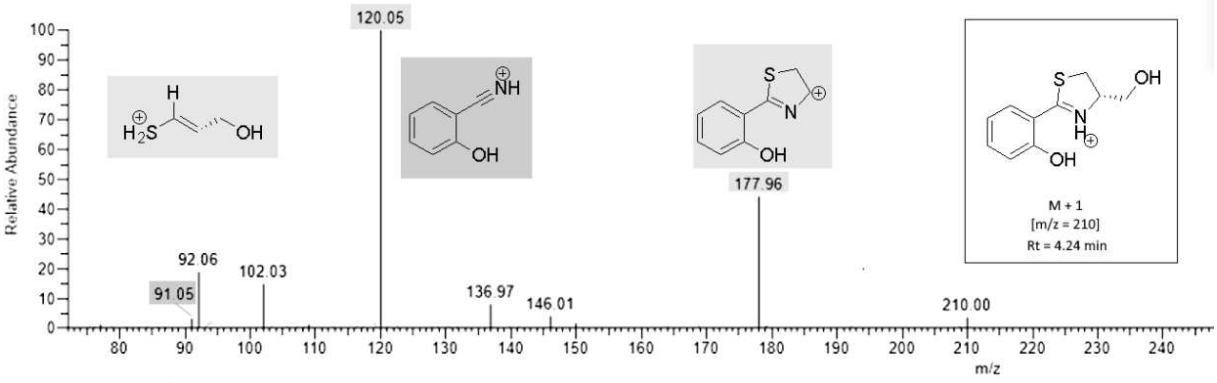

B

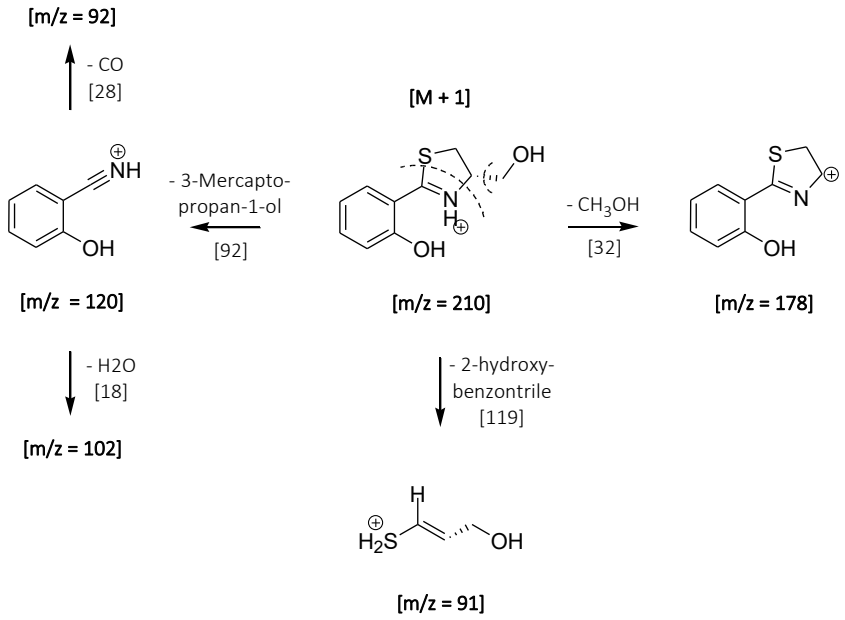

Figure 3-6 MS^2 reference spectrum of aerugine (compound 1) with proposed fragments and proposed fragmentation pattern of aerugine. A: MS^2 reference spectrum obtained in Product Ion Scan mode after injection of synthetic aerugine with assignment of proposed fragments. B: Most abundant fragments of the MS^2 spectrum and neutral losses with the corresponding *m/z* value in brackets.

The molecule peak with *m/z* 210 represents the non-fragmented molecule after addition of one hydrogen atom and is also the peak with the highest *m/z* value in the spectrum. The most abundant fragment *m/z* 120 is probably formed by cleavage of carbon heteroatom bonds, which results in thiazole ring opening. The positive charge is retained at the heteroatom (N) by hydrogen rearrangement and the resulting fragment with *m/z* 120 represents the base peak of the mass spectrum. After cleavage of the carbon-heteroatom bond, the charge could also migrate to the α-carbon. The fragment with *m/z* 91 might be formed, due to further charge migration to the sulfur atom and neutral loss of 2-hydroxybenzonitrile. Reactions leading to such fragments have been referred to as competitive or complementary reactions following carbon-heteroatom bond cleavage. According to the [M + 1H] + 1 rule, the sum of the *m/z* values of these fragments adds up to the molecule peaks *m/z* value + 1.[84] In other words, the

sum of the fragments *m/z* 120 and *m/z* 91 corresponds to the molecule peak´s *m/z* value 210 + 1, which gives 211. Further fragments that can be seen in the Product Ion Scan spectrum are probably obtained by neutral loss of -CO, -H_2O and -CH_3OH (fragments: *m/z* 92, *m/z* 102 and *m/z* 178). These neutral losses have been studied by Levesen and coworkers and are very common for dissociation reactions after ESI.[107] Due to the lack of understanding of dissociation reactions and complex rearrangement of the structures, the structures of some fragments that are found in the spectrum cannot be proposed in a plausible way.[84]

Figure **3-7** shows the MS^2 spectrum of aerugine-d_4 with assignment of the most abundant fragments and a probable fragmentation pattern.

A

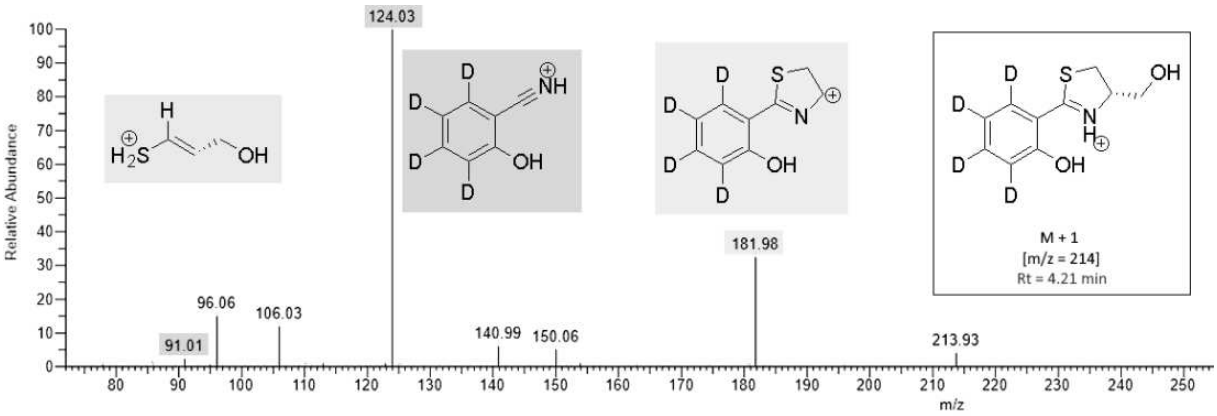

B

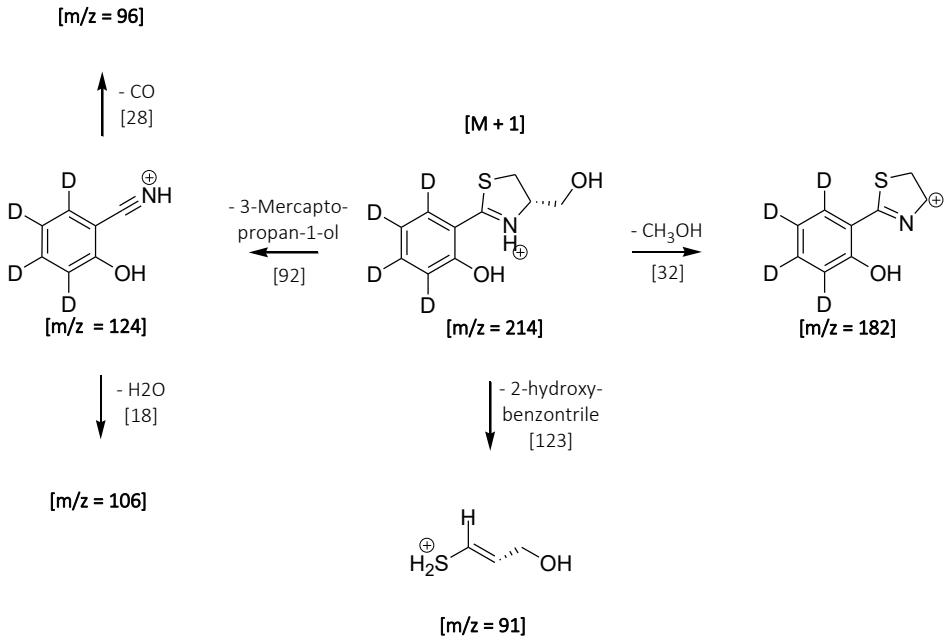

Figure 3-7 MS^2 reference spectrum of aerugine-d_4 (compound 1-d) with proposed fragments and a probable fragmentation pattern of aerugine-d_4. A: MS^2 reference spectrum obtained in Product Ion Scan mode after injection of internal standard aerugine-d_4 with assignment of proposed fragments. B: Most abundant fragments of the MS^2 spectrum and neutral losses with the corresponding *m/z* value in brackets.

Fragmentation of aerugine-d_4 probably takes place in the same pattern as fragmentation of aerugine. When comparing mass spectra of aerugine and aerugine-d_4, the *m/z* values of fragments containing the aromatic ring differ by *m/z* 4. This is due to the four adjacent heavy deuterium atoms. Furthermore, the assumption that only fragment *m/z* 91 is not derived from the aromatic part of the molecule is reassured, as it is the only fragment that does not differ by *m/z* 4.

Figure **3-8** shows the MS^2 spectrum of pyochelin with assignment of the most abundant fragments and a probable fragmentation pattern.

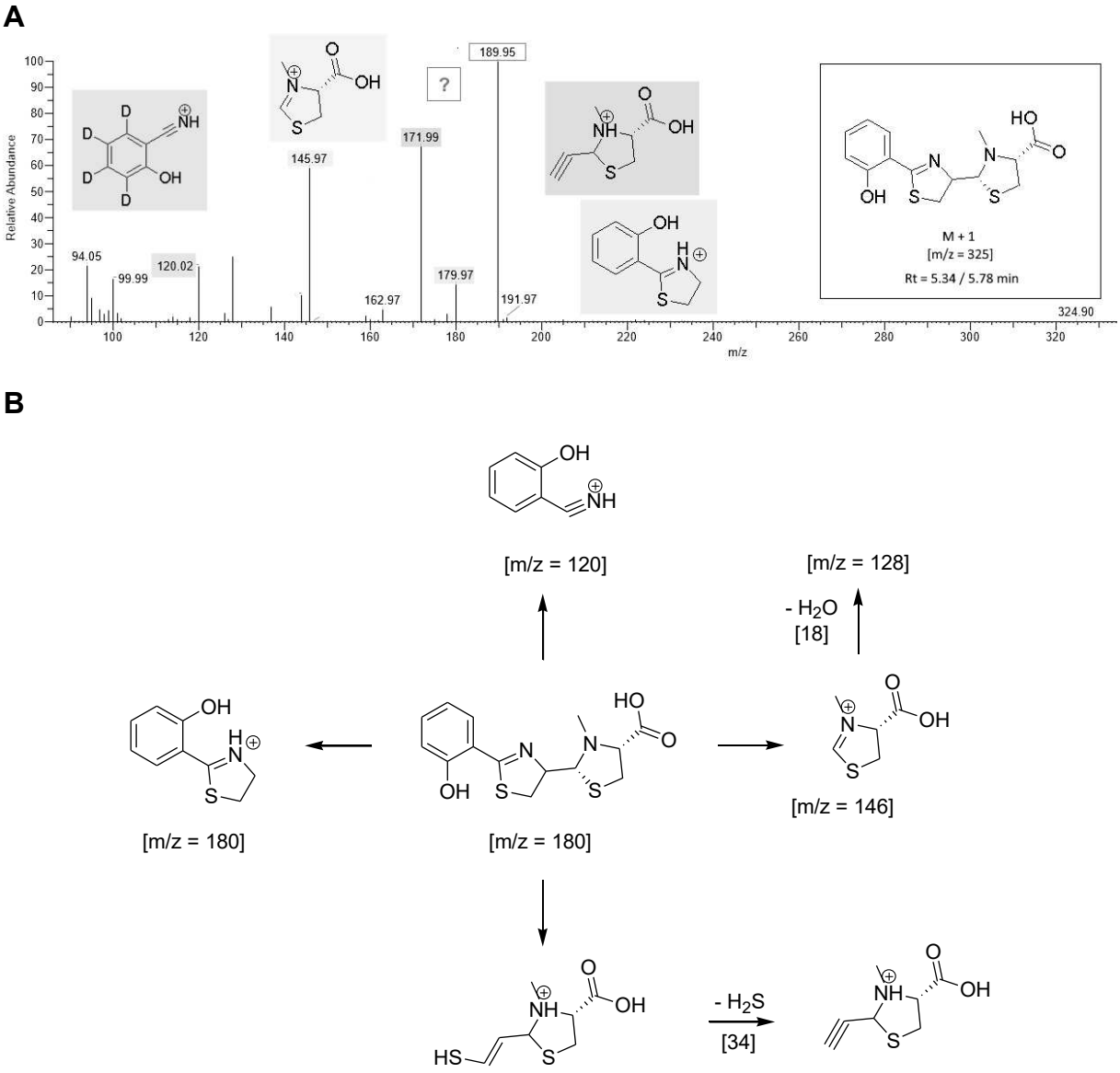

Figure 3-8 MS^2 reference spectrum of pyochelin with proposed fragments and a probable fragmentation pattern. A: MS^2 reference spectrum obtained in Product Ion Scan mode after injection of synthesized pyochlein with assignment of proposed fragments. B: Most abundant fragments of the MS^2 spectrum and neutral losses with the corresponding *m/z* value in brackets.

The molecule peak with *m/z* 325 (see Figure **3-8**) corresponds to non-fragmented pyochelin with addition of one proton. Fragments *m/z* 120 and *m/z* 206 presumably emerge in a similar way as fragments *m/z* 91 and *m/z* 120 from fragmentation of aerugine. Two carbon-heteroatom bonds are cleaved, and the thiazole ring is opened. For this cleavage, the [M + 1H] + 1 rule applies. [84] The sum of the fragments *m/z* 120 and *m/z* 206 corresponds to the molecule peak´s *m/z* value 325 + 1, which gives 326. It appears that also a carbon-carbon bond that is connecting the thiazolin and the thiazolidine ring is cleaved during the fragmentation process; giving

fragments *m/z* 180 and *m/z* 146. Again the [M + 1H] + 1 rule applies. The sum of the fragments *m/z* 180 and *m/z* 146 corresponds to the molecule peak´s *m/z* value 325 + 1, which gives 326.[84] Fragments *m/z* 128 and *m/z* 172 are generated by neutral loss of -H_2O and -H_2S from fragments *m/z* 146 and *m/z* 206. With the data obtained from this low-resolution Product Ion Scan, no plausible structure for the *m/z* 190 fragment can be suggested. Nevertheless, also in a previously published LC-MS/MS quantification method, this fragment has been used for SRM-mode quantification of pyochelin.[89]

3.4. Quantification of aerugine in bacterial liquid culture supernatants

Quantification was performed *via* external calibration in the 0.01-2.0 mg/L range and the corresponding calibration curves can be found in the appendix. For parallel detection of pyochelin it was necessary to redissolve extracted supernatants in 100% MeOH, before measurements. Probably solubility of pyochelin in 50% MeOH in H_2O is not sufficient for detection. Furthermore, using 100% MeOH as solvent resulted in a limit of detection (LOD) of 0.015 mg/L instead of 0.023 mg/L and therefore, a slight increase in sensitivity of the method.

First, detection of aerugine in supernatant extracts of *P. aeruginosa* strain PAO1 was performed showing that extraction and measurement conditions were suitable for detection of aerugine. PAO1 is known to produce aerugine and therefore, was used as a positive control to test the quantification method. Furthermore, secreted aerugine concentrations were within the calibration range and therefore, no dilution of samples or adaptation of the calibration range had to be performed.

In the following, results from LC-MS/MS measurements of bacterial liquid cultures are shown. Supernatants of bacterial liquid cultures were collected after centrifugation and extracted with ethyl acetate (EA). Before extraction, internal standard aerugine-d_4 was added as extraction control.

3.4.1 Analysis of aerugine levels during bacterial growth

Production of aerugine was monitored during bacterial growth over time. PAO1 was cultured in M8 at 37 °C and aerugine concentration was measured after 6 and 24 h. Figure **3-9** shows data corresponding to measurements of three independent biological replicates and supernatant extraction was performed in triplicates.

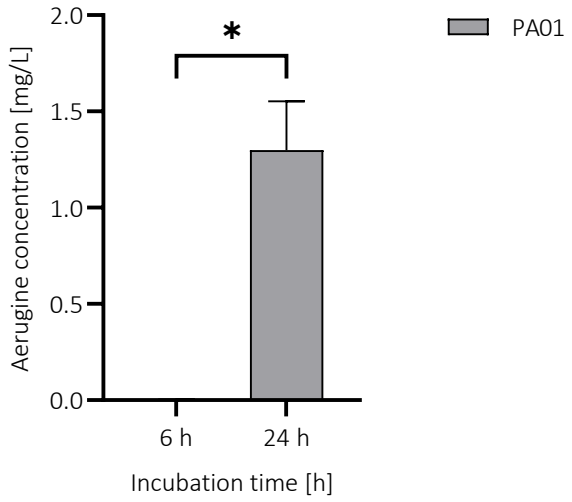

Figure 3-9: Aerugine production of PAO1 in M8 after incubation for 6 h and 24 h at 37 °C. Data represent mean ± standard deviation from three independent biological subcultures. Extraction of the samples was performed in technical triplicates and using an internal standard as extraction control. Two-tailed paired t-test was performed. Statistically significant differences are indicated by asterisks ($p^* < 0.05$).

Aerugine could not be detected in PAO1 supernatants after 6 h. However, after 24 h, the concentration of secreted aerugine was 1.34 ± 0.23 mg/L which corresponds to a concentration of 6.43 ± 1.09 µM. This shows that the extraction and quantification method developed in this work is suitable to measure the production of aerugine and the calibration was performed in a realistic concentration range. Furthermore, M8 is a suitable minimal medium to induce aerugine production in PAO1. Interestingly, this concentration lies above the half-maximal effective concentration of 3–4 µM for aerugine's neurotoxicity in human dopaminergic neurons (LUHMES cells) documented by Ückert and coworkers.[1] For further investigations it may be of interest to monitor aerugine production by PAO1 up to 48 h to determine whether the concentration has reached a plateau after 24 h or continues to rise.

3.4.2 Screening of conditions inducing aerugine production in *Y. enterocolitica* and *K. pneumoniae*

To induce aerugine production in *Y. enterocolitica* and *K. pneumoniae*, different growth media were investigated. Figure **3-10** and Figure **3-11** show screenings to find growth conditions for further investigation. Various growth media, the addition of the aerugine biosynthesis-substrates L-cysteine and salicylic acid and deferration of growth media were investigated. In this first screening of the growth conditions only individual measurements were carried out. The use of the deuterated internal standard assured that negative measurements were not due to poor extraction efficiency.

3.4.3 Screening of various growth media

A variety of growth media were tested in an initial screening. Minimal medium 8 (M8) is of interest as it has already been used for aerugine production by PAO1 (see Figure **3-9**). Peptone growth medium (PGM), trypticase soy yeast medium (TSYM) and marine broth (MB) represent undefined growth media with a variety of nutrient sources. PMH is a chemically defined minimal medium developed to study siderophore production in *Yersiniae*.[74] After cultivation of PAO1 in M8 and TSYM for 48 h, the experiment was terminated due to poor phase separation during extraction.

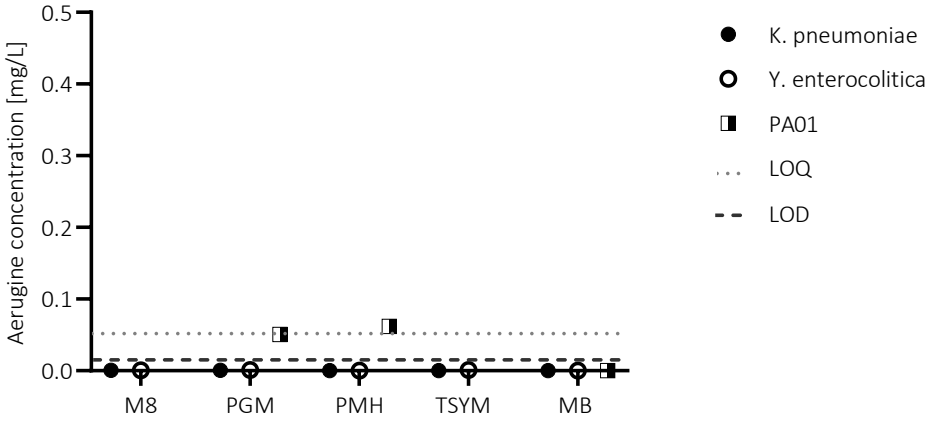

Figure 3-10 Screening for growth media inducing aerugine production in *K. pneumoniae and Y. enterocolitica.* After incubation, supernatants were collected after centrifugation and extraction was performed after adding aerugine-d_4 as internal standard. Incubation of *K. pneumoniae* DSM 30104, *Y. enterocolitica* DSM 4780 and PAO1 DSM 22644 in indicated growth media (M8: minimal medium 8; PGM: peptone growth medium, PMH: chemically defined minimal medium; TSYM: trypticase soy yeast medium, MB: marine broth) at 37 °C for 48 h.

As shown in Figure **3-10**, no aerugine production was observed in M8, PGM, PMH, TSYM or MB by *K. pneumoniae* or *Y. enterocolitica*. PAO1 appears to produce small amounts of aerugine in PGM and PMH after 48 h (0.05 and 0.06 mg/L, corresponding to 0.24 µM and 0.29 µM). This is far below the concentration of 6 µM detected after 24 h culturing PAO1 in M8 and below the concentration of 3-4 µM causing neurotoxicity documented by Ückert *et al.*[1] For this reason, the cultivation of PAO1 in these media was not investigated further in this thesis. However, it would be of particular interest to obtain data on the aerugine concentration after 48 h of cultivation of PAO1 in M8. It could therefore be suggested to increase the centrifugation time for the cell pelleting step to improve phase separation during extraction.

Screening upon feeding salicylic acid and L-cysteine

For further investigations, substrates of the biosynthetic pathway (Figure **3-11**) of aerugine production were added to the growth media.

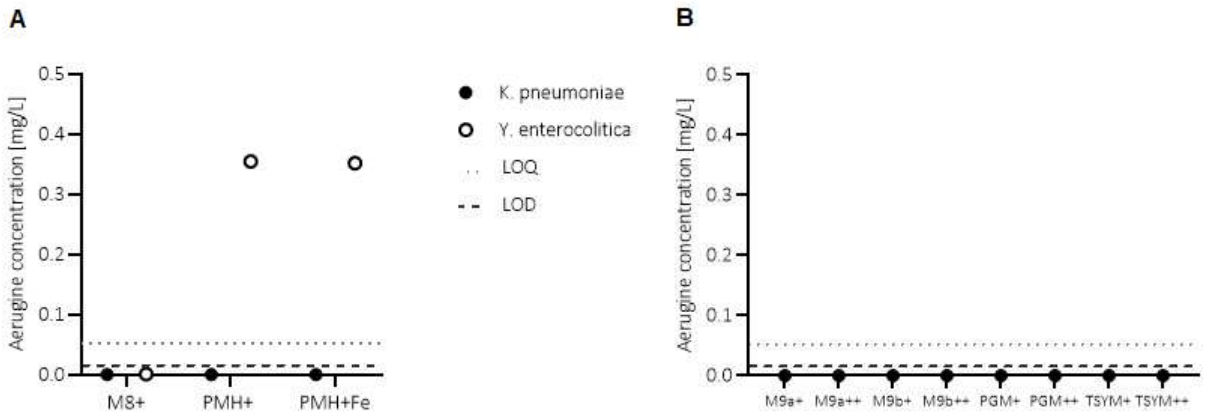

Figure 3-11 Screening for growth media inducing aerugine production in *K. pneumoniae and Y. enterocolitica* upon feeding salicylic acid and L-cysteine. After incubation, supernatants were collected after centrifugation and extraction was performed after adding aerugine-d_4 as internal standard. A: Incubation of *K. pneumoniae* in indicated growth media (M9a: minimal medium M9 + 0.5 % casamino acids; M9b: M9 + 0.5 % casamino acids and 1 mM $CaCl_2$, PGM; TSYM) with addition of salicylic acid and L-cysteine (100 µM each: +; 200 µM each: ++) at 37 °C for 24 h. B: Incubation of *K. pneumoniae* and *Y. enterocolitica* in indicated growth media (M8, PMH) with addition of salicylic acid and L-cysteine (100 µM each: +; 200 µM each: ++) and iron (Fe: 0.1 µM $FeCl_3$) at 37 °C for 24 h.

Figure **3-11 A** shows aerugine production in *Y. enterocolitica* after feeding salicylic acid and L-cysteine (100 µM each) in PMH. To confirm these findings, the experiment has been repeated in biological triplicates and the results are shown in Figure **3-13**. *K. pneumoniae* showed no aerugine production under other growth conditions, including cultivation in M9 containing casamino acids with and without $CaCl_2$, or in PGM and PMH. Feeding salicylic acid and L-cysteine at concentrations of up to 200 µM also did not induce aerugine production in *K. pneumoniae* (Figure **3-11 B**).

PMH was developed for siderophore production in *Yersiniae*.[4] It undergoes a deferration step during its preparation and therefore, presents iron depleted growth conditions. *K. pneumoniae* also produced its siderophore enterochelin in this medium.[80] Though, also after feeding the substrates salicylic acid and L-cysteine, aerugine was not detected in K. pneumoniae cutured in PMH. Growth media including complex nutrient sources such as casamino acids, yeast extract, or tryptone have been used to induce siderophore production in *K. pneumoniae*.[77] As figure **B** shows, the introduction of complex nutrient sources and the addition of substrates did not stimulate the production of aerugine in *K. pneumoniae*. It could be that aerugine production in *K. pneumoniae* is very sensitive to the iron concentration-in the growth medium. The detection of siderophores in *K. pneumoniae,* that is of course also sensitive to the iron concentration in growth media, has been reported for complex growth media that have undergone a deferration step.[78,79] Therefore, in this thesis work next a deferrated complex medium was investigated.

Deferratation of growth media

K. pneumoniae was incubated in deferrated PGM, with or without feeding salicylic acid and L-cysteine, for 24 h at 25 or 37 °C. Due to a mistake in sample preparation a known amount of synthetic aerugine was added together with the internal standard and centrifugation during collecting supernatants of bacterial cultures was performed at varying speed. Figure **3-12** shows the detected quantity of aerugine "as measured", and after subtracting the known amount of aerugine added as "corrected". The "**!**" in the diagram legend indicates this error in sample preparation.

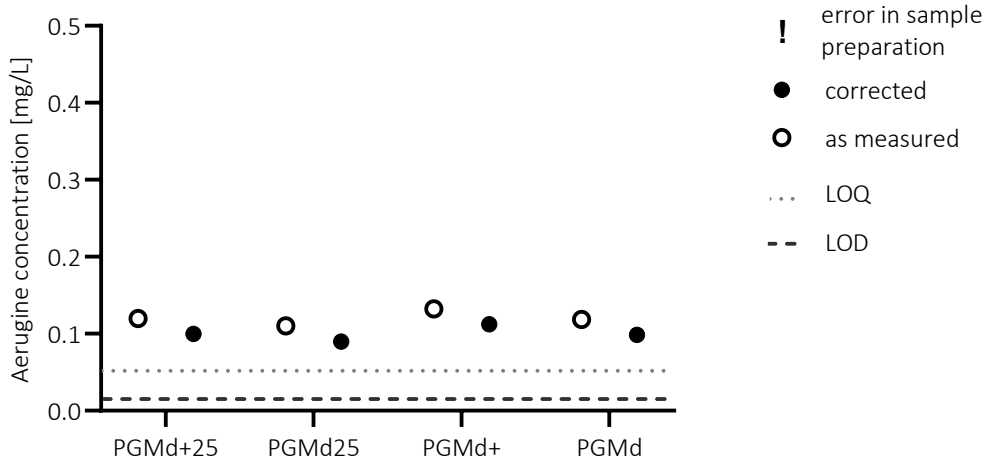

Figure 3-12 Screening for growth media inducing aerugine production in *K. pneumoniae*. (PGMd: PGM after 1 h deferration step with Chelex 100; +. feeding with 100 µM salicylic acid and 100 µM L-cysteine) (**!** Before extraction 0.02 mg/L aerugine were added, due to a mistake in sample preparation.) Aerugine concentration is shown "as measured" before, and as "corrected", after subtracting 0.02 mg/L from the detected concentration.

Figure **3-12** shows detection of aerugine in deferrated PGM. No obvious effect due to substrate feeding or decreased incubation temperature can be seen in the graph. The detected concentrations of at least 0.11 mg/L in each sample, are above the LOQ. Therefore, the accidentally added amount of 0.02 mg/L synthetic aerugine can be subtracted.

In ESI-MS coeluting matrix components can enhance or suppress ionization of analytes. According to the literature, it seems that strong ion enhancement of SSE > 150% is observed rarely and furthermore ion suppression seems to be more frequent.[97–100,108–110] Only certain analytes showed ion enhancement of >200%, if ammonium hydroxide was used as pH additive.[110] It seems not very probable that the aerugine signal above the LOQ is due to ion enhancement effects of the accidentally added 0.02 mg/L synthetic aerugine. For detection of the signal observed, this would mean the detected signal is five times higher due to matrix effects. If ion enhancement effects for ESI MS/MS experiments that are described in the literature are considered, ion enhancement at this level is not very probable. From this it can be

concluded that the detected signals are probably not due to ion enhancement. At the very least, it can be suggested to repeat this experiment and investigate whether *K. pneumoniae* produces aerugine when incubated in deferrated PGM at 37 °C within a time frame of 48 h.

Analysis of aerugine levels upon L-cysteine/salicylic acid feeding

Substrates for the biosynthetic pathway of aerugine production (see Introduction, Figure **1-2**) were added to the growth media. Production of aerugine upon feeding these substrates, namely salicylic acid and L-cysteine, was monitored during bacterial growth over time. *Y. enterocolitica* was cultured in PMH at 37 °C and aerugine concentration was measured after 6 and 24 h. Figure **3-13** shows data corresponding to measurements of three independent biological cultures and extraction of supernatants performed in triplicates. Due to a mistake in sample preparation a known amount of synthetic aerugine was added together with the internal standard and centrifugation during collecting supernatants of bacterial cultures was performed at varying speeds. Data from technical replicas showing a relative standard deviation above 30% were excluded.

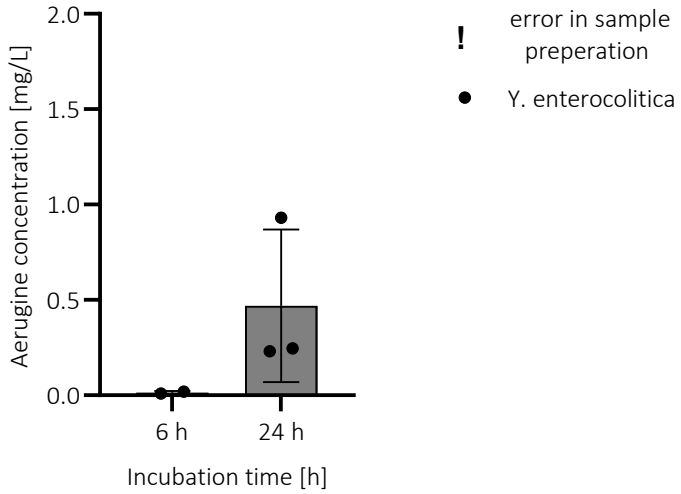

Figure 3-13 Aerugine production of Y. enterocolitica in PMH upon feeding salicylic acid and L-cysteine (100 µM each), after 6 h and 24 h of incubation time. Data represent mean ± standard deviation of three independent biological cultures. Extraction of the samples was performed in technical triplicates and using an internal standard as extraction control (**!** Before extraction 0.02 mg/L aerugine were added, due to a mistake in sample preparation. Therefore, 0.02 mg/L were subtracted from the measured concentrations, before transferring raw data to Graph Pad Prism.).

It can be observed that aerugine seems to be accumulating within a time frame of 24 h (Figure **3-13**). Although accumulation of aerugine can be observed within 24 h the whole experiment must be repeated. Due to the errors in sample preparation, these data are not reliable proof that

Y. enterocolitca produces aerugine. Further, it would be of interest to monitor aerugine production up to 48 h.

Analysis of aerugine levels upon Fe(III) addition

Production of aerugine by PAO1 and by *Y. enterocolitica* under increasing concentrations of iron from 0.1-100 µM $FeCl_3$ was measured. Figure **3-14** shows data corresponding to measurements of three independent biological cultures and extraction of supernatants performed in triplicates. Due to a mistake in sample preparation of one biological replicate for PAO1 and of all three biological replicates for *Y. enterocolitica*, a known amount of synthetic aerugine was added together with the internal standard and centrifugation during collecting supernatants of bacterial cultures was performed at varying speeds. Furthermore, some results were excluded as in some replicate's extraction was not successful at all (internal standard was not found), or the relative standard deviation of technical replicates was above 30%.

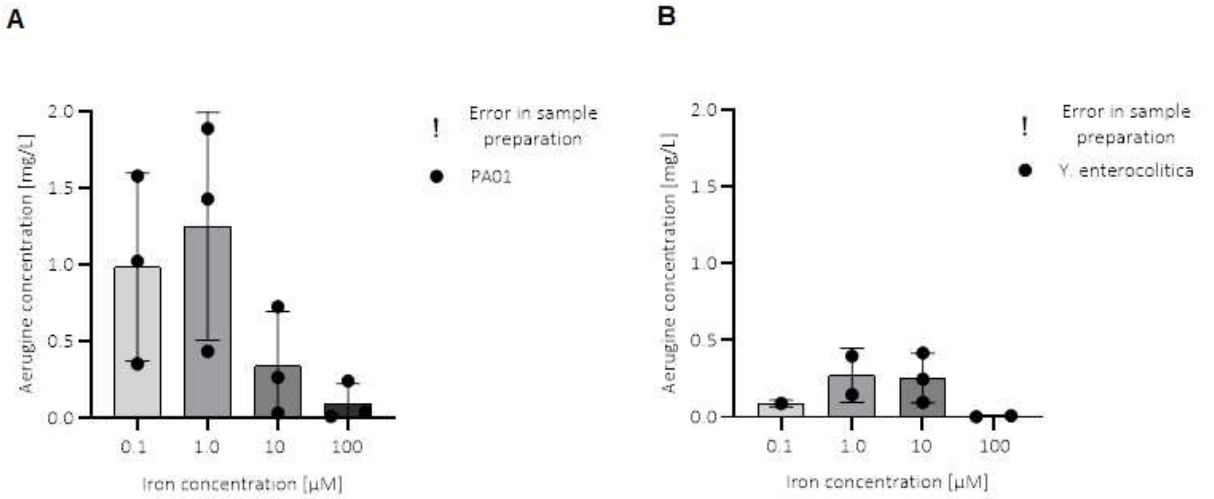

Figure 3-14: Aerugine production of PAO1 (A) and *Y. enterocolitica* (B) depending on increasing iron concentrations (0.1 µM; 1.0 µM; 10.0 µM; 100 µM $FeCl_3$). Incubation of PAO1 in M8 and *Y. enterocolitica* in PMH (including salicylic acid and L-cysteine, 100 µM each) at 37 °C for 24 h. A: Data represent mean ± standard deviation from three independent biological cultures for iron concentrations of 0.1-100 µM. Extraction of the samples was performed in technical triplicates and using an internal standard as extraction control (**!** Before extraction 0.02 mg/L aerugine was added to one biological replicate, due to a mistake in sample preparation. Therefore, 0.02 mg/L were subtracted from the measured concentrations of this replica, before transferring raw data to Graph Pad Prism.). Ordinary one-way ANOVA was performed. No statistically significant differences were identified. B: Data represent mean ± standard deviation from three independent biological subcultures. Extraction of the samples was performed in technical triplicates and using an internal standard as extraction control (**!** 0.02 mg/L aerugine was added, due to a mistake in sample preparation. Therefore, 0.02 mg/L were subtracted from the measured concentrations, before transferring raw data to Graph Pad Prism.):

Figure **3-14 A** shows detected aerugine concentrations at increasing iron concentrations in the growth medium after cultureing PAO1. The concentrations were 0.98 mg/L ± 0.62 mg/L at 0.1 µM $FeCl_3$, 1.25 mg/L ± 0.74 mg/L at 1.0 µM $FeCl_3$, 0.34 mg/L ± 0.36 mg/L at

10.0 µM $FeCl_3$ and 0.09 mg/L ± 0.12 mg/L at 100.0 µM $FeCl_3$ (corresponding to 4.69 µM ± 2.97 µM, 5.98 µM ± 3.54 µM, 1.63µM ± 1.72 µM and 0.43 µM ± 0.57 µM aerugine). Relative standard deviations lie between 60 and 130% and therefore, results should be handled with care. Ordinary one-way ANOVA did not show significant differences of aerugine production due to increasing concentrations of iron in the growth medium. As indicated in the figure, one sample underwent differences during sample preparation. As can be seen in more detail in the appendix, this biological replicate has much lower aerugine concentrations. Therefore, it is possible that high standard deviations and the lack of significance of the concentration differences is due to variations in the centrifugation step during cell pelleting. Therefore, it is strongly recommended to repeat at least this biological replicate to obtain reliable data from the experiment.

Figure **3-14 B** shows detected aerugine concentrations in *Y. enterocolitica* supernatant extracts of 0.25 ± 0.16 mg/L at 10.0 µM $FeCl_3$ (corresponding to 1.20 µM ± 0.77 µM aerugine) and signals after culturing at 100.0 µM $FeCl_3$ below the LOD. These findings must be handled with care as the data belong to samples that were affected by inequalities during sample preparation. Especially because of incompleteness of the data it is recommended to repeat the whole experiment to investigate whether aerugine production is inhibited at 100 µM $FeCl_3$.

3.5. Quantification of pyochelin in PAO1

Pyochelin is an important siderophore of *P. aeruginosa*. As with aerugine, neurotoxicity has been observed by the Leist group at the University of Konstanz, Germany. Therefore, its quantification would be of interest. Pyochelin production was monitored in parallel with the production of aerugine by PAO1. Figure **3-15** shows signals measured after incubation after 6 h and 24 h and at iron concentrations of 0.1-100 µM. Data corresponds to measurements of three independent subcultures and extraction of supernatants performed in triplicates.

A: **B:**

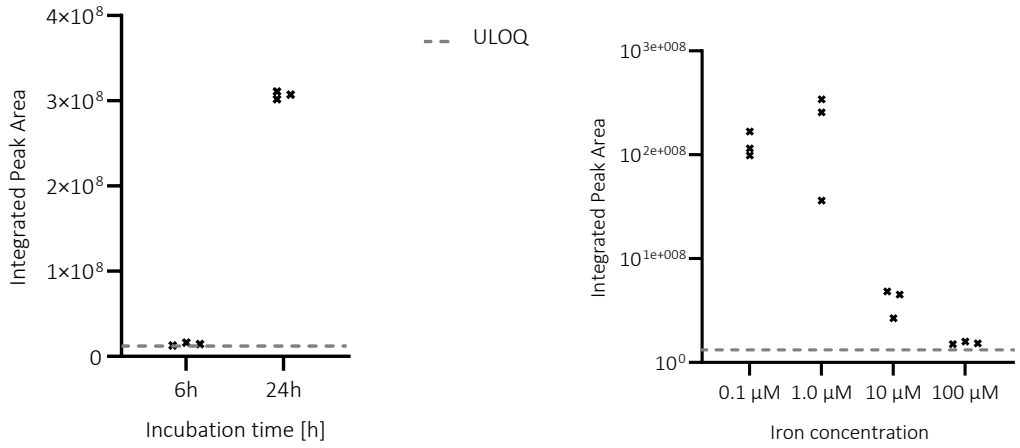

Figure 3-15 Detection of Pyochelin. Data represent means of technical triplicates from three independent biological subcultures. Upper limit of quantification (ULOQ) defined as the integrated peak area of the signal corresponding to 2 mg/mL pyochelin. A: Pyochelin production of PAO1 in M8 depending on incubation time. B: Pyochelin production of PAO1 in M8 with increasing iron concentrations.

Figure **3-15** shows that the pyochelin concentration in the samples exceeds the upper limit of quantification (ULOQ). For example, the detected pyochelin concentration after 6 h would be 2.39 mg/L ± 0.55 mg/L and after 24 mg/L ± 8.19 mg/L, which is clearly out of the calibrated range. Therefore, the Integrated Peak Area is plotted in the diagram instead of the concentration.

In consideration of this result, it is suggested that the concentration range of the calibration needs to be adjusted. Quantification via LC-MS/MS is usually performed in the range of 0.1-1 mg/L.[87] To suggest a suitable calibration range already existing LC-MS/MS methods should be considered. Periplasmic and cytoplasmic pyochelin has been detected after culturing *P. aeruginosa* mutant strains in iron deficient growth medium in concentrations up to 100 µM.[89] Due to the experimental set up in this publication, pyochelin-Fe complexes were added to the growth medium to investigate the bacterial ABC transporter system. Secreted pyochelin concentrations are expected to be smaller. Another publication presents an LC-MS/MS method for quantification of pyochelin in sputum samples of cystic fibrosis patients.[50] For detection as a biomarker only secreted pyochelin is measured. Calibration was performed in the range of 0.25-25 µM or 0.04-8.13 mg/L. Consequently, adjusting the calibration range to 0.04-8.00 mg/L should be considered for further experiments. If the calibrated area still does not include the detected signals that are shown for example in Figure **3-15**, the samples should be diluted before injection into the mass spectrometer. In this case, simultaneous quantification of aerugine and pyochelin would not be possible without additional sample preparation steps.

3.6. Synthesis of aerugine derivatives

The synthesis of aerugine derivatives for structure-activity relationship (SAR) studies was performed. Condensation reactions of L-cysteinol with various benzonitriles were carried out to obtain aerugine derivatives with changes in the phenyl group (Figure **3-16**). Theoretically, a large variety of compounds can be obtained in this simple way. Synthesis of compounds **8**, **9**, **10** and **12** (Table **3-2**) was performed to investigate the influence of the position and methylation of the hydroxyl group, which may be involved in important stabilizing hydrogen bonds. Compound **11** was synthesized to investigate whether halogen bonds play a role.

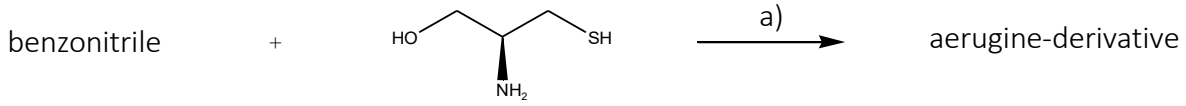

Figure 3-16 Synthesis of aerugine derivatives by condensation reaction of L-cysteinol to various benzonitriles. Conditions: a) 0.1 M phosphate buffer pH = 6.4, 72 h at 65 °C, sealed under N_2.

Table **3-2** shows the derivatives that were synthesized as part of this thesis.

Table 3-2 Aerugine derivatives. Yields correspond to amounts obtained after flash chromatography.

Structure	Compound	Yield
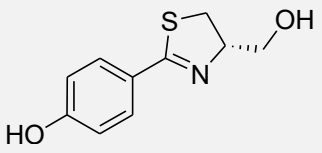	8	11%
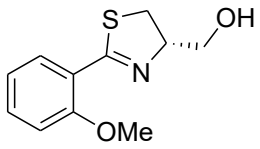	9	0%
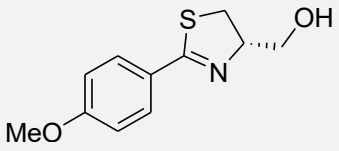	10	30%
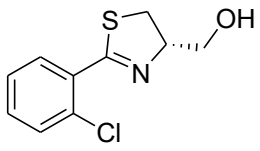	11	38%
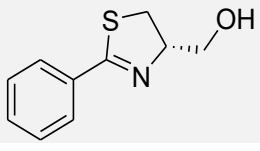	12	50%

Only the synthesis of compound **9** was not successful. It is very likely that this compound was lost during purification, as it was later successfully synthesized by Nathalie Wörz, PhD student in the Böttcher group. The methylation of the 2-hydroxyl group is of particular interest to determine whether this group is involved in important stabilizing hydrogen bonds that are crucial for bioactivity. In addition to investigating the influence of methylation of hydroxyl groups, the effect of different positions of hydroxyl groups is also frequently investigated in SAR studies.[111,112] The importance of the aliphatic hydroxyl group of aerugine has already been demonstrated by Ückert and co-workers.[1] The formation and influence of halogen bonds can also be investigated by introducing halogen atoms.[113–115] In this work, a chloro group (compound **11**) was introduced as one example. In conclusion, it can be stated that the synthesis of four aerugine derivatives was successful and it could be shown that this derivative library can be easily extended. The synthesized derivatives were sent to the Leist Group at the University of Konstanz for biological testing. The results were not yet available when this work was completed.

4. Conclusion and Outlook

This thesis work aimed at detection and quantification of the production of the neurotoxic metabolite aerugine in human pathogenic bacteria. To achieve this, an LC-MS/MS method enabling the detection and quantification of aerugine from liquid cultures was developed. This included the synthesis of an internal deuterated standard as extraction control. Another aim was to investigate whether aerugine is produced as its (*R*)- or (*S*)-enantiomer *via* chiral HPLC.

(*R*)-aerugine was synthesized via an already established stereospecific synthesis pathway for usage as reference material for LC-MS/MS method development. In addition, deuterated aerugine was synthesized as an internal standard for the use as extraction control. During this, in-house deuteration of salicylic amide was performed, based on prior work about the deuteration of arenes *via* H-D exchange.[2,3] The LC-MS/MS method for detection and quantification of aerugine from liquid cultures was established using *Pseudomonas aeruginosa*. Neurotoxic effects of aerugine have been observed at exposure of 3-4 µM.[1] By means of this successfully established quantification method, it could be shown that *P. aeruginosa* produces aerugine in a concentration of 6.43 ± 1:09 µM within 24 h. This finding can be emphasized with regard to the discovery of the effects of neurotoxic metabolites from human pathogenic bacteria on the development of neurodegenerative diseases such as Parkinson's disease. In the future would be of interest to monitor accumulation of aerugine within a time frame of up to 48 h and compare aerugine production in various growth media and upon feeding of salicylic acid or L-cysteine. Furthermore, it was shown that quantification of pyochelin in *P. aeruginosa* is dependent on the solvent that is used for redissolving samples before the measurement and that calibration in the 0.01-2.00 mg/L range is not suitable for quantification of pyochelin. It may be suggested to increase the calibration up to 8.00 mg/L.

A screening for culturing conditions to induce aerugine production in other human pathogenic bacteria was performed. By this the chemically defined minimal medium PMH, after feeding of salicylic acid and L-cysteine, was identified to possibly induce aerugine production in *Y. enterocolitica.*[4] Further measurements seemed to confirm this finding, but due to errors during sample preparation and incompleteness of data, it was not possible to fully proof aerugine production by *Y. enterocolitica.* Furthermore, the screening identified deferrated PGM to be an interesting growth medium for further investigations of aerugine production by *K. pneumoniae*. Due to unlucky circumstances resulting in downtime of the mass spectrometer and the limited time frame, further measurements could not be performed within the scope of this master thesis. Initial tests to inhibit aerugine production of *P. aeruginosa* and

Y. enterocolitica by adding increasing iron concentrations did not give statistically significant results. It is suggested to repeat these experiments in the future.

Followingly, it was not possible to investigate whether aerugine is produced as its (*R*)- or (*S*)-enantiomer by the human pathogenic bacteria that were investigated in this study. Therefore, it is only possible to suggest the chemically defined minimal medium PMH, after feeding of salicylic acid and L-cysteine and deferrated PGM for further investigation. If aerugine production of *Y. enterocolitica* and *K. pneumoniae* can be verified in the future, production as its (*R*)- or (*S*)-enantiomer should be investigated using these growth conditions.

Finally, four aerugine derivatives for SAR studies were synthesized successfully by condensation reaction of various benzonitriles and L-cysteine. It is suggested to further increase this derivative library in the future. The synthesized derivatives were sent to the Leist Group at the University of Konstanz for biological testing. The results were not yet available when this work was completed.

5. Experimentals

5.1. General

Chemicals and solvents were purchased from Sigma-Aldrich, Carl Roth, BLD pharmaceuticals or VWR Chemicals and were used as received.

Thin layer chromatography (TLC) was performed using technical grade solvents and Standard SIL G Silica Layers on Aluminum Sheets UV254 (Macherey-Nagel™, Alugram™) and detection by short/long wave UV-light and permanganate staining. Column chromatography was performed with Silica gel 60 (40 – 63 µm, Merck Millipore) and technical grade solvents.

NMR spectra were recorded on Bruker Avance-III 400 spectrometers with chemical shifts (δ) in ppm relative to residual solvent signals. Multiplicities are indicated by s – singlet, d - doublet, t - triplet, q - quartet, quint. - quintet, m – multiplet and coupling constant J is given in Hz. NMR data were analyzed with MestReNova version 6.0.2 - 5475.

LC-MS/MS analysis was performed on Vanquish™ Horizon/Flex UHPLC system (Thermo Fisher Scientific) in combination with TSQ® Series II Quantum (Thermo Fisher Scientific) using LC-MS grade solvents only. LC-MS/MS data were processed using Xcalibur Version 4.5. Statistical analysis and visualization of data was performed using a test version of Graph Pad Prism 10.2.0 (392).

Standards for LC-MS/MS and HPLC and synthesis products were sterile filtered using syringe sterile filters (0.2 µm, PTFE membrane, minispike outlet 25 mm, VWR), before injection. Filtrates were dried under a gentle stream of nitrogen and on the lyophilizer (alpha 2-4 lsc basic, CHRIST). HPLC was performed using Shimadzu HPLC system (LC-20AT pump, DGU-20A degassing unit, CBM-20A system controller, SPD-M20A detector).

Media and buffers were prepared using milliQ water (Purelab ultra, Elga) and sterilized by autoclaving (VX-120, SYSTEC) if not stated otherwise. If stated, pH was adjusted using diluted aqueous HCl or NaOH (SevenCompact, Mettler Toledo).

Bacterial liquid cultures were pelleted using Centrifuge 5430 R (Eppendorf). Supernatants of bacterial liquid cultures were sterile filtered using 1 mL syringes and sterile syringe-filters (0.2µm, Acrodisc™ syringe filter, wwPTFE, Minispike outlet, 13 mm).

5.2. Synthesis

5.2.1. General procedure A - stereospecific synthesis of aerugine and derivatives

The stereospecific synthesis of (*R*)-aerugine was carried out according to the procedure established by Dr. Felix Anderl, senior scientist of the Böttcher Group. The conditions of the reaction are shown in Figure **5-1**.

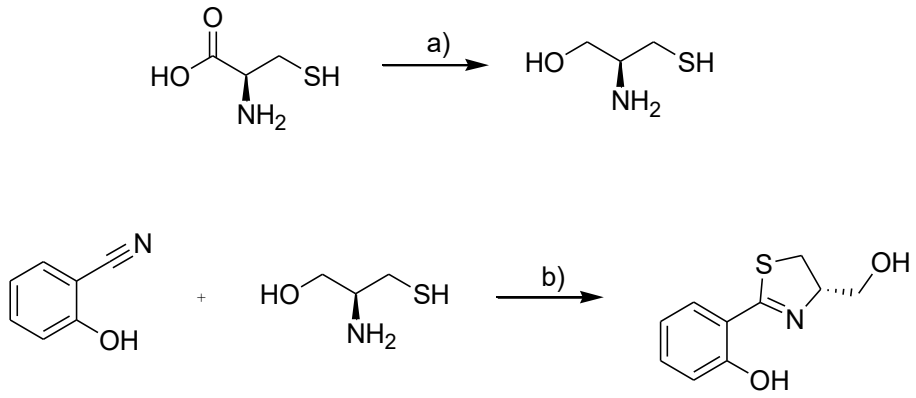

Figure 5-1: Reduction of L-cysteine to L-cysteinol and condensation of 2-hydroxybenzonitrile and L-cysteinol. Conditions: a) BH_3SMe_2, THF, 0 °C to rt, 16 h, sealed under N_2. b) 0.1 M phosphate buffer pH = 6.4, 16 h at 65 °C, sealed under N_2.

Borane dimethyl sulfide complex (6.0 eq) was added to a stirred suspension of L-cysteine (1.0 eq) in dry tetrahydrofuran (THF) (0.2 M) at 0°C. Reaction process was monitored by addition of MeOH (0.2 mL) to 0.1 mL of the reaction mixture, evaporation of solvents, and subsequent ^{1}H-NMR spectroscopy in D_2O. After 6 h, the ^{1}H-NMR spectrum showed full conversion of L-cysteine to L-cysteinol. The reaction mixture was slowly warmed to ambient temperature and MeOH (1.0 mL/eq) was carefully added. 2-hydroxybenzonitrile (0.7 eq) and aqueous KH_2PO_4/K_2HPO_4 buffer (pH 6.4, 0.1 M, 1.5 mL/eq) were added and the resulting mixture was heated to 65 °C. After 16 h, the reaction mixture was cooled to ambient temperature and extracted with dichloromethane (DCM) (3 x 4 mL). Combined organic layers were dried over Na_2SO_4 and concentrated under reduced pressure.

For synthesis of aerugine derivates L-cysteine (1.0 eq), borane dimethyl sulfide complex (3.6 eq), (THF) (1.1 M), MeOH (4.5 mL/eq), benzonitrile (0.5 - 1.1 eq) and aqueous KH_2PO_4/K_2HPO_4 buffer (pH 6.4, 0.1 M, 8.0 mL/eq) was used. The condensation reaction was performed for 72 h at 90 °C.

5.2.2. General procedure B - deuteration of arenes, aerugine and derivatives

The H-D exchange reaction was performed according to Sawama *et al.*[2] 10% platinum on activated char coil (Pt/C) (0.05 – 0.06 eq) was added to a stirred solution of the substrate (1.0 eq) in D_2O (1 mL/eq) and isopropanol (2-PrOH) (0.5 mL/eq). The reaction mixture was

stirred for 16 h at 90 °C, until ^{1}H-NMR spectroscopy indicated sufficient deuteration. Pt/C was removed from the reaction mixture through filtration (Celite). Deviations from the general procedure are stated for each compound.

5.2.3. (*R*)-aerugine (Compound 1)

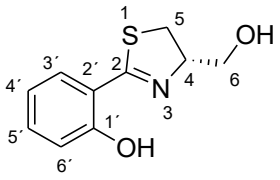

Figure 5-2 (*R*)-2-(4-(Hydroxymethyl)-4,5-dihydrothiazol-2-yl)phenol ((*R*)-aerugine, Compound **1**).

Reduction of L-cysteine followed by condensation reaction with 2-hydroxybenronitrile (20 mg, 0.16 mmol, 0.7 eq) was carried out according to general procedure A. Purification of the residue by column chromatography (SiO_2; PE/EA = 2:1) yielded (*R*)-aerugine (compound **1**) as a pale yellow solid (8.4 mg, 0.04 mmol, 25%).

1:

R_f: 0.4 (PE/EA=1:1).

^{1}H NMR (400 MHz, MeOD) δ 7.43 (dd, *J* = 8.5, 1.5 Hz, 1H, H3´), 7.38 – 7.32 (m, 1H, H-5´), 6.94 (d, *J* = 7.6 Hz, 1H, H-6´), 6.91 – 6.86 (m, 1H, H-4´), 4.84 – 4.79 (m, 4.2 Hz, 1H, H-4), 3.83 – 3.78 (m, 2H, H-6), 3.51 – 3.45 (m, 1H, H-5a), 3.33 (d, *J* = 3.0 Hz, 1H, H5b).

^{13}C NMR (101 MHz, MeOD) δ 173.58 (C2), 160.19 (C1´), 134.06 (C5´), 131.60 (C3´), 119.95 (C6´), 117.81 (C4´), 79.51 (C4), 64.25 (C6), 33.71 (C5).

5.2.4. Deuteration of salicylic acid (Compound 2-d)

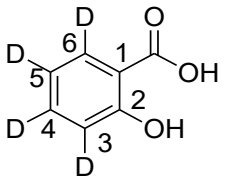

Figure 5-3 Salicylic acid-d_4 (Compound **2-d**)

The H-D exchange reaction of salicylic acid (35 mg, 0.25 mmol, 1.0 eq) was performed according to general procedure B. In this case, the reaction was performed at ambient temperature before heating to 90 °C. After 23 h a ^{1}H-NMR spectrum was recorded indicating slow proceeding of the reaction. The reaction mixture was stirred for another 16 h at 90 °C, until ^{1}H-NMR spectroscopy indicated sufficient deuteration. The mixture was dried under reduced pressure yielding pure compound **2-d** (15 mg, 0.11 mmol, 42%) as an off-white solid.

2-d:

^{1}H NMR (400 MHz, D_2O) δ 7.68 (m, 0.05H, H-6), 7.34 (t, 0.02H, H-4), 6.78 (m, 0.02H, H-3, H-5).

5.2.5. Deuteration of 2-hydroxybenzonitrile (Compound 3-d)

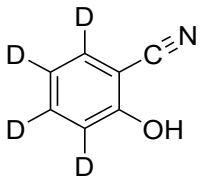

Figure 5-4 2-hydroxybenzonitrile (Compound **3-d**).

Deuteration of 2-hydroxybenzonitrile (12 mg, 0.10 mmol, 1.0 eq) was performed using Pt/C (0.05 eq), D_2O (1 mL/eq), 2-PrOH (0.5 mL/eq) according to general procedure B. Nitromethane (5.4 µL, 0.1 mmol, 1.0 eq) was added as an internal standard to the stirred reaction mixture. ^{1}H-NMR spectroscopy of the reaction did not show deuteration and the reaction mixture was discarded.

5.2.6. Deuteration of (*R*)-aerugine (Compound 1-d)

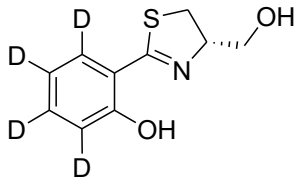

Figure 5-5 (*R*)-2-(4-(Hydroxymethyl)-4,5-dihydrothiazol-2-yl)phenol ((*R*)-aerugine, Compound **1-d**).

Deuteration was performed using (*R*)-aerugine (21 mg, 0.10 mmol, 1.0 eq), Pt/C (0.06 eq), D_2O (1 mL/eq), 2-PrOH (0.5 mL/eq) according to general procedure B. Nitromethane (5.4 µL, 0.1 mmol, 1.0 eq) was added as an internal standard to the stirred reaction mixture. ^{1}H-NMR spectroscopy of the reaction did not show deuteration and the reaction mixture was discarded.

5.2.7. Deuteration of (*R*)-2-(2'-hydroxyphenyl)-4-methoxycarbonyl-4,5-dihydrothiazole (Compound 4-d)

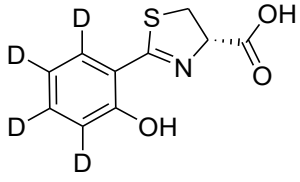

Figure 5-6 (*R*)-2-(2'-hydroxyphenyl)-4-methoxycarbonyl-4,5-dihydrothiazole (Compound **4-d**).

Deuteration was performed using (*R*)-2-(2'-hydroxyphenyl)-4-methoxycarbonyl-4,5-dihydrothiazole (27 mg, 0.12 mmol, 1.0 eq), Pt/C (0.06 eq), D_2O (1 mL/eq), 2-PrOH (0.5 mL/eq) according to general procedure B. Nitromethane (5.4 µL, 0.1 mmol, 1.0 eq) was

added as an internal standard to the stirred reaction mixture. ^{1}H-NMR spectroscopy of the reaction did not show deuteration and the reaction mixture was discarded.

5.2.8. Deuteration of (*R*)-dihydroaeruginoic acid (Compound 5-d)

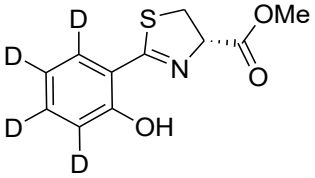

Figure 5-7 (*R*)-dihydroaeruginoic acid (Compound **5-d**).

Deuteration was performed using (*R*)-dihydroaeruginoic acid (22 mg, 0.09 mmol, 1.0 eq), Pt/C (0.06 eq), D_2O (1 mL/eq), 2-PrOH (0.5 mL/eq) according to general procedure B. Nitromethane (5.4 µL, 0.1 mmol, 1.0 eq) was added as an internal standard to the stirred reaction mixture. ^{1}H-NMR spectroscopy of the reaction did not show deuteration and the reaction mixture was discarded.

5.2.9. Deuteration of salicylic amide (Compound 6-d)

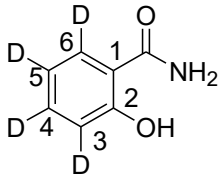

Figure 5-8 Salicylic amide-d_4 (Compound **6-d**)

Deuteration of salicylic amide (279 mg, 2 mmol, 1.0 eq) was performed according to general procedure B using Pt/C (0.06 eq), D_2O (8 mL/eq) and 2-PrOH (4 mL/eq) and yielding the product as orange solid (184 mg, 1.3 mmol, 64%).

6-d:

^{1}H NMR (400 MHz, D_2O) δ 7.71 – 7.55 (m, 0.19H, H-6), 7.31 – 7.25 (m, 0.22H, H-4), 6.83 – 6.73 (m, 0.15 H, H-3, H-5).

5.2.10. Salicylic acid methyl ester (Compound 7)

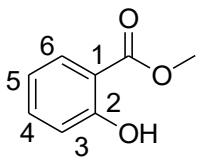

Figure 5-9: Salicylic acid methyl ester; Methyl 2-hydroxybenzoate (Compound **7**).

Acetyl chloride (2 mL, 28 mmol, 2.8 eq) was added to MeOH (100 mL), and the resulting mixture was stirred at ambient temperature for 15 min. Then, salicylic acid (1.38 g, 10 mmol, 1.0 eq) was added, and the resulting mixture was heated to reflux. After 16 h, the reaction mixture was cooled to ambient temperature and concentrated under reduced pressure. The product was dissolved in DCM (2 mL) and purification of the residue by column chromatography (SiO_2; PE/EA = 4:1) yielded the product as pale-yellow oil (1.45 g, 9.54 mmol, 95%) with the characteristic smell of wintergreen.

7:

R_f: 0.8 (PE/EA = 2:1).

^{1}H NMR (400 MHz, MeOD) δ 7.84 – 7.78 (m, 1H, H-6), 7.51 – 7.42 (m, 1H, H-4), 6.90 – 6.80 (m, 2H, H-3, H-5).

5.2.11. Salicylic amide (Compound 6)

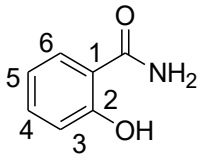

Figure 5-10: Salicylic amide; 2-hydroxybenzamide (Compound **6**).

Salicylic acid methyl ester **7** (120 mg, 0.79 mmol, 1.0 eq) was transferred to a pressure vial and 7 M ammonia in MeOH (0.8 mL, 5.6 mmol, 7.1 eq) was added. The orange reaction mixture was stirred at 85 °C overnight. TLC (PE/EA = 2:1) of the clear yellow reaction mixture showed incomplete conversion to a more polar product. The reaction mixture was dried under reduced pressure yielding the product as orange solid (80 mg, 0.59 mmol, 74%) that was used without further purification.

6:

R_f: 0.3 (PE/EA = 2:1).

^{1}H NMR (400 MHz, $CDCl_3$) δ 7.37 (t, J = 7.8 Hz, 1H, H-4), 7.31 (d, J = 7.8 Hz, 1H, H-6), 6.93 (d, J = 9.2 Hz, 1H, H-3), 6.84 – 6.76 (m, 1H, H-5).

5.2.12. 2-hydroxybenzonitrile (Compound 3)

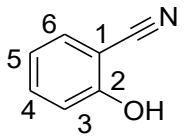

Figure 5-11: 2-hydroxybenzonitrile (Compound **3**).

The following reaction was adapted from the work of Einhorn *et al.*[104] Triphosgen (16 mg, 0.05 mmol, 0.33 eq) was added to a solution of salicylic amide (20 mg, 0.15 mmol, 1.0 eq) in anhydrous pyridine (0.25 mL) under nitrogen at 0 °C. The reaction was diluted with diethyl ether and washed with H_2O (10 mL), 2 M aqueous HCl (10 mL), and H_2O (10 mL). The organic layer was dried over Na_2SO_4, filtrated, and concentrated under reduced pressure. Purification by column chromatography (SiO_2; PE/EA = 3:1 to 1:1) yielded 2-hydroxybenzonitrile as a pure off-white solid (7.1 mg, 0.060 mmol, 41%).

3:

R_f: 0.5 (PE/EA=1:1).

^{1}H NMR (400 MHz, $CDCl_3$) δ 7.57 – 7.47 (m, 2H, H-4, H-6), 7.06 – 6.97 (m, 2H, H-3, H-5).

5.2.13. 2-hydroxybenzonitrile-d$_4$ (Compound 3-d)

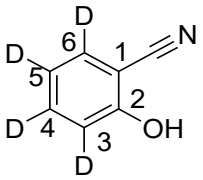

Figure 5-12: 2-hydroxybenzonitrile-d$_4$ (Compound **3-d**).

The dehydration reaction using Burgess reagent was based on the work of Claremon *et al.*[106] 1-Methoxy-*N*-triethylammoniosulfonyl-methanimidate (Burgess reagent) (343 mg, 1.44 mmol, 1.1 eq) provided by Dr. Felix Anderl, senior scientist of the Böttcher Group, was added to deuterated salicylic amide (184 mg, 1.3 mmol, 1.0 eq) under nitrogen. Dry THF (4.8 mL) was added, and the reaction mixture was stirred at ambient temperature. After 1 h, TLC (n-hexane/EA = 1:1) showed incomplete conversion to 2-hydroxybenzonitrilie and therefore, Burgess reagent (147 mg, 0.62 mmol, 0.48 eq) was added to the reaction mixture again. After 1.5 h, TLC (n-hexane/EA = 1:1) showed full conversion to a less polar product. Purification of the product by column chromatography (SiO_2; PE/EA = 3:1 to 1:1) yielded 2-hydroxybenzonitrile as off-white solid (0.68 mmol, 84 mg, 52%) that was used for condensation reaction to L-cysteinol.

3-d:

R_f: 0.6 (n-hexane/EA=1:1).

^{1}H NMR (600 MHz, $CDCl_3$) δ 7.54 – 7.50 (m, 0.3H, H-4), 7.56 – 7.43 (m, 0.1H, H-6), 7.01 – 6.99 (m, 0.19H, H-3, H-5), 6.13 (s, 1H, -OH).

^{13}C NMR (151 MHz, $CDCl_3$) δ 158.19 (C2), 134.26 (C4), 132.33 (C6), 120.63 (C5), 116.36 (C3), 116.05 (-CN), 99.46 (C1).

5.2.14. (*R*)-aerugine-d4 (Compound 1-d)

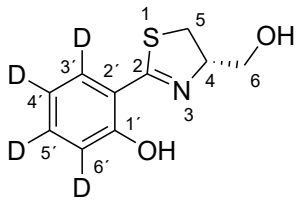

Figure 5-13 (*R*)-aerugine-d_4; 2-[4-(hydroxymethyl)-4,5-dihydro-1,3-thiazol-2-yl]phenol-d4 (Compound **1-d**).

Reduction of L-cysteine followed by condensation reaction with 2-hydroxybenronitrile-d_4 (41 mg, 0.33 mmol, 0.7 eq) was carried out according to general procedure A. Purification of the residue was performed by column chromatography (SiO_2; PE/EA = 2:1) and extraction of fat impurities with acetonitrile (ACN) (3 mL) and n-hexane (3 x 3 mL). The organic layer was dried under reduced pressure yielding (*R*)-aerugine-d_4 (compound **1-d**) as a pale yellow solid (8.7 mg, 0.04 mmol, 12%).

1-d:

R_f: 0.4 (PE/EA=1:1).

^{1}H NMR (600 MHz, MeOD) δ 7.45 – 7.42 (m, 0.29H, H-5´), 7.36 (s, 0.10H, H-3´), 6.95 – 6.92 (m, 0.10H, H-6´), 6.89 (t, *J* = 3.8 Hz, 0.11H, H-4´), 4.85 – 4.80 (m, 1H, H-4), 3.83 – 3.77 (m, 2H, H-6), 3.52 – 3.46 (m, 1H, H-5a), 3.36 – 3.32 (m, 1H, H-5b).

^{13}C NMR (151 MHz, MeOD) δ 173.90 (C2), 160.15 (C1´), 134.01 (C5´), 131.54 (C3´), 119.77 (C6´), 117.70 (C2´), 117.45 (C4´), 79.24 (C4), 64.19 (C6), 33.65 (C5).

Analytical HPLC was performed to control purity of the internal standard. For analytical HPLC, 20 µL of sterile filtered aerugine-d_4 in MeOH (1 mg/100 µL) were injected. Analytical HPLC of aerugine-d4 was performed using a C-18 Reprospher LC column (250 x 10 mm, 5 µm, Dr. Maish Gmbh). LC-method with solvent A = H_2O + 0.1% FA; B = MeOH + 0.1% FA: T_{0min} B = 50%; T_{5min} B = 50%; T_{20min} B = 90%; T_{30min} B = 90%; T_{40min} B = 90%. The flow rate was 2 mL/min and detection was performed at 190, 254 and 355 nm.

5.2.15. 4-[4-(hydroxymethyl)-4,5-dihydro-1,3-thiazol-2-yl]phenol (Compound 8)

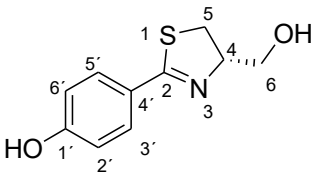

Figure 5-14: 4-[4-(hydroxymethyl)-4,5-dihydro-1,3-thiazol-2-yl]phenol **(**Compound **8**).

Reduction of L-cysteine followed by condensation reaction with 4-hydroxybenzonitrile (107 mg, 1.0 mmol, 1.0 eq) was carried out according to general procedure A. Purification of the residue was performed by column chromatography (SiO_2; PE/EA = 1:1) yielding the product as a pale yellow solid (21 mg, 0.10 mmol, 11%)**.** 21 mg of the product were injected for preparative HPLC using a C-18 Reprospher LC column (250 x 10 mm, 5 µm, Dr. Maish Gmbh). LC-method with solvent A = H_2O + 0.1% FA; B = MeOH + 0.1% FA: T_{0min} B = 50%; T_{40min} B = 50%; T_{50min} B = 90%; T_{60min} B = 90%. The flow rate was 2 mL/min, and detection was performed at 190, 254 and 355 nm. Fraction 12.5-15.0 min was collected and dried under reduced pressure yielding 20 mg. The compound was further purified by Nathalie Wörz, PhD student of the Böttcher group.

8:

R_f: 0.2 (PE/EA=1:1).

^{1}H NMR (700 MHz, MeOD) δ 7.71 – 7.66 (m, 2H, H-3´, H-5´), 6.85 – 6.81 (m, 2H, H-2´, H-6´), 4.74 – 4.68 (m, 1H, H-4), 3.82 (m, 1H, H-6a), 3.74 – 3.69 (m, 1H, H-6b), 3.52 – 3.47 (m, 1H, H-5a), 3.40 – 3.36 (m, 1H, H-5b).

^{13}C NMR (176 MHz, MeOD) δ 171.56 (C2), 162.11 (C1´), 131.43 (C3´), 131.25 (C5´), 125.66 (C4´), 116.27 (C2´, C6´), 80.00 (C4), 63.97 (C6), 35.30 (C5).

5.2.16. 2-[4-(hydroxymethyl)-4,5-dihydro-1,3-thiazol-2-yl]methoxybenzol (Compound 9)

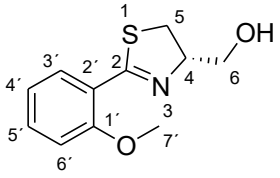

Figure 5-15: 2-[4-(hydroxymethyl)-4,5-dihydro-1,3-thiazol-2-yl]methoxybenzol (Compound **9**).

Reduction of L-cysteine followed by condensation reaction with 2-methoxybenzontrile (100 µL, 1.44 mmol, 1.1 eq) was carried out according to general procedure A. Purification of the solid product by column chromatography (SiO_2; PE/EA = 1:1) gave 199 mg of an impure yellow solid. Further purification by column chromatography did not result in isolation of the desired product. ^{1}H-NMR spectra of these compounds did not indicate that the desired product had formed and therefore, the fractions were discarded.

5.2.17. 4-[4-(hydroxymethyl)-4,5-dihydro-1,3-thiazol-2-yl]methoxybenzol (Compound 10)

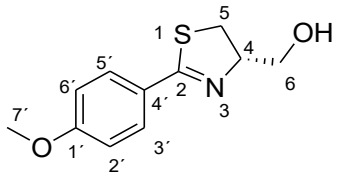

Figure 5-16: 4-[4-(hydroxymethyl)-4,5-dihydro-1,3-thiazol-2-yl]methoxybenzol (Compound **10)**.

Reduction of L-cysteine followed by condensation reaction with 4-methoxybenzonitrile (83 mg, 0.62 mmol, 0.49 eq) was carried out according to general procedure A. Purification of the residue was performed by column chromatography (SiO_2; PE/EA = 4:1 to 100% EA) yielding the product as a pale yellow solid (41 mg, 0.19 mmol, 30%). 41 mg of the product were injected for preparative HPLC using a C-18 Reprospher LC column (250 x 10 mm, 5 µm, Dr. Maish Gmbh). LC-method with solvent A = H_2O + 0.1% FA; B = MeOH + 0.1% FA: T_{0min} B = 50%; T_{5min} B = 50%; T_{20min} B = 90%; T_{30min} B = 90%; T_{40min} B = 90%. The flow rate was 2 mL/min and detection was performed at 190, 254 and 355 nm. Fraction 9.0-21.5 min was collected and dried under reduced pressure yielding 27 mg. The compound was further purified by Nathalie Wörz, Phd student of the Böttcher group.

10:

R_f: 0.2 (PE/EA=1:1).

^{1}H NMR (700 MHz, MeOD) δ 7.81 – 7.75 (m, 2H, H-3´, H-5´), 7.01 – 6.97 (m, 2H, H-2´, H-6´), 4.76 – 4.70 (m, 1H, H-4), 3.87 (s, 3H, H-7´), 3.85 – 3.81 (m, 1H, H-6a), 3.77 – 3.71 (m, 1H, H-6b), 3.55 – 3.49 (m, 1H, H-5a), 3.43 – 3.37 (m, 1H, H-5b).

^{13}C NMR (176 MHz, MeOD) δ 171.20 (C2), 163.92 (C1´), 131.20 (C5´), 131.10 (C3´), 126.87 (C4´), 114.92 (C2´), 114.68 (C6´), 80.15 (C4), 64.00 (C6), 55.94 (C7´), 35.39 (C5).

5.2.18. 2-[4-(hydroxymethyl)-4,5-dihydro-1,3-thiazol-2-yl]chlorophenol (Compound 11)

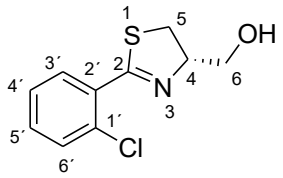

Figure 5-17: 2-[4-(hydroxymethyl)-4,5-dihydro-1,3-thiazol-2-yl]chlorophenol (Compound **11**).

Reduction of L-cysteine followed by condensation reaction with 2-chlorobenzonitrile (80 mg, 0.58 mmol, 0.46 eq) was carried out according to general procedure A. Purification of the residue was performed by column chromatography (SiO_2; PE/EA = 9:1 to 100% EA) yielding the product as pale yellow solid (51 mg, 0.22 mmol, 38%). 50 mg of the product were injected for preparative HPLC using a C-18 Reprospher LC column (250 x 10 mm, 5 µm, Dr. Maish Gmbh). LC-method with solvent A = H_2O + 0.1% FA; B = MeOH + 0.1% FA: T_{0min} B = 50%; T_{5min} B = 50%; T_{20min} B = 90%; T_{30min} B = 90%; T_{40min} B = 90%. The flow rate was 2 mL/min and detection was performed at 190, 254 and 355 nm. Fraction 13.0-22.0 min was collected and dried under reduced pressure yielding 26 mg. The compound was further purified by Nathalie Wörz, Phd student of the Böttcher group.

11:

R_f: 0.9 (PE/EE=1:2).

^{1}H NMR (700 MHz, MeOD) δ 7.60 – 7.58 (m, 1H, H-3´), 7.53 – 7.50 (m, 1H, H-6´), 7.48 – 7.44 (m, 1H, H-5´), 7.41 – 7.38 (m, 1H, H-4´), 4.82 – 4.78 (m, 1H, H-4), 3.86 (dd, *J* = 11.1, 4.6 Hz, 1H, H-6a), 3.81 – 3.75 (m, 1H, H-6b), 3.66 – 3.60 (m, 1H, H-5a), 3.55 – 3.50 (m, 1H, H-5b).

^{13}C NMR (176 MHz, MeOD) δ 170.08 (C2), 134.24 (C2´), 132.60 (C5´), 131.42 (C3´), 131.39 (C6´), 128.12 (C4´), 80.22 (C4), 63.62 (C6), 36.76 (C5).

5.2.19. [4-(hydroxymethyl)-4,5-dihydro-1,3-thiazol-2-yl]benzol (Compound 12)

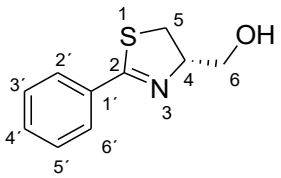

Figure 5-18: [4-(hydroxymethyl)-4,5-dihydro-1,3-thiazol-2-yl]benzol (Compound **12**).

Reduction of L-cysteine followed by condensation reaction with benzonitrile (80 µL, 80 mg, 0.78 mmol, 0.61 eq) was carried out according to general procedure A. Purification of the residue was performed by column chromatography (SiO_2; PE/EA = 1:1) yielding the product as pale yellow solid (75 mg, 0.39 mmol, 50%). 56 mg of compound **12** were injected for preparative HPLC using a C-18 Reprospher LC column (250 x 10 mm, 5 µm, Dr. Maish Gmbh). LC-method with solvent A = H_2O + 0.1% FA; B = MeOH + 0.1% FA: T_{0min} B = 50%; T_{5min} B = 50%; T_{20min} B = 90%; T_{30min} B = 90%; T_{40min} B = 90%. The flow rate was 2 mL/min and detection was performed at 190, 254 and 355 nm. Fraction 19.0-22.5 min was collected and dried under reduced pressure yielding 19 mg. The compound was further purified by Nathalie Wörz, Phd student of the Böttcher group.

12:

R_f: 0.2 (PE/EE=1:1).

^{1}H NMR (600 MHz, MeOD) δ 7.85 – 7.79 (m, 2H, H-2´, H-6´), 7.54 – 7.49 (m, 1H, H-4´), 7.48 – 7.41 (m, 2H, H-3´, H-5´), 4.79 – 4.74 (m, 1H, H-4), 3.86 – 3.81 (m, 1H, H-6a), 3.78 – 3.73 (m, 1H, H-6b), 3.57 – 3.51 (m, 1H, H-5a), 3.45 – 3.40 (m, 1H, H-5b).

^{13}C NMR (151 MHz, MeOD) δ 171.39 (C2), 134.07 (C1´), 132.36 (C4´), 129.46 (2C, C3´, C5´), 129.08 (2C, C2´, C6´), 80.14 (C4), 63.71 (C6), 35.12 (C5).

5.3. Biological experiments

5.3.1 Media and buffer compositions

Y. enterocolitica (DSM 4780), *K. pneumoniae* (DSM 30104) and PAO1 (DSM 22644) were cultured in Trypticase soy yeast medium (TSYM) (30 g/L CASO broth, 3 g/L yeast extract, pH = 7 - 7.2), lysogeny broth (LB) (20 g/L LB, pH = 7 - 7.2), minimal medium (M8) (1 mM $MgSO_4 \cdot 7\ H_2O$, 8.6 mM NaCl, 22 mM KH_2PO_4, 12 mM Na_2HPO_4, 0.2% D-glucose, 0.5% Casamino acids, pH = 7 - 7.2), minimal medium M9 (M9 salts (8.6 mM NaCl, 20 mM NH_4Cl, 22 mM KH_2PO_4, 12 mM Na_2HPO_4), 1 mM $MgSO_4$, 0.2% D-glucose) and peptone growth medium (PGM) (1 mM $MgSO_4$, 50 mM NaCl, 1 mM $CaCl_2$, 10 mM KH_2PO_4/K_2HPO_4 buffer [pH 6], 0.32% peptone). Directly before use, M9 was prepared from stock solutions that were autoclaved separately beforehand (5x M9 salts, 100x $MgSO_4$, 100x glucose). In some cases, M9 was substituted with 0.5% Casamino acids from a 200 g/L stock or 1 mM $CaCl_2$ from a 100x stock. KH_2PO_4/K_2HPO_4 buffer (pH 6) was added to PGM from a 1 M stock directly before use.

The defined minimal medium PMH was prepared according to Table **5-1** as a 2x concentrated stock, adapted from Staggs *et al*.[74] The components were dissolved in 750 mL milliQ water and pH was adjusted to 7.5. The medium was filled up to 1 L with millliQ water and deferrated while stirring with 4.14 g Chelex 100 resin (Bio-Rad) for 1 h. After the deferration step, Chelex 100 resin was filtered off and the medium was sterile filtered using vacuum filtration units (0.22 µm, BT 1000 PES Bottle Top Filters, Sartolab®). The defined minimal medium was not autoclaved. Aliquots of the 2x concentrated medium were diluted 1:1 with autoclaved milliQ water and $MgCl_2$ was added to a final concentration of 20 mM from a 2.0 M stock solution, directly before use.

Table 5-1: Composition of 1x PMH. (* $MgCl_2$ was added to 1x PMH directly before use from a 2 M stock to a final concentration of 20 mM; adapted from Staggs *et al.*[74]).

Component		mM (1x PMH)	mM (2x PMH stock)
HEPES		25.0	50.0
K_2HPO_4		2.5	5.0
$MgCl_2$	*	20.0	40.0
$Na_2S_2O_3$		2.5	5.0
NH_4Cl		10.0	20.0
Glucose		10.0	20.0
D, L-alanine		2.5	5.0
L-arginine hydrochloride		1.0	2.0
L-Asparagine		2.5	5.0
L-Aspartic acid		1.0	2.0
L-Glutamic acid		5.0	10.0
L-Glutamine		1.0	2.0
Glycine		5.0	10.0
L-Histidine		1.0	2.0
L-Isoleucine		1.0	2.0
L-Leucine		1.0	2.0
L-Lysine		1.0	2.0
L-Methionine		1.0	2.0
L-Phenylalanine		1.0	2.0
L-Proline		5.0	10.0
L-Serine		5.0	10.0
L-Threonine		2.5	5.0
L-Tryptophan		0.1	0.2
L-Tyrosine		1.0	2.0
L-Valine		1.0	2.0
D-Biotin		0.002	0.004
Calcium pantothenate		0.004	0.008
Thiamine hydrochloride		0.003	0.006

Solutions for addition of substrates to growth media and for the examination of the effect of different $FeCl_3$ concentrations were prepared as shown in Table **5-2**. Components were dissolved in 50 mL milliQ water and autoclaved.

Table 5-2: Preparation of substrate solutions.

Component	MW [g/mol]	final concentration [mM]
Salicylic acid	138.1	10
L-cysteine · HCl · H_2O	175.6	10
Iron (III)-chloride Hexahydrate	270.3	10

Furthermore, a 1.0 mM $FeCl_3$ solution was prepared by diluting 5 mL 10 mM $FeCl_3$ solution with 45 mL autoclaved milliQ water.

5.3.2 Preparation of cryo stocks

Cryo stocks (trypticase soy yeast extract medium [TSYM], 25% glycerol) of *Yersinia enterocolitica subsp. enterocolitica* DSM 4780 (*Y. enterocolitica*) and *Klebsiella pneumoniae subsp. pneumoniae* DSM 30104 (*K. pneumoniae*) and a cryo stock of *Pseudomonas aeruginosa* DSM 22644 (PAO1) (LB; 25% glycerol) were prepared and stored at -80 °C. PAO1 was derived from Shubham Joge, Phd. Student of the Böttcher group. *Y. enterocolitica* and *K. pneumoniae* were prepared from DSMZ glass ampoules according to the procedure that is described by the Leibniz-institute DSMZ, using TSYM as growth medium.[116]

5.3.3 Preparation of overnight cultures (ONCs) and subcultures

5 mL ONCs in LB medium were inoculated from cryo stocks and incubated at 37 °C overnight. 20 mL or 10 mL subcultures were inoculated with 200 µL or 100 µL ONC and incubated at 37 °C, unless otherwise indicated.

5.3.4 Extraction conditions

Supernatants were collected according to the procedure described in chapter **5.1** and extracted as described in chapter **5.4.1**.

5.3.4.1 Analysis of aerugine and pyochelin levels during bacterial growth

Aerugine production by PAO1 in minimal medium M8 was followed over time. The experiment was performed in biological triplicates derived from three independent ONCs, as shown in Table **5-3**. Extraction was performed in technical triplicates.

Table 5-3 Aerugine production by PAO1 over time.

Organism	Medium, incubation temperature	Incubation time [h]
PAO1	M8; 37 °C	6 h; 24 h
PAO1	M8; 37 °C	6 h; 24 h
PAO1	M8; 37 °C	6 h; 24 h

To find conditions for *K. pneumoniae* and *Y. enterocolitica* to produce aerugine, a screening for aerugine production in various growth media was performed in single biological and technical replicates. An overview of the examined conditions can be seen in Table **5-4** and Table **5-5**.

Time dependency of aerugine production by *Y. enterocolitica* was measured in parallel with the dependency on iron concentration in the growth medium (see Table **5-9**).

Table 5-4: Overview of conditions screened for aerugine production in *K. pneumoniae* and *Y. enterocolitica*.

Organism	Medium, incubation temperature	Incubation time
K. pneumoniae	M8; 37 °C	48 h
Y. enterocolitica	M8; 37 °C	48 h
PAO1	PGM; 37 °C	48 h
K. pneumoniae	PGM; 37 °C	48 h
Y. enterocolitica	PGM; 37 °C	48 h
PAO1	PMH; 37 °C	48 h
K. pneumoniae	PMH; 37 °C	48 h
Y. enterocolitica	PMH; 37 °C	48 h
K. pneumoniae	TSYM; 37 °C	48 h
Y. enterocolitica	TSYM; 37 °C	48 h
K. pneumoniae	Marine broth; 37 °C	48 h
Y. enterocolitica	Marine broth; 37 °C	48 h

5.3.4.2 Analysis of aerugine and pyochelin levels upon L-cysteine/salicylic acid feeding

To induce aerugine production in *K. pneumoniae* and *Y. enterocolitica*, M8 and PMH were substituted with salicylic acid and L-cysteine by adding 100 µL of 0.01 M stock solutions to 10 mL medium to obtain final concentrations of 100 µM each. Furthermore, $FeCl_3$ was added to a final concentration of 0.1 µM by adding 1 µL of a 1.0 mM stock to 10 mL medium. These experiments were performed in single biological and technical replicates. An overview is given in Table **5-5**.

Table 5-5: Inducing aerugine production by feeding salicylic acid and L-cysteine, incubation at 37 °C.

Organism	Medium	Incubation time
K. pneumoniae	M8 (100 µM salicylic acid; 100 µM L-cysteine)	24 h
Y. enterocolitica	M8 (100 µM salicylic acid; 100 µM L-cysteine)	24 h
K. pneumoniae	PMH (100 µM salicylic acid; 100 µM L-cysteine)	24 h
Y. enterocolitica	PMH (100 µM salicylic acid; 100 µM L-cysteine)	24 h
K. pneumoniae	PMH (100 µM salicylic acid; 100 µM L-cysteine; 0.1 µM $FeCl_3$)	24 h
Y. enterocolitica	PMH (100 µM salicylic acid; 100 µM L-cysteine; 0.1 µM $FeCl_3$)	24 h

Further screenings for aerugine production in *K. pneumoniae* were performed and are summarized in Table **5-6**. Media were substituted with salicylic acid and L-cysteine in 100 µM and 200 µM final concentrations each. 10 mL aliquots minimal medium M9 were further substituted with 250 µL Casamino acids (200 g/L) to a final concentration of 0.5% or 100 µL 100x $CaCl_2$ to obtain a final concentration of 1 mM $CaCl_2$.

Table 5-6: Substituting M9, PGM and TSYM to induce aerugine production in *K. pneumoniae*.

Organism	Medium, incubation temperature	Incubation time
K. pneumoniae	M9 (0.5% Casamino acids; 100 µM salicylic acid; 100 µM L-cysteine); 37 °C	24 h
K. pneumoniae	M9 (0.5% Casamino acids; 1 mM $CaCl_2$; 100 µM salicylic acid; 100 µM L-cysteine); 37 °C	24 h
K. pneumoniae	PGM (100 µM salicylic acid; 100 µM L-cysteine); 37 °C	24 h
K. pneumoniae	TSYM (100 µM salicylic acid; 100 µM L-cysteine); 37 °C	24 h
K. pneumoniae	M9 (0.5% Casamino acids; 200 µM salicylic acid; 200 µM L-cysteine); 37 °C	24 h
K. pneumoniae	M9 (0.5% Casamino acids; 1 mM $CaCl_2$; 200 µM salicylic acid; 200 µM L-cysteine); 37 °C	24 h
K. pneumoniae	PGM (200 µM salicylic acid; 200 µM L-cysteine); 37 °C	24 h
K. pneumoniae	TSYM (200 µM salicylic acid; 200 µM L-cysteine); 37 °C	24 h

Furthermore, *K. pneumoniae* was cultured in deferrated PGM, with and without adding salicylic acid and L-cysteine, and at 25 °C or 37 °C (Table **5-7**). Due to a mistake in sample preparation of one biological replicate, a known amount of synthetic aerugine was added together with the internal standard and centrifugation during collecting supernatants of bacterial cultures was performed at varying speeds.

Table 5-7 Incubation of *K. pneumoniae* in PGM, after 1 h deferration using Chelex 100 resin. (**!**) indicates mistake in sample preparation.

Organism	Medium, incubation temperature	Incubation time
***K. pneumoniae* (!)**	PGM (deferrated, 100 µM salicylic acid; 100 µM L-cysteine); 25 °C	24 h
***K. pneumoniae* (!)**	PGM (deferrated); 25 °C	24 h
***K. pneumoniae* (!)**	PGM (deferrated, 100 µM salicylic acid; 100 µM L-cysteine); 37 °C	24 h
***K. pneumoniae* (!)**	PGM (deferrated); 37 °C	24 h

5.3.4.3 Analysis of aerugine and pyochelin levels upon Fe(III) addition

The effects of substituting iron were examined by adding $FeCl_3$ in increasing concentrations to the growth medium. $FeCl_3$ was added to 10 mL aliquots of medium. Aerugine production by PAO1 in M8 and *Y. enterocolitica* in PMH (including salicylic acid and L-cysteine, 100 µM each) with 0.1 µM, 1.0 µM, 10.0 µM and 100.0 µM $FeCl_3$ was examined (Table **5-8**). Four or five subcultures with the four/five different $FeCl_3$ concentrations were inoculated from one ONC and considered as one biological replicate. Supernatants were collected after 24 h and extracted in three technical replicates.

Due to a mistake in sample preparation to some biological replicates, a known amount of synthetic aerugine was added together with the internal standard and centrifugation during collecting supernatants of bacterial cultures was performed at varying speeds.

Table 5-8: Effect of $FeCl_3$ concentration on aerugine production in PAO1. (**!**) indicates mistake in sample preparation.

Organism	ONC	$FeCl_3$ [µM]	Medium, incubation temperature	Incubation time [h]
PAO1	ONC1	0.1	M8; 37 °C	24 h
PAO1	ONC1	1.0	M8; 37 °C	24 h
PAO1	ONC1	10.0	M8; 37 °C	24 h
PAO1	ONC1	100.0	M8; 37 °C	24 h
PAO1	ONC2	0.1	M8; 37 °C	24 h
PAO1	ONC2	1.0	M8; 37 °C	24 h
PAO1	ONC2	10.0	M8; 37 °C	24 h
PAO1	ONC2	100.0	M8; 37 °C	24 h
PAO1 (!)	ONC3	0.1	M8; 37 °C	24 h
PAO1 (!)	ONC3	1.0	M8; 37 °C	24 h
PAO1 (!)	ONC3	10.0	M8; 37 °C	24 h
PAO1 (!)	ONC3	100.0	M8; 37 °C	24 h

Conditions for investigating aerugine production by *Y. enterocolitica* over time (6 h and 24 h) and upon increasing iron concentrations (0.0-100.0 µM) in the growth medium are shown in Table **5-9**.

Table 5-9 Effect of $FeCl_3$ concentration on aerugine production in *Y. enterocolitica*. (**!**) indicates mistake in sample preparation.

Organism	ONC	$FeCl_3$ [µM]	Medium, incubation temperature	Incubation time [h]
***Y. enterocolitica* (!)**	ONC1	0.0	PMH+SA/L-cys; 37 °C	6 h, 24 h
***Y. enterocolitica* (!)**	ONC1	0.1	PMH+SA/L-cys; 37 °C	24 h
***Y. enterocolitica* (!)**	ONC1	1.0	PMH+SA/L-cys; 37 °C	24 h
***Y. enterocolitica* (!)**	ONC1	10.0	PMH+SA/L-cys; 37 °C	24 h
***Y. enterocolitica* (!)**	ONC1	100.0	PMH+SA/L-cys; 37 °C	24 h
***Y. enterocolitica* (!)**	ONC2	0.0	PMH+SA/L-cys; 37 °C	6 h, 24 h
***Y. enterocolitica* (!)**	ONC2	0.1	PMH+SA/L-cys; 37 °C	24 h
***Y. enterocolitica* (!)**	ONC2	1.0	PMH+SA/L-cys; 37 °C	24 h
***Y. enterocolitica* (!)**	ONC2	10.0	PMH+SA/L-cys; 37 °C	24 h
***Y. enterocolitica* (!)**	ONC2	100.0	PMH+SA/L-cys; 37 °C	24 h
***Y. enterocolitica* (!)**	ONC3	0.0	PMH+SA/L-cys; 37 °C	6 h, 24 h
***Y. enterocolitica* (!)**	ONC3	0.1	PMH+SA/L-cys; 37 °C	24 h
***Y. enterocolitica* (!)**	ONC3	1.0	PMH+SA/L-cys; 37 °C	24 h
***Y. enterocolitica* (!)**	ONC3	10.0	PMH+SA/L-cys; 37 °C	24 h
***Y. enterocolitica* (!)**	ONC3	100.0	PMH+SA/L-cys; 37 °C	24 h

5.4 Analytical methods

5.4.1 General extraction procedure of secondary metabolites from bacterial liquid cultures

1 mL samples of 10 mL or 20 mL subcultures were taken at indicated timepoints and bacteria were pelleted by centrifugation (4500 rcf, 5 min). Supernatants were sterile filtered and then stored at -80 °C in 1 mL Eppendorf tubes. Prior to extraction of 300 µL aliquots with 300 µL HPLC grade EA in technical triplicates, samples were thawed and 3 µL of internal standard aerugine-d4 in MeOH (2 µg/mL) were added. Extraction was performed in MS vials with FEP membrane caps (REF 702732, FEP 1.0 mm, Macherey Nagel) by vortexing for 5 seconds. To improve phase separation, MS vials were centrifuged (41 rcf, 1 min) in MS racks. 100 µL aliquots of organic layer were pipetted into MS vials (LABSOLUTE, Art: No. 7663222) with 100 µL inlets (LABSOLUTE, Art: No. 7615290), dried under a gentle stream of nitrogen and stored at -80 °C. Directly before measurement, samples were redissolved in 100 µL of indicated solvent (50% MeOH in H_2O or 100% MeOH).

5.4.2 Calibration curves for quantification

For calibration, a dilution series of aerugine (2.00 mg/L, 1.00 mg/L, 0.50 mg/L, 0.25 mg/L, 0.05 mg/L, 0.01 mg/L) was prepared by serial dilution of 10 mg/L stocks in triplicates. Dilutions were prepared in 50% MeOH / H_2O and in 100% MeOH. Furthermore, a dilution series of pyochelin in 100% MeOH according to the same scheme was prepared.

Calibration was performed using the methods SRM-210-120 and SRM-325-190 (see chapters **5.4.4** and **5.4.5**) and subsequently, regression function and value of determination (R^2) were calculated using Xcalibur Version 4.5. For pyochelin, integration was performed for two peaks (pyochelin exists in an equilibrium of two diastereomers that are separated by chromatography) and therefore, two calibration curves were obtained. The signals of both retention times were added for each dilution to obtain a regression function for total pyochelin. Regression functions are shown in Table **5-10**.

Table 5-10: Regression function and value of determination (R^2)

Solvent	Regression function	R^2
Aerugine 50% MeOH	y = 4170 * x - 24776	0.9998
Aerugine 100% MeOH	y = 6129 * x - 3659	0.9995
Pyochelin I 100% MeOH	y = 4258 * x - 39516	0.9999
Pyochelin II 100% MeOH	Y = 1925 * x - 6636	0.9998
Pyochelin total 100% MeOH	y = 6183 * x - 46152	0.9999

LOD and limit of quantification (LOQ) were determined according to formula I and II after regression analysis using Excel Version 2312.

$$\text{LOD} \qquad \frac{3 * standard\ error}{slope} \qquad \text{(I)}$$

$$\text{LOQ} \qquad \frac{10 * standard\ error}{slope} \qquad \text{(II)}$$

Calculated LOD and LOQ values of synthetic aerugine in 50% MeOH / H_2O and 100% MeOH are shown in Table **5-11**.

Table 5-11: LOD and LOQ values of synthetic aerugine.

Solvent	LOD [mg/L]	LOQ [mg/L]
Aerugine 50% MeOH	0.023	0.076
Aerugine 100% MeOH	0.015	0.051
Pyochelin 100% MeOH	0.007	0.023

5.4.3 LC-MS/MS analysis

Ultra-high performance liquid chromatography (U-HPLC) was performed on a Vanquish™ UHPLC system (Thermo Fisher Scientific) equipped with a Nucleodur C18 Gravity-SB 150 x 2 mm, 3 µm column (Macherey-Nagel) and Nucleodur C18 Gravity-SB 4 x 2 mm, 3µm precolumn with the column heated to 40 °C. LC-method with 5 µL injection volume and solvent A = water + 0.1% FA; B = ACN + 0.1% FA: T_{0min} B = 20%; T_{10min} B = 100%; T_{12min} B = 100%; T_{13min} B = 20%; T_{15min} B = 20%. The flow rate was 0.5 mL/min and detection by MS/MS analysis was performed using TSQ® Series II Quantum (Thermo Fisher Scientific) mass spectrometer with heated electrospray ionization H-ESI (HESI-II probe, Thermo Scientific), Ion Source in positive mode, with ion spray voltage = 3500 V, vaporizer temperature = 300 °C, capillary temperature = 380 °C, sheath gas pressure = 60 psi, ion sweep gas pressure = 2 psi, and auxiliary gas = 10 psi. Fragmentation patterns were obtained *via* Product Ion Scan mode, with a fixed collision energy of 30 eV and a mass range of *m/z* = 75 - 350 for aerugine and aerugine-d_4 and a mass range of *m/z* = 90 – 400 for pyochelin.

5.4.4 Quantification of aerugine in bacterial cultures

To measure the concentration of aerugine in bacterial extracts, a Single Reaction Monitoring (SRM) mode tandem mass spectrometry method was developed. Fragmentation patterns were obtained by Product Ion Scan.

A Precursor Ion Scan of synthetic aerugine in 50 % MeOH / H_2O (1.0 mg/L) gave retention time (Rt) = 4.24 min for the *m/z* = 210 precursor. Subsequently, a fragment with *m/z* = 120 was identified *via* a Product Ion Scan and selected for development of a Single Reaction Mode (SRM) method. A Precursor Ion Scan of the deuterated internal standard aerugine-d_4 in MeOH (1 mg/L) gave Rt = 4.21 min for the *m/z* = 214 precursor and a fragment with *m/z* = 124 identified by a Product Ion Scan. Settings for SRM scan methods can be obtained in Table **5-12**.

Table 5-12: SRM methods for LC-MS/MS quantification of aerugine.

Compound	R_t	Precursor	Product ion	Method
Aerugine	4.24	*m/z* = 210	*m/z* = 120	SRM-210-120
Aerugine-d_4	4.21	*m/z* = 214	*m/z* = 124	SRM-214-124

5.4.5 Quantification of pyochelin in bacterial cultures

A Precursor Ion Scan and a Product Ion Scan was performed for pyochelin in MeOH (0.5 mg/L). Settings for SRM scan methods are shown in Table **5-13**.

Table 5-13 SRM method for LC-MS/MS quantification of pyochelin.

Compound	R_t	Precursor	Product ion	Method
Pyochelin I	5.34	m/z = 325	m/z = 190	SRM-325-190
Pyochelin II	5.78	m/z = 325	m/z = 190	SRM-325-190

Pyochelin was synthesized by Dr .Felix Anderl, senior scientist of the Böttcher Group, and his student Patrick Schimpl. The resulting four pyochelin diastereomers were separated by Dr. Gina Porras Brenes, postdoctoral researcher of the Böttcher group, by reversed phase chromatography. Pyochelin I and II are in a natural equilibrium and were used for calibration. Therefore, method SRM-325-190 gives signals at R_t = 5.34 and R_t = 5.78.

6. Literature

1. Ückert, A. K. *et al.* Identification of the bacterial metabolite aerugine as potential trigger of human dopaminergic neurodegeneration. *Environ Int* **180**, (2023).
2. Sawama, Y. *et al.* H-D Exchange Deuteration of Arenes at Room Temperature. *Org Process Res Dev* **23**, 648–653 (2019).
3. Ito, N. *et al.* Efficient and selective Pt/C-catalyzed H-D exchange reaction of aromatic rings. *Bull Chem Soc Jpn* **81**, 278–286 (2008).
4. Perry, R. D. & Brubaker, R. R. Accumulation of Iron by Yersiniae. *J Bacteriol* **137**, 1290–1298 (1979).
5. Margulis L. Symbiosis as a source of evolutionary innovation: speciation and morphogenesis. in *Symbiogenesis and Symbionticism* 1–14 (MIT Press, 1991).
6. Barraud, N. *et al.* Involvement of nitric oxide in biofilm dispersal of Pseudomonas aeruginosa. *J Bacteriol* **188**, 7344–7353 (2006).
7. Braniste, V. *et al.* The gut microbiota influences blood-brain barrier permeability in mice. *ScienceTranslationalMedicine* **6**, (2014).
8. Shishov, V. A., Kirovskaya, T. A., Kudrin, V. S. & Oleskin, A. V. Amine neuromediators, their precursors, and oxidation products in the culture of Escherichia coli k-12. *Appl Biochem Microbiol* **45**, 494–497 (2009).
9. Savchenko, V., Szamosvári, D., Bao, Y., Pignitter, M. & Böttcher, T. Biosynthetic flexibility of Pseudomonas aeruginosa leads to hydroxylated 2-alkylquinolones with proinflammatory host response. *Commun Chem* **6**, (2023).
10. Egland, K. A. & Greenberg, E. P. Quorum sensing in Vibrio fischeri: Elements of the luxl promoter. *Mol Microbiol* **31**, 1197–1204 (1999).
11. Atkinson, S., Chang, C. Y., Sockett, R. E., Cámara, M. & Williams, P. Quorum sensing in Yersinia enterocolitica controls swimming and swarming motility. *J Bacteriol* **188**, 1451–1461 (2006).
12. Inahashi, Y. *et al.* Watasemycin biosynthesis in Streptomyces venezuelae: thiazoline C-methylation by a type B radical-SAM methylase homologue. *Chem Sci* **8**, 2823–2831 (2017).
13. Meyer, J.-M. *et al.* Use of siderophores to type pseudomonads: the three Pseudornonas aeruginosa pyoverdine systems. *Microbiology (N Y)* **143**, 35–43 (1997).

14. Lawlor, M. S., O'Connor, C. & Miller, V. L. Yersiniabactin is a virulence factor for Klebsiella pneumoniae during pulmonary infection. *Infect Immun* **75**, 1463–1472 (2007).
15. Lloyd-Price, J. *et al.* Strains, functions and dynamics in the expanded Human Microbiome Project. *Nature* **550**, 61–66 (2017).
16. Sampson, T. R. *et al.* Gut Microbiota Regulate Motor Deficits and Neuroinflammation in a Model of Parkinson's Disease. *Cell* **167**, 1469–1480 (2016).
17. Villarán, R. F. *et al.* Ulcerative colitis exacerbates lipopolysaccharide-induced damage to the nigral dopaminergic system: Potential risk factor in Parkinson's disease. *J Neurochem* **114**, 1687–1700 (2010).
18. Scheperjans, F. *et al.* Gut microbiota are related to Parkinson's disease and clinical phenotype. *Movement Disorders* **30**, 350–358 (2015).
19. O'Donnell, M. P., Fox, B. W., Chao, P. H., Schroeder, F. C. & Sengupta, P. A neurotransmitter produced by gut bacteria modulates host sensory behaviour. *Nature* **583**, 415–420 (2020).
20. Marvel, F. A., Chen, C. C., Badr, N., Gaykema, R. P. A. & Goehler, L. E. Reversible inactivation of the dorsal vagal complex blocks lipopolysaccharide-induced social withdrawal and c-Fos expression in central autonomic nuclei. *Brain Behav Immun* **18**, 123–134 (2004).
21. Desbonnet, L. *et al.* Gut microbiota depletion from early adolescence in mice: Implications for brain and behaviour. *Brain Behav Immun* **48**, 165–173 (2015).
22. Sherwin, E., Sandhu, K. V., Dinan, T. G. & Cryan, J. F. May the Force Be With You: The Light and Dark Sides of the Microbiota–Gut–Brain Axis in Neuropsychiatry. *CNS Drugs* **30**, 1019–1041 (2016).
23. Marvel, F. A., Chen, C. C., Badr, N., Gaykema, R. P. A. & Goehler, L. E. Reversible inactivation of the dorsal vagal complex blocks lipopolysaccharide-induced social withdrawal and c-Fos expression in central autonomic nuclei. *Brain Behav Immun* **18**, 123–134 (2004).
24. Bravo, J. A. *et al.* Ingestion of Lactobacillus strain regulates emotional behavior and central GABA receptor expression in a mouse via the vagus nerve. *Proc Natl Acad Sci U S A* **108**, 16050–16055 (2011).
25. Vogt, N. M. *et al.* Gut microbiome alterations in Alzheimer's disease. *Sci Rep* **7**, (2017).

26. Yang, J. *et al.* Landscapes of bacterial and metabolic signatures and their interaction in major depressive disorders. *Sci. Adv* **6**, (2020).
27. Johnstone, T. C. & Nolan, E. M. Beyond iron: Non-classical biological functions of bacterial siderophores. *Dalton Transactions* vol. 44 6320–6339 Preprint at https://doi.org/10.1039/c4dt03559c (2015).
28. Cox, C. D. Deferration of Laboratory Media and Assays for Ferric and Ferrous Ions. in *Methods in Enzymology* vol. 235 315–329 (1994).
29. Baker, H. M., Anderson, B. F. & Baker, E. N. Dealing with iron: Common structural principles in proteins that transport iron and heme. *PNAS* **100**, 3579–3583 (2003).
30. Baker, H. M. & Baker, E. N. Lactoferrin and Iron: structural and dynamic aspects of binding and release. *BioMetals* **17**, 209–216 (2004).
31. Lazarovi, P. The structure and function of pardaxin. *Toxin Rev* **21**, 321–359 (2002).
32. Locht, C. & Antoine, R. The history of pertussis toxin. *Toxins* vol. 13 Preprint at https://doi.org/10.3390/toxins13090623 (2021).
33. W. E. Van Heyningen, S. V. H. C. A. K. The Nature and Action of Cholera Toxin. *Ciba Foundation Symposium 42 - Acute Diarrhoea in Childhood* **42**, (1976).
34. Popoff, M. R. & Bouvet, P. Clostridial toxins. *Future Microbiol* **4**, 1021–1064 (2009).
35. Lin, Z. *et al.* Pulicatins A-E, neuroactive thiazoline metabolites from cone snail-associated bacteria. *J Nat Prod* **73**, 1922–1926 (2010).
36. Watkins, A. L., Ray, A., Roberts, L. R., Caldwell, K. A. & Olson, J. B. The Prevalence and Distribution of Neurodegenerative Compound-Producing Soil Streptomyces spp. *Sci Rep* **6**, (2016).
37. Tangamornsuksan, W. *et al.* Paraquat exposure and Parkinson's disease: A systematic review and meta-analysis. *Arch Environ Occup Health* **74**, 225–238 (2019).
38. Jankovic, J. Pathophysiology and clinical assessment of parkinsonian symptoms and signs. *Handbook of Parkinson's Disease, Third Edition* 71–107 (2003) doi:10.1201/9780203912164.ch4.
39. Davie, C. A. A review of Parkinson's disease. *Br Med Bull* **86**, 109–127 (2008).

40. Maroteaux, L., Campanelli, J. T. & Scheller, R. H. Synuclein: A Neuron-Specific Protein Localized to the Nucleus and Presynaptic Nerve Terminal. *The Journal of Neuroscience* **8**, 2804–2815 (1988).
41. Polymeropoulos, M. H. *et al.* Mutation in the α-synuclein gene identified in families with Parkinson's disease. *Science (1979)* **276**, 2045–2047 (1997).
42. Singleton, A. B. *et al.* Synuclein Locus Triplication Causes Parkinson's Disease. *Science (1979)* **302**, (2003).
43. Okarmus, J. *et al.* Lysosomal perturbations in human dopaminergic neurons derived from induced pluripotent stem cells with PARK2 mutation. *Sci Rep* **10**, (2020).
44. Tohru Kitada. A hippocampal GluR5 kainate receptor regulating inhibitory synaptic transmission. *Nature* **392**, (1998).
45. Tanner, C. M. *et al.* Rotenone, paraquat, and Parkinson's disease. *Environ Health Perspect* **119**, 866–872 (2011).
46. Costello, S., Cockburn, M., Bronstein, J., Zhang, X. & Ritz, B. Parkinson's disease and residential exposure to maneb and paraquat from agricultural applications in the central valley of California. *Am J Epidemiol* **169**, 919–926 (2009).
47. Caldwell, K. A., Thies, J. L. & Caldwell, G. A. No country for old worms: A systematic review of the application of C. elegans to investigate a bacterial source of environmental neurotoxicity in parkinson's disease. *Metabolites* **8**, (2018).
48. Okamoto, T. *et al.* Structure of Aerugine from Pseudomonas aeruginosa. *Yunusov, Khim. Prir. Soedin* **104**, (1984).
49. Drechsel, H. *et al.* Structure Elucidation of Yersiniabactin, a Siderophore from Highly Virulent Yersinia Strains. *Liebigs Ann.* 1727–1733 (1995).
50. Cox, C. D., Rinehart, K. L., Mooret, M. L. & Cook, J. C. Pyochelin: Novel structure of an iron-chelating growth promoter for Pseudomonas aeruginosa. *Proc.Natl.Acad.Sci. USA* **78**, 4256–4260 (1981).
51. Sasaki, T., Igarashi, Y., Saitoa, N. & Furumai, T. Watasemycins A and B, New Antibiotics Produced by Streptomyces sp. TP-A0597. *Journal of Antibiotics* **55**, 249–255 (2002).
52. Reimer, J. M., Haque, A. S., Tarry, M. J. & Schmeing, T. M. Piecing together nonribosomal peptide synthesis. *Curr Opin Struct Biol* **49**, 104–113 (2018).

53. Gaille, C., Reimmann, C. & Haas, D. Isochorismate synthase (PchA), the first and rate-limiting enzyme in salicylate biosynthesis of Pseudomonas aeruginosa. *Journal of Biological Chemistry* **278**, 16893–16898 (2003).
54. Abe, K., Nomura, N. & Suzuki, S. Biofilms: Hot spots of horizontal gene transfer (HGT) in aquatic environments, with a focus on a new HGT mechanism. *FEMS Microbiol Ecol* **96**, (2021).
55. Jiang, X. *et al.* Dissemination of antibiotic resistance genes from antibiotic producers to pathogens. *Nat Commun* **8**, (2017).
56. Handley, K., Bonham, K. S., Wolfe, B. E. & Dutton, R. J. Extensive horizontal gene transfer in cheese-associated bacteria. *elifesciences* (2017).
57. Shepherdson, E. M. F. & Elliot, M. A. Cryptic specialized metabolites drive Streptomyces exploration and provide a competitive advantage during growth with other microbes. *PNAS* **119**, (2022).
58. Karp, A. & Snyder, J. C. In Vitro Effect of Aureomycin, Terramycin. and Chloramphenicol on Typhus Rickettsiae.'. *P.S.E.B.M.* **79**, 216–219 (1952).
59. Vaz Jauri, P., Bakker, M. G., Salomon, C. E. & Kinkel, L. L. Subinhibitory antibiotic concentrations mediate nutrient use and competition among soil streptomyces. *PLoS One* **8**, (2013).
60. Campana, S. *et al.* Molecular epidemiology of Pseudomonas aeruginosa, Burkholderia cepacia complex and methicillin-resistant Staphylococcus aureus in a cystic fibrosis center. *Journal of Cystic Fibrosis* **3**, 159–163 (2004).
61. Bottone, E. J. Yersinia enterocolitica: The Charisma Continues. *Clin Microbiol Rev* **10**, 257–276 (1997).
62. Saebo, A., Nylandf, H. & Lassens, J. Yersinia Enterocolitica Infection - An Unrecognized Cause of Acute and Chronic Neurological Diesease? A 10-Year Follow-up Study on 458 Hospitalized Patients. *Medical Hypothesis* **41**, 282–286 (1993).
63. Pelludat, C., Rakin, A., Jacobi, C. A., Schubert, S. & Heesemann, J. The Yersiniabactin Biosynthetic Gene Cluster of Yersinia enterocolitica: Organization and Siderophore-Dependent Regulation. *J Bacteriol* **180**, 538–546 (1998).
64. Chambers, C. E., Mcintyre, D. D., Mouckt, M. & Sokol, P. A. Physical and structural characterization of yersiniophore, a siderophore produced by clinical isolates of Yersinia enterocolitica. *BioMetals* **9**, 157–169 (1996).

65. Paczosa, M. K. & Mecsas, J. Klebsiella pneumoniae: Going on the Offense with a Strong Defense. *Microbiology and Molecular Biology Reviews* **80**, 629–661 (2016).
66. El Fertas-Aissani, R., Messai, Y., Alouache, S. & Bakour, R. Virulence profiles and antibiotic susceptibility patterns of Klebsiella pneumoniae strains isolated from different clinical specimens. *Pathologie Biologie* **61**, 209–216 (2013).
67. Yu, W. L. *et al.* Comparison of prevalence of virulence factors for Klebsiella pneumoniae liver abscesses between isolates with capsular K1/K2 and non-K1/K2 serotypes. *Diagn Microbiol Infect Dis* **62**, 1–6 (2008).
68. Balado, M. *et al.* The siderophore piscibactin is a relevant virulence factor for vibrio anguillarum favored at low temperatures. *Front Microbiol* **9**, (2018).
69. Chiadò, A., Varani, L., Bosco, F. & Marmo, L. Opening study on the development of a new biosensor for metal toxicity based on pseudomonas fluorescens pyoverdine. *Biosensors (Basel)* **3**, 385–399 (2013).
70. Meiwes, J., Fiedler, H.-P., Z~ihner, H., Konetschny-Rapp, S. & Jung, G. Production of desferrioxamine E and new analogues by directed fermentation and feeding fermentation. *Appl Microbiol Biotechnol* **32**, 505–510 (1990).
71. Virpiranta, H. *et al.* Isolation of efficient metal-binding bacteria from boreal peat soils and development of microbial biosorbents for improved nickel scavenging. *Water* **12**, (2020).
72. Konetschny-Rapp, S., Jung, G., Meiwes, J. & Zähner, H. Staphyloferrin A: a structurally new siderophore from staphylococci. *Eur J Biochem* **191**, 65–74 (1990).
73. Neidhardt, F. C., Bloch, P. L. & Smith1, D. F. Culture Medium for Enterobacteria. *J Bacteriol* **119**, 736–747 (1974).
74. Staggs, T. M. & Perry, R. D. Identification and Cloning of a fur Regulatory Gene in Yersinia pestist. *J Bacteriol* **173**, 417–425 (1991).
75. Gong, S., Bearden, S. W., Geoffroy, V. A., Fetherston, J. D. & Perry, R. D. Characterization of the Yersinia pestis Yfu ABC inorganic iron transport system. *Infect Immun* **69**, 2829–2837 (2001).
76. Miller, M. C. & DeMoll, E. Extraction, purification, and identification of yersiniabactin, the siderophore of Yersinia pestis. *Curr Protoc Microbiol* **5B.3.1–3.2**, (2011).

77. Podschun, R., Fischer, A. & Ullmann, U. Siderophore Production of Klebsiella Species Isolated from Different Sources. *Zentralblatt fur Bakteriologie* **276**, 481–486 (1992).
78. Russo, T. A. *et al.* An Assessment of Siderophore Production, Mucoviscosity, and Mouse Infection Models for Defining the Virulence Spectrum of Hypervirulent Klebsiella pneumoniae. *mSphere* **6**, (2021).
79. Bachman, M. A., Lenio, S., Schmidt, L., Oyler, J. E. & Weiser, J. N. Interaction of Lipocalin 2, Transferrin, and Siderophores Determines the Replicative Niche of Klebsiella pneumoniae during Pneumonia. *mBio* **3**, (2012).
80. Perry::, R. D. & Clemente, C. L. S. Siderophore Synthesis in Klebsiella pneumoniae and Shigella sonnei During Iron Deficiencyt. *J Bacteriol* **140**, 1129–1132 (1979).
81. Díaz-Cruz, M. S., López de Alda, M. J., López, R. & Barceló, D. Determination of estrogens and progestogens by mass spectrometric techniques (GC/MS, LC/MS and LC/MS/MS). *Journal of Mass Spectrometry* **38**, 917–923 (2003).
82. Ihling, C. *et al.* Mass Spectrometric Identification of SARS-CoV-2 Proteins from Gargle Solution Samples of COVID-19 Patients. *J Proteome Res* **19**, 4389–4392 (2020).
83. Frederiksen, H. *et al.* Sex-specific Estrogen Levels and Reference Intervals from Infancy to Late Adulthood Determined by LC-MS/MS. *Journal of Clinical Endocrinology and Metabolism* **105**, (2020).
84. Niessen, W. M. A. Fragmentation of toxicologically relevant drugs in positive-ion liquid chromatography-tandem mass spectrometry. *Mass Spectrometry Reviews* vol. 30 626–663 Preprint at https://doi.org/10.1002/mas.20332 (2011).
85. Niessen, W. M. A. Group-specific fragmentation of pesticides and related compounds in liquid chromatography-tandem mass spectrometry. *Journal of Chromatography* **1217**, 4061–4070 (2010).
86. Thomas, S. N., French, D., Jannetto, P. J., Rappold, B. A. & Clarke, W. A. Liquid chromatography–tandem mass spectrometry for clinical diagnostics. *Nature Reviews Methods Primers* **2**, (2022).
87. *Thermo Scientific TM Altis TM Triple-Stage Quadrupole Mass Spectrometer, Mass Spectrometer Operations Course*.

88. Ji, A. *et al.* A Novel and Sensitive LC/MS/MS Method for Quantitation of Pyochelin in Human Sputum Samples from Cystic Fibrosis Patients. *Biomark Appl* **3**, (2019).
89. Roche, B. *et al.* A role for PchHI as the ABC transporter in iron acquisition by the siderophore pyochelin in Pseudomonas aeruginosa. *Environ Microbiol* **24**, 866–877 (2022).
90. Garcie, C. *et al.* The Bacterial Stress-Responsive Hsp90 Chaperone (HtpG) Is Required for the Production of the Genotoxin Colibactin and the Siderophore Yersiniabactin in Escherichia coli. *Journal of Infectious Diseases* **214**, 916–924 (2016).
91. Bachman, M. A. *et al.* Klebsiella pneumoniae yersiniabactin promotes respiratory tract infection through evasion of lipocalin 2. *Infect Immun* **79**, 3309–3316 (2011).
92. Caza, M., Lépine, F. & Dozois, C. M. Secretion, but not overall synthesis, of catecholate siderophores contributes to virulence of extraintestinal pathogenic Escherichia coli. *Mol Microbiol* **80**, 266–282 (2011).
93. Szamosvári, D., Prothiwa, M., Dieterich, C. L. & Böttcher, T. Profiling structural diversity and activity of 2-alkyl-4(1H)-quinoloneN-oxides of Pseudomonas and Burkholderia. *Chemical Communications* **56**, 6328–6331 (2020).
94. Rai, V., Fisher, N., Duckworth, O. W. & Baars, O. Extraction and Detection of Structurally Diverse Siderophores in Soil. *Front Microbiol* **11**, (2020).
95. Boiteau, R. M. *et al.* Siderophore profiling of co-habitating soil bacteria by ultra-high resolution mass spectrometry. *Metallomics* **11**, 166–175 (2019).
96. Holmström, S. J. M. *et al.* Siderophores in forest soil solution. *Biogeochemistry* **71**, 247–258 (2004).
97. Van Eeckhaut, A., Lanckmans, K., Sarre, S., Smolders, I. & Michotte, Y. Validation of bioanalytical LC-MS/MS assays: Evaluation of matrix effects. *J Chromatogr B Analyt Technol Biomed Life Sci* **877**, 2198–2207 (2009).
98. Steiner, D., Krska, R., Malachová, A., Taschl, I. & Sulyok, M. Evaluation of Matrix Effects and Extraction Efficiencies of LC-MS/MS Methods as the Essential Part for Proper Validation of Multiclass Contaminants in Complex Feed. *J Agric Food Chem* **68**, 3868–3880 (2020).
99. Liang, H. R., Foltz, R. L., Meng, M. & Bennett, P. Ionization enhancement in atmospheric pressure chemical ionization and suppression in electrospray ionization between target drugs and stable-isotope-labeled internal standards in

quantitative liquid chromatography/tandem mass spectrometry. *Rapid Communications in Mass Spectrometry* **17**, 2815–2821 (2003).

100. George, R. *et al.* Enhancement and Suppression of Ionization in Drug Analysis Using HPLC-MS/MS in Support of Therapeutic Drug Monitoring: A Review of Current Knowledge of Its Minimization and Assessment. *Ther Drug Monit* **40**, (2018).
101. Tan, A., Boudreau, N. & Lévesque, A. Internal standards for quantitative LC-MS bioanalysis. *LC-MS in Drug Bioanalysis* 1–32 (2012).
102. Pirman, D. A., Reich, R. F., Kiss, A., Heeren, R. M. A. & Yost, R. A. Quantitative MALDI tandem mass spectrometric imaging of cocaine from brain tissue with a deuterated internal standard. *Anal Chem* **85**, 1081–1089 (2013).
103. Rodriguez, D. *et al.* Synthesis and characterization of tritylthioethanamine derivatives with potent KSP inhibitory activity. *Bioorg Med Chem* **19**, 5446–5453 (2011).
104. Einhorn, A. & Mettler, C. Über die Einwirkung von Phosgen und Pyridin auf Säureamide. *Berichte d. D. chem. Gesellschaft* 3647–3653 (1902).
105. lacamas Laboratories, Inc. . https://www.lacamaslabs.com/phosgene-chemistry/.
106. Claremonx, D. A. & Phillips, B. T. An Efficient Chemoselective Synthesis of Nitriles from primary Amides. *Tetrahedron Lett* **29**, 2155–2158 (1988).
107. Levsen, K. *et al.* Even-electron ions: A systematic study of the neutral species lost in the dissociation of quasi-molecular ions. *Journal of Mass Spectrometry* **42**, 1024–1044 (2007).
108. Sulyok, M., Stadler, D., Steiner, D. & Krska, R. Validation of an LC-MS/MS-based dilute-and-shoot approach for the quantification of > 500 mycotoxins and other secondary metabolites in food crops: challenges and solutions. *Anal Bioanal Chem* **412**, 2607–2620 (2020).
109. Ferrer Amate, C., Unterluggauer, H., Fischer, R. J., Fernández-Alba, A. R. & Masselter, S. Development and validation of a LC-MS/MS method for the simultaneous determination of aflatoxins, dyes and pesticides in spices. in *Analytical and Bioanalytical Chemistry* vol. 397 93–107 (2010).
110. Mallet, C. R., Lu, Z. & Mazzeo, J. R. A study of ion suppression effects in electrospray ionization from mobile phase additives and solid-phase extracts. *Rapid Communications in Mass Spectrometry* **18**, 49–58 (2004).

111. Pereira Ávilla, H., Fátima Albino Smania, E., Delle Monache, F. & Smania Júnior, A. Structure-activity relationship of antibacterial chalcones. *Bioorg Med Chem* **16**, 9790–9794 (2008).
112. Chen, J. *et al.* Structure-antioxidant activity relationship of methoxy, phenolic hydroxyl, and carboxylic acid groups of phenolic acids. *Sci Rep* **10**, (2020).
113. Elsocht, M. *et al.* Structure–activity relationship (SAR) study of spautin-1 to entail the discovery of novel nek4 inhibitors. *Int J Mol Sci* **22**, 1–40 (2021).
114. Politzer, P., Lane, P., Concha, M. C., Ma, Y. & Murray, J. S. An overview of halogen bonding. *Journal of Molecular Modeling* vol. 13 305–311 Preprint at https://doi.org/10.1007/s00894-006-0154-7 (2007).
115. Castagnolo, D. *et al.* Synthesis, biological evaluation and SAR study of novel pyrazole analogues as inhibitors of Mycobacterium tuberculosis. *Bioorg Med Chem* **16**, 8587–8591 (2008).
116. Leibniz-Institut DSMZ-Deutsche Sammlung von Mikroorganismen und Zellkulturen GmbH. Opening of Ampoules and Rehydration of Dried Cultures, Microsoft PowerPoint - InternetOpening_Oeffnen.pptx (dsmz.de), accessed at 25/01/2024.

7. Abbreviations

Δ	chemical shifts
ACN	acetonitrile
CAS	chrome azurol S
$CDCl_3$	deuterated chloroform
CNS	central nervous system
DCM	dichloromethane
D_2O	deuterium oxide
EA	ethyl acetate
FA	formic acid
H-ESI	heated electrospray ionization
HGT	horizontal gene transfer
H	hours
MeOD	deuterated methanol
MeOH	methanol
PA01	*Pseudomonas aeruginosa*
PE	petroleum ether
PD	Parkinson´s disease
PGM	peptone growth medium
Pt/C	platinum on activated char coil
2-PrOH	isopropanol
Rt	retention time
SAR	Structure Activity Relationship
THF	tetrahydrofuran
TLC	thin layer chromatography
TSYM	trypticase soy yeast extract medium
U-HPLC	ultra-high performance liquid chromatography
ULOQ	upper limit of quantification

8. Appendix

8.1 List of figures

8.2 List of tables

8.3 List of supplementary figures

8.4 List of supplementary tables

8.5 NMR-spectra

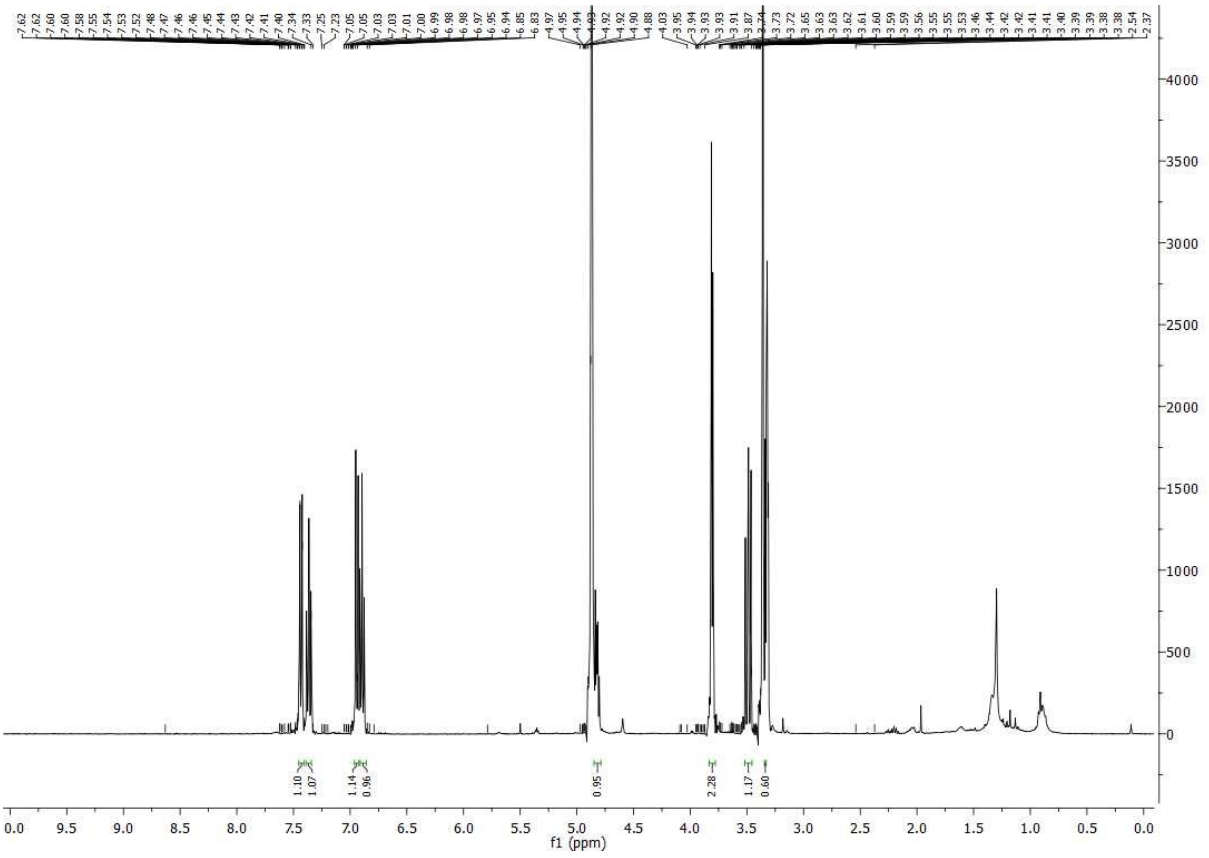

Supplementary Figure 1 ^{1}H-NMR of (R)-aerugine, compound **1**.

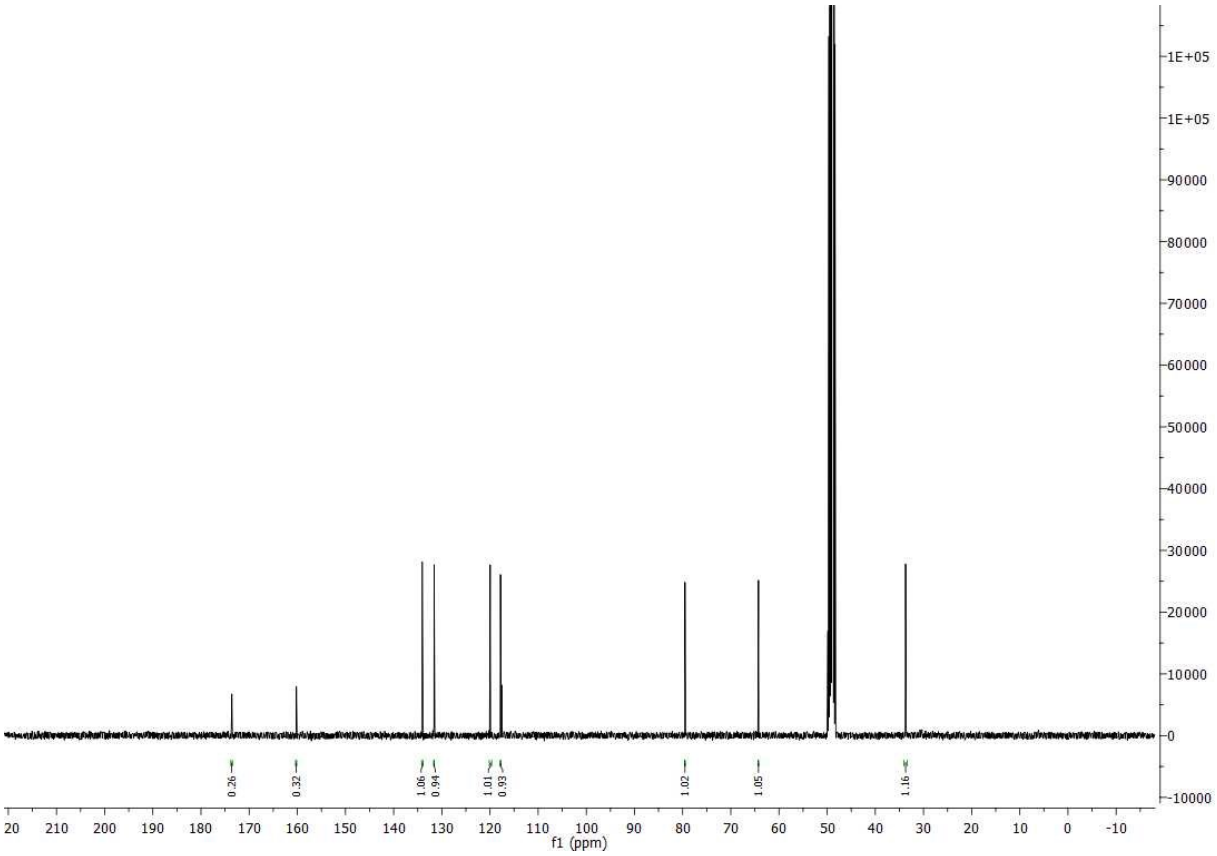

Supplementary Figure 2 ^{13}C-NMR of (R)-aerugine, Compound **1**.

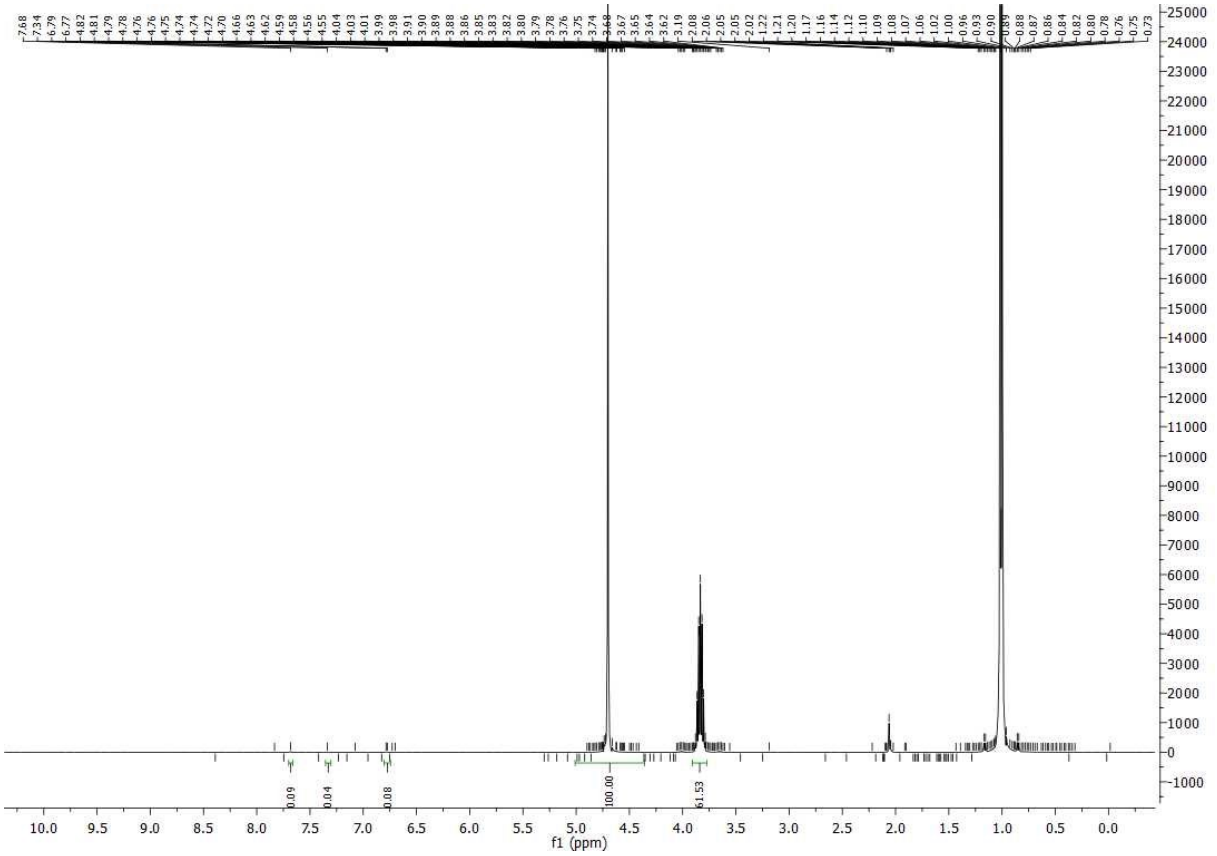

Supplementary Figure 3 ^{1}H-NMR of salicylic acid-d_4, compound **2-d**.

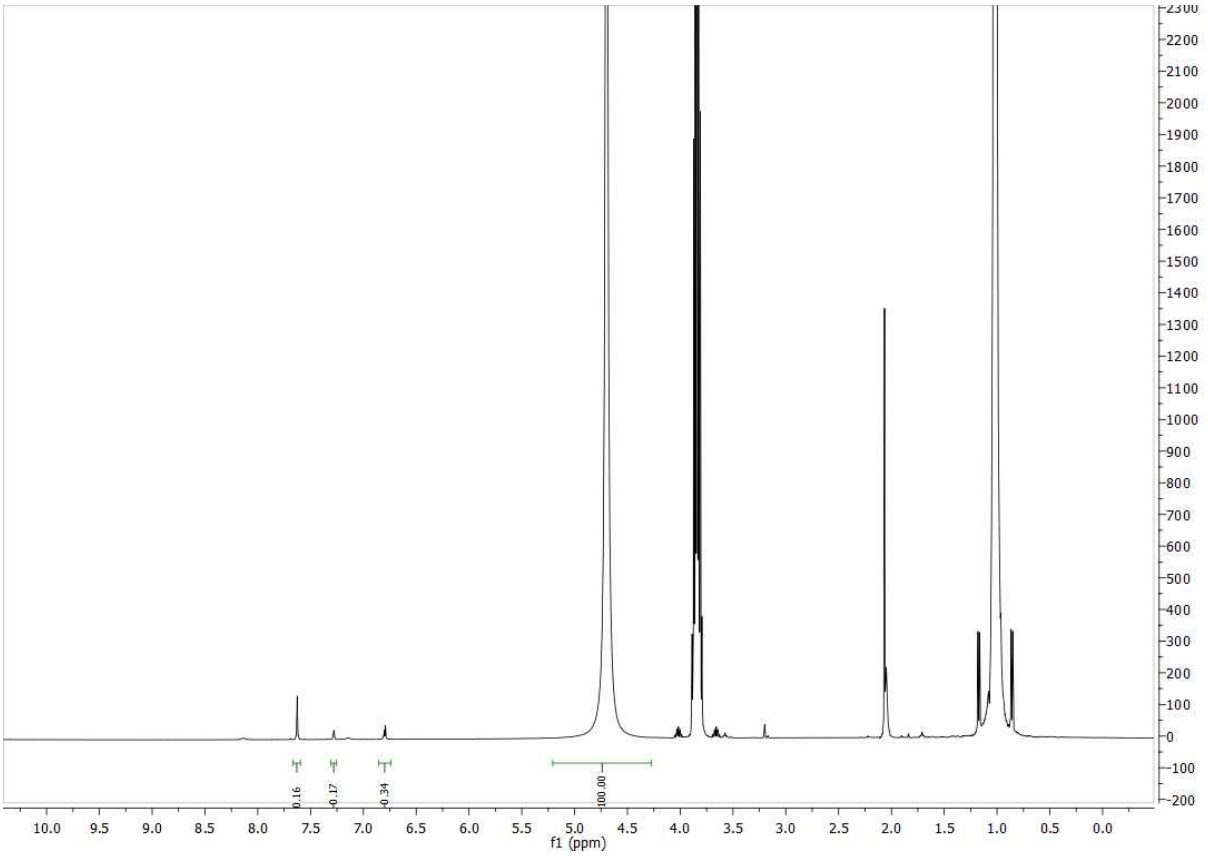

Supplementary Figure 4 ^{1}H-NMR of salicylic amide-d_4, compound **6-d**.

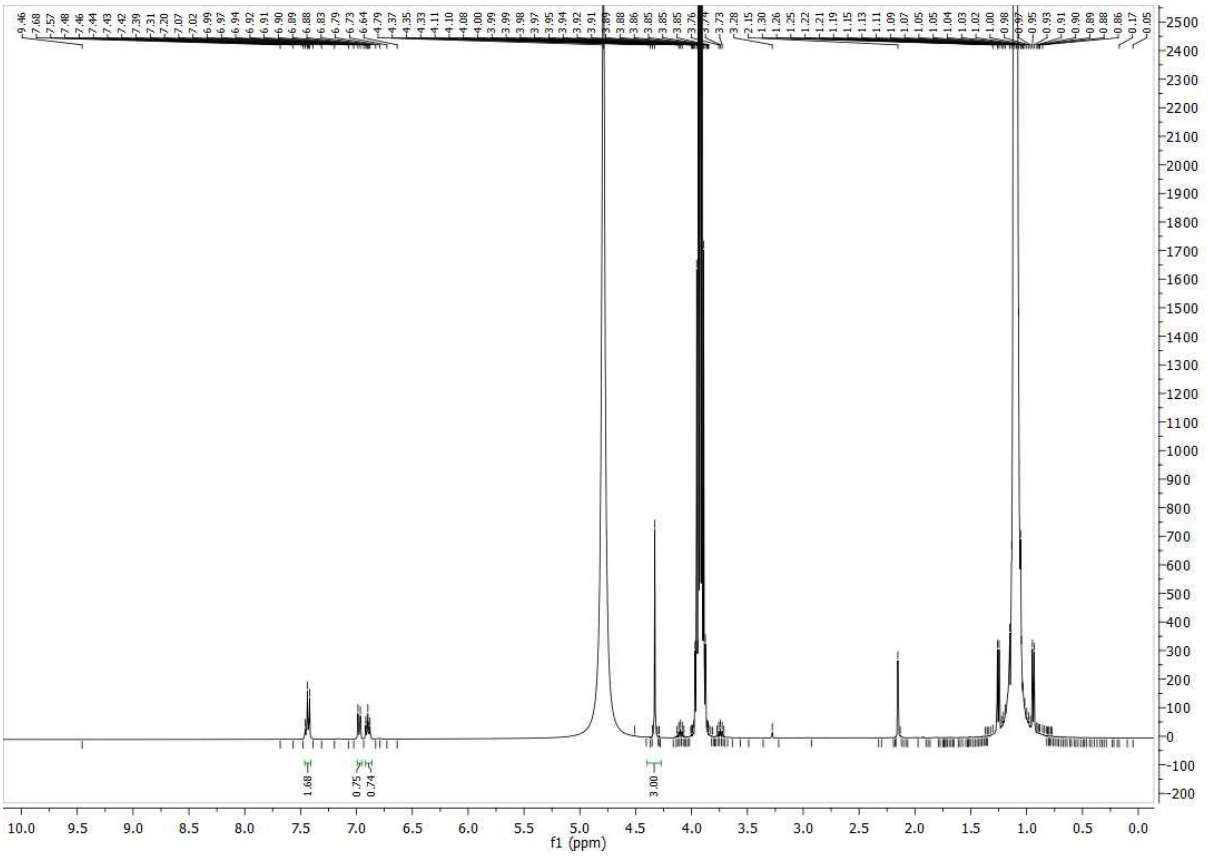

Supplementary Figure 5 ^{1}H-NMR. Deuteration of 2-hydroxybenzonitrile (Compound **3-d**) with nitromethane reference.

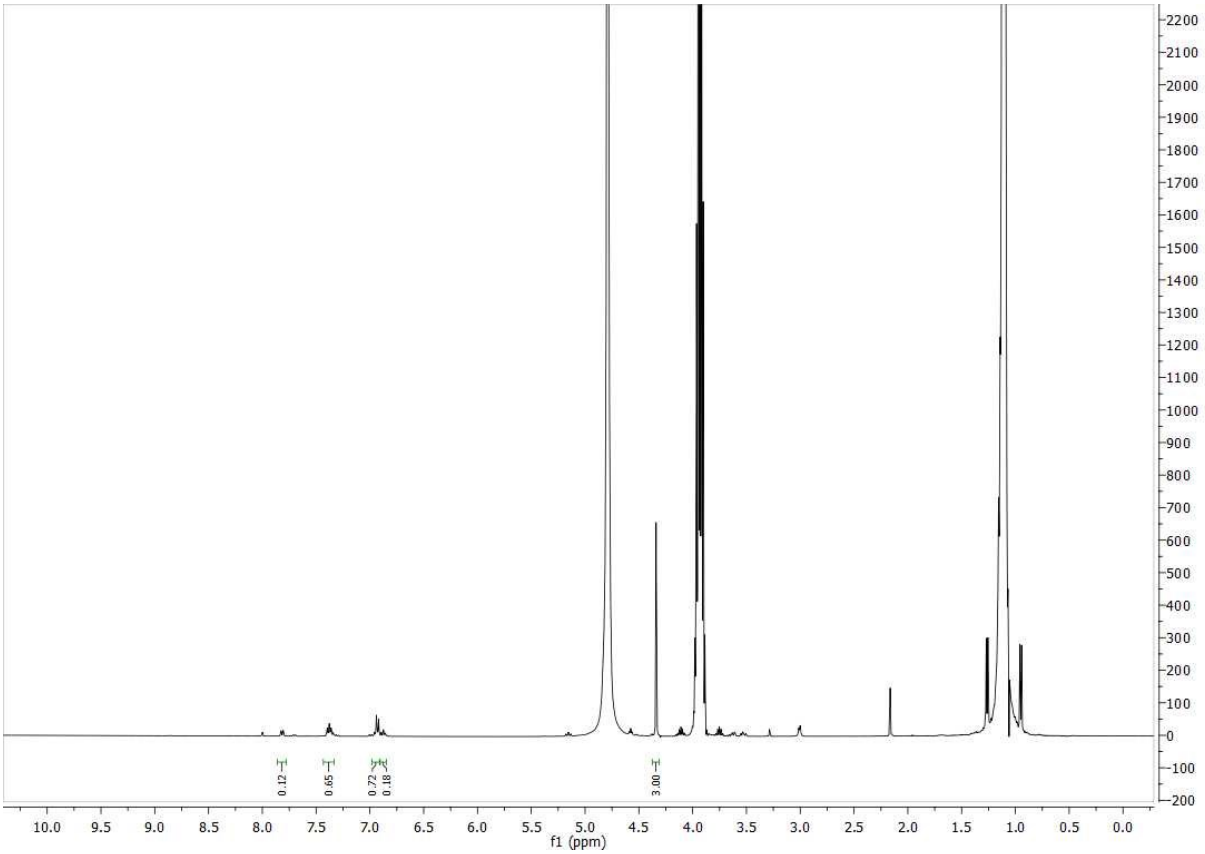

Supplementary Figure 6 ^{1}H-NMR. Deuteration of (*R*)-2-(4-(Hydroxymethyl)-4,5-dihydrothiazol-2-yl)phenol ((*R*)-aerugine, Compound **1-d**) with nitromethane reference.

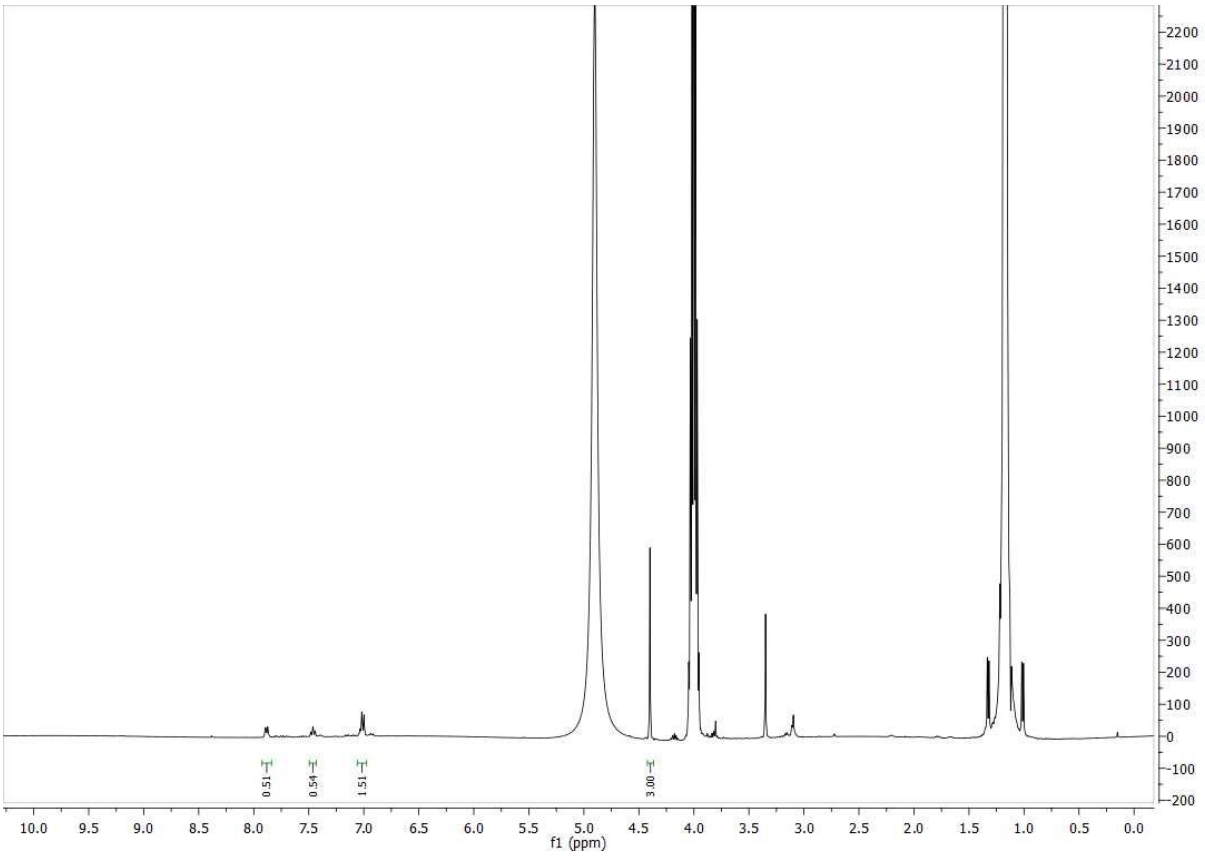

Supplementary Figure 7 ^{1}H-NMR. Deuteration of (*R*)-2-(2'-hydroxyphenyl)-4-methoxycarbonyl-4,5-dihydrothiazole (Compound 4-**d**) with nitromethane reference.

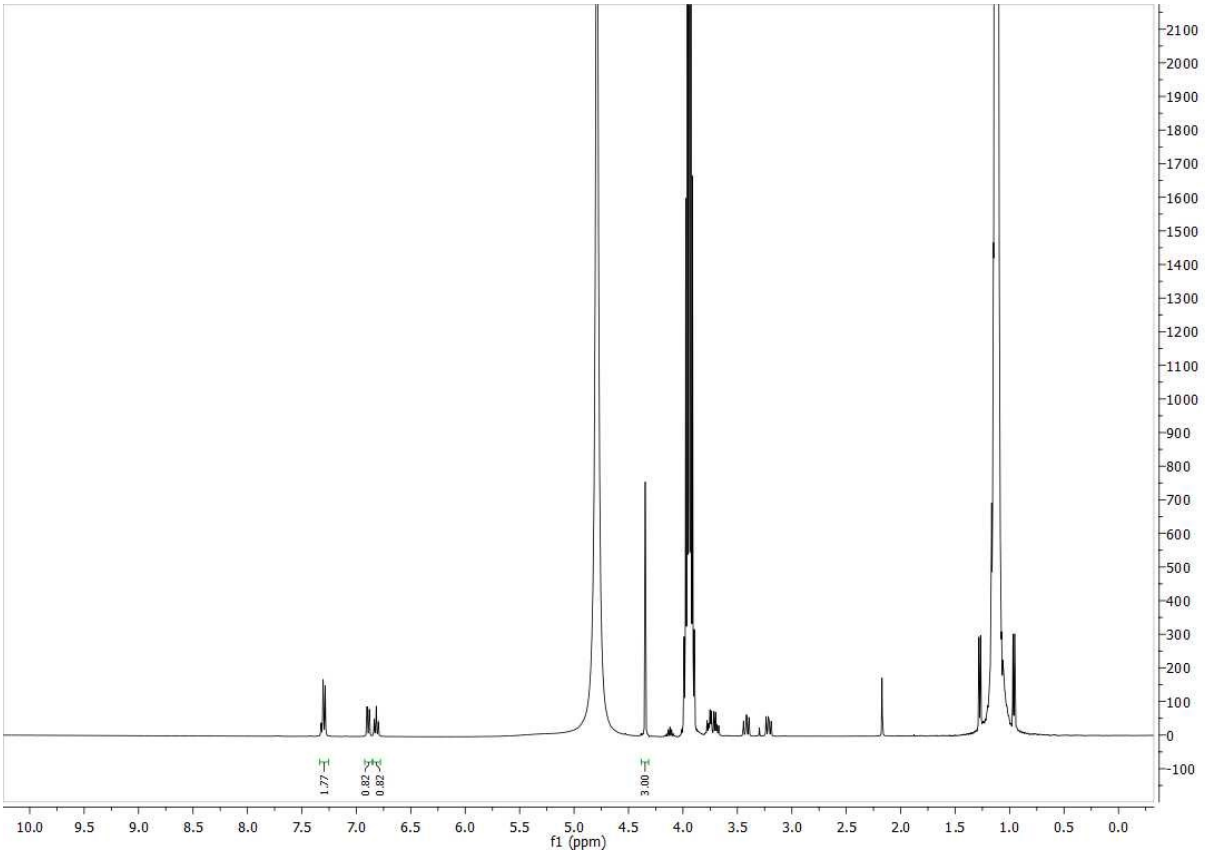

Supplementary Figure 8 ^{1}H-NMR. Deuteration of (*R*)-dihydroaeruginoic acid (Compound **5-d**) with nitromethane reference.

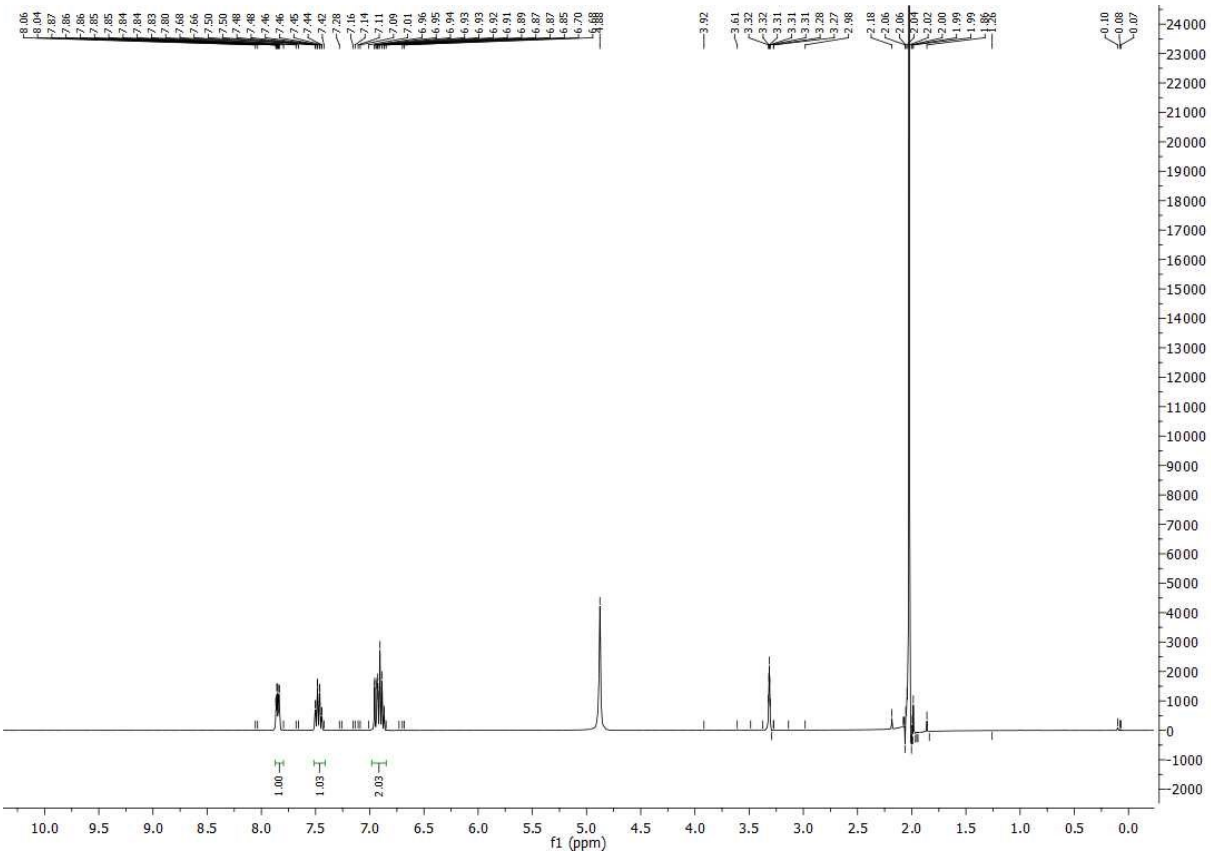

Supplementary Figure 9 ^{1}H-NMR of salicylic acid methyl ester (Compound **7**).

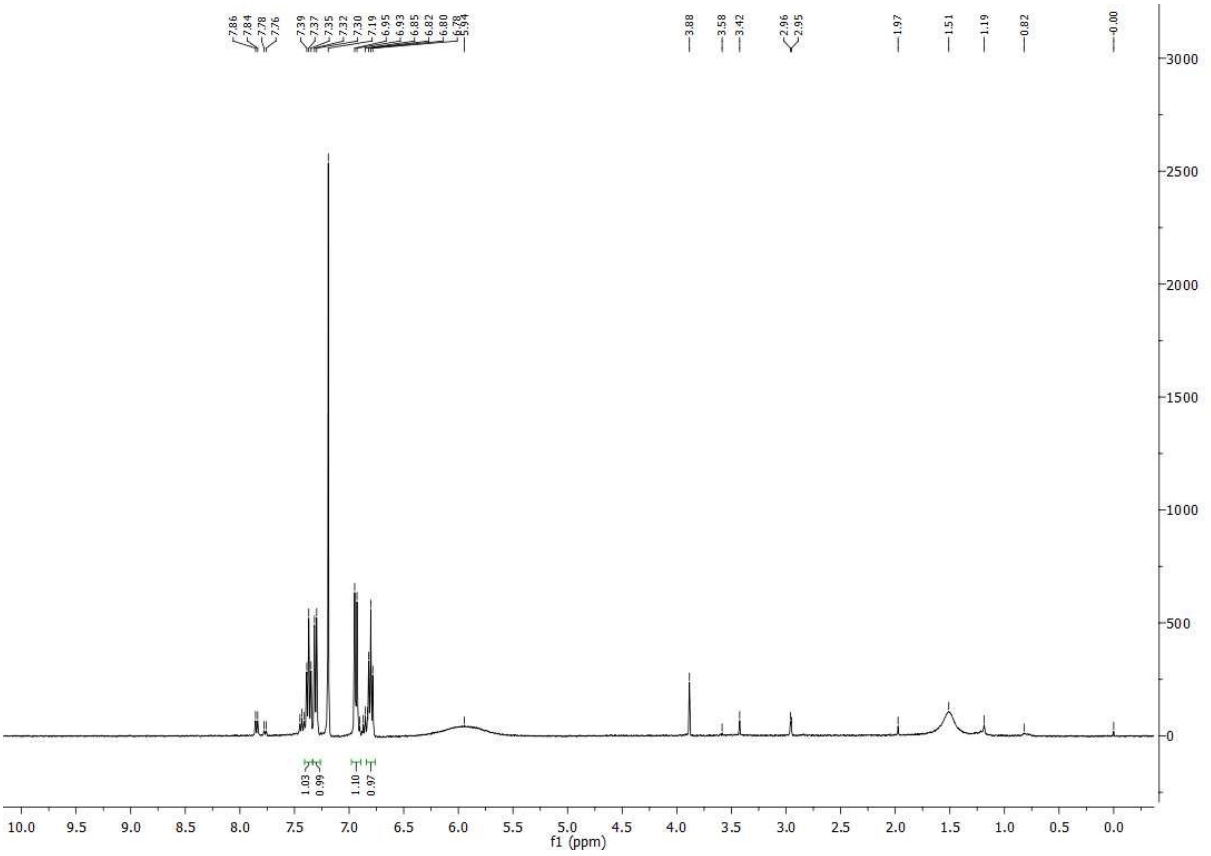

Supplementary Figure 10 ^{1}H-NMR of salicylic amide (Compound **6**).

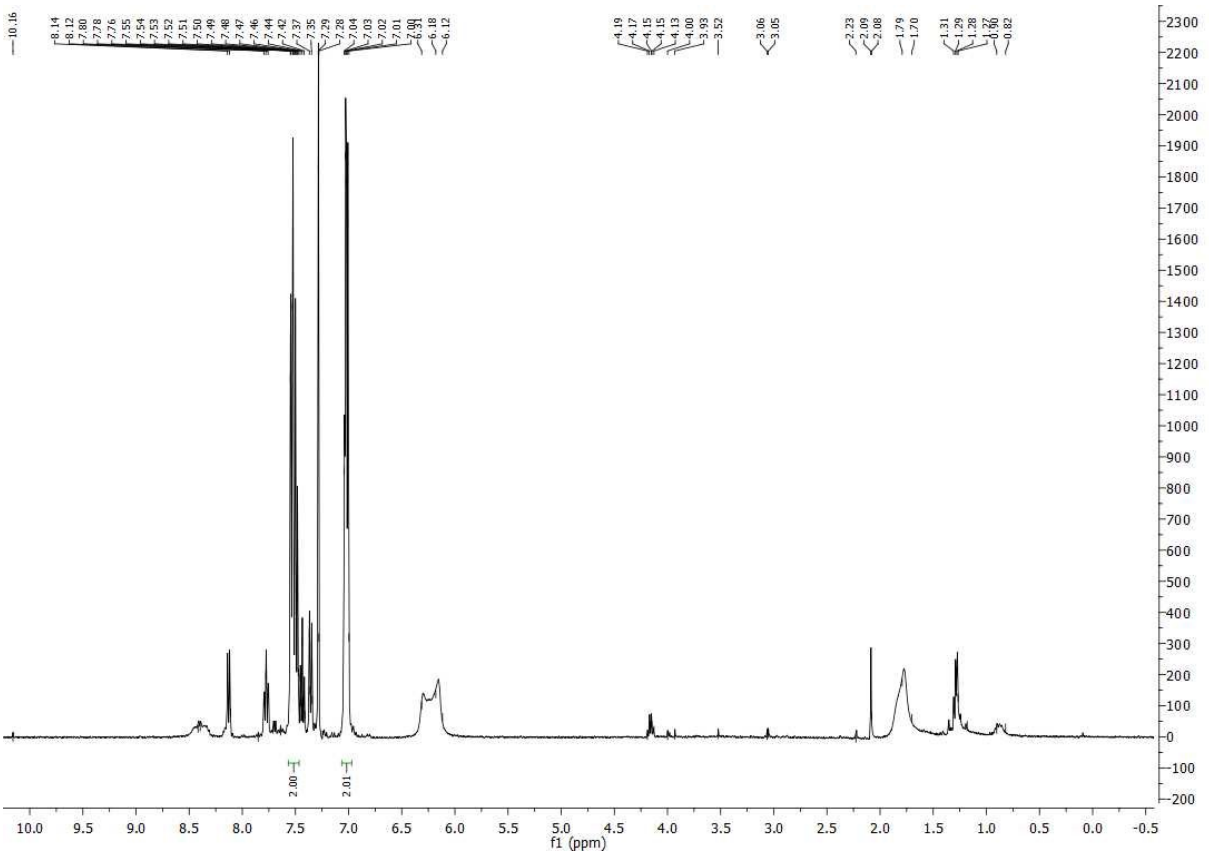

Supplementary Figure 11 ^{1}H-NMR of 2-hydroxybenzonitrile (Compound **3**).

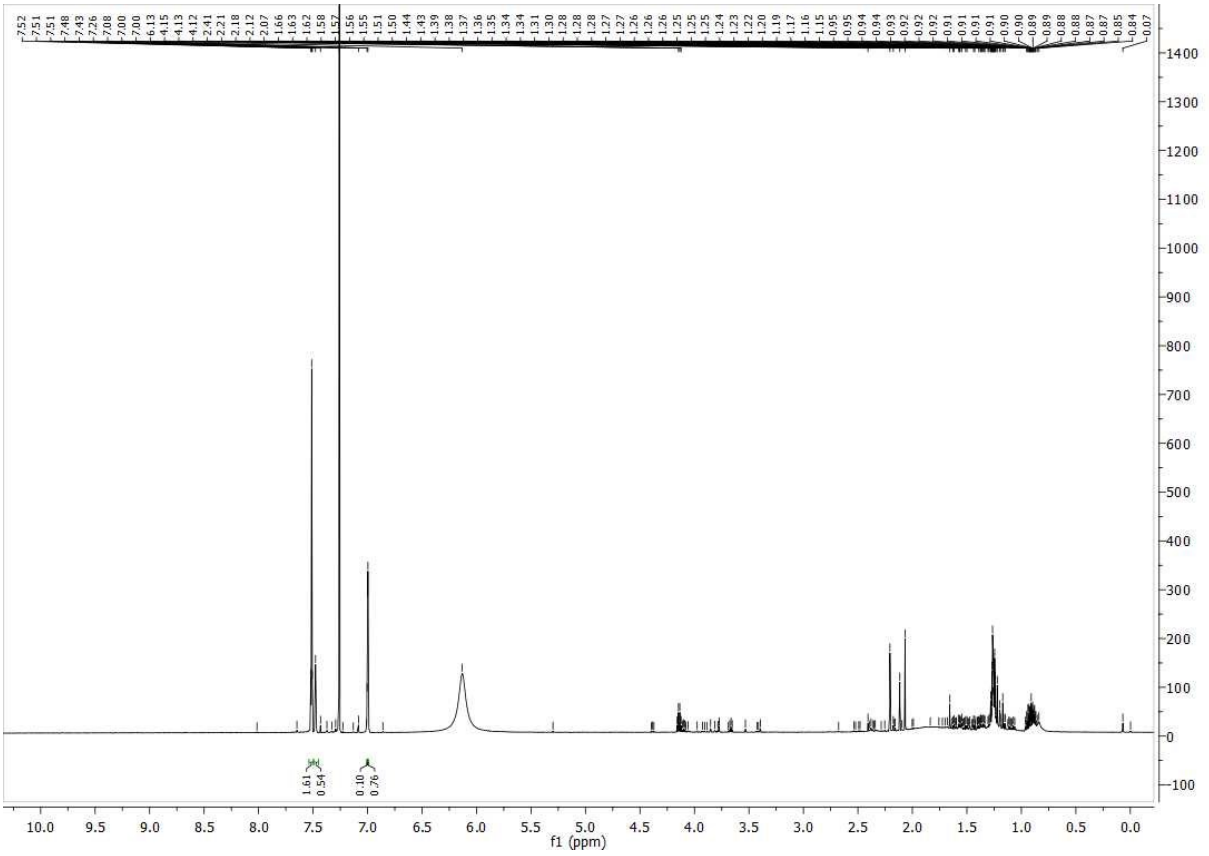

Supplementary Figure 12 ^{1}H-NMR of 2-hydroxybenzonitrile-d_4 (Compound **3-d**).

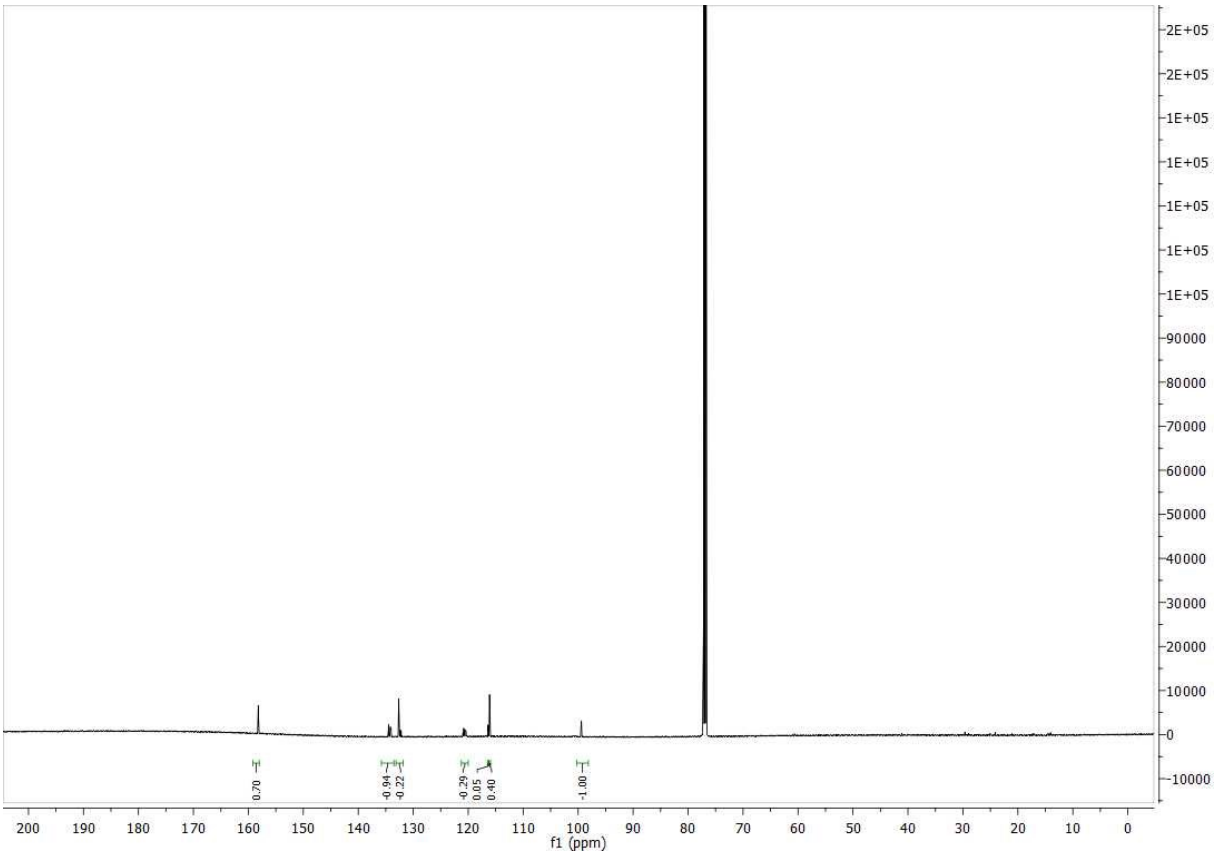

Supplementary Figure 13 ^{13}C-NMR of 2-hydroxybenzonitrile-d_4 (Compound **3-d**).

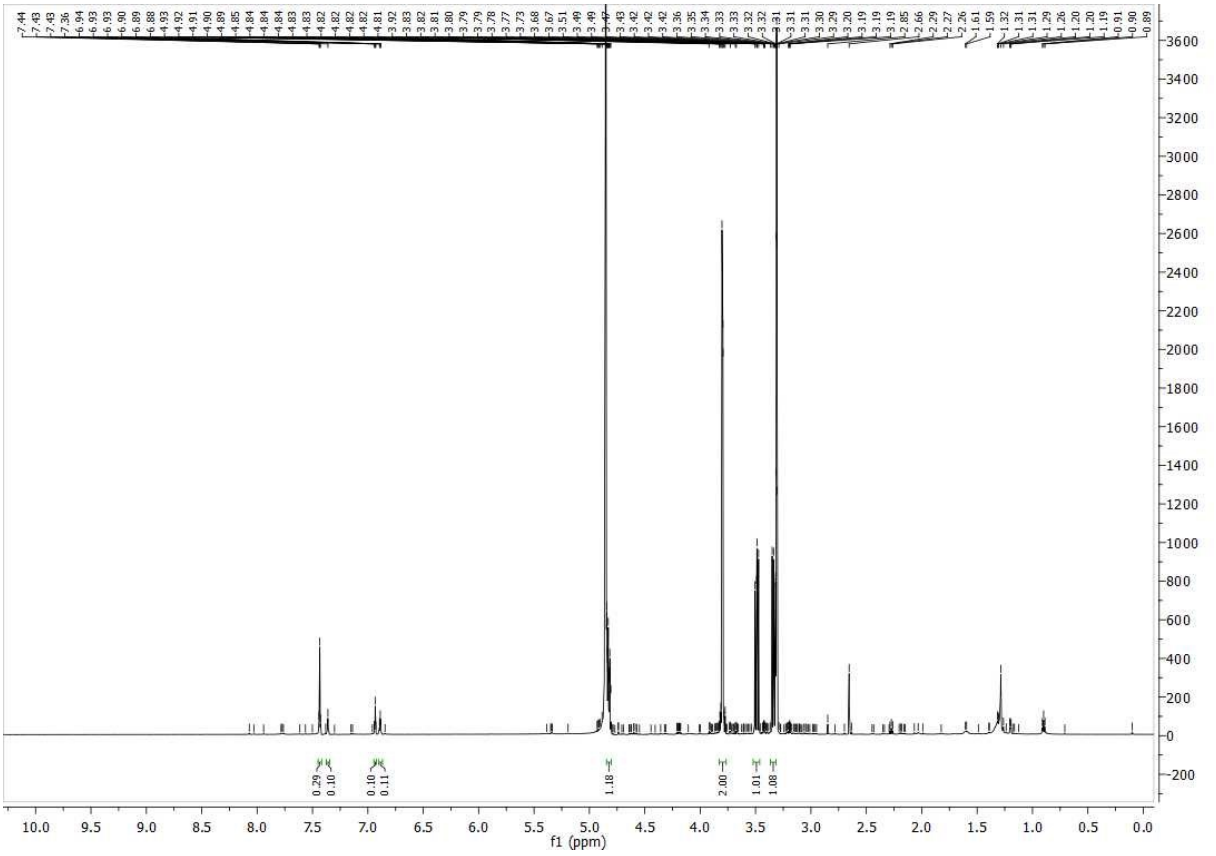

Supplementary Figure 14 ^{1}H-NMR of aerugine-d_4 (Compound **1-d**).

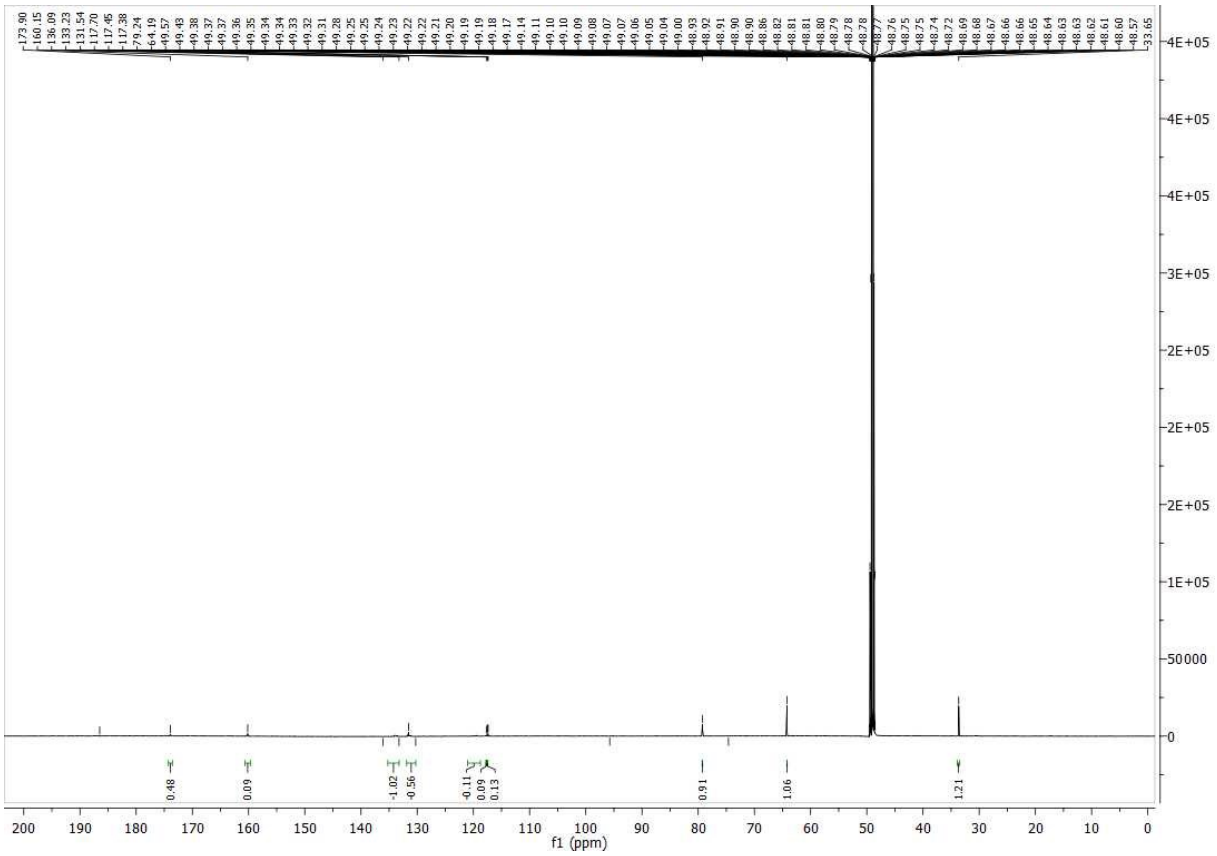

Supplementary Figure 15 ^{13}C-NMR of aerugine-d_4 (Compound **1-d**).

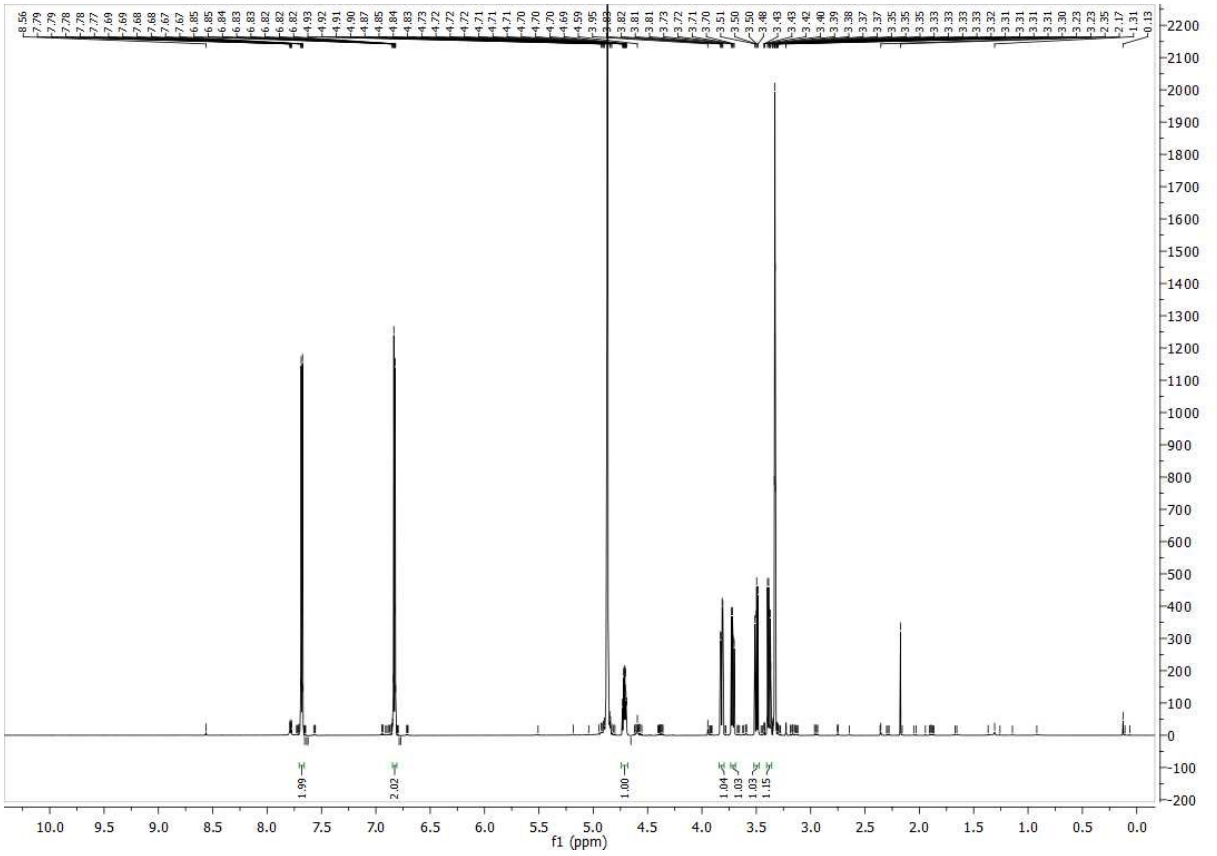

Supplementary Figure 16 ^{1}H-NMR of 4-[4-(hydroxymethyl)-4,5-dihydro-1,3-thiazol-2-yl]phenol **(**Compound **8**).

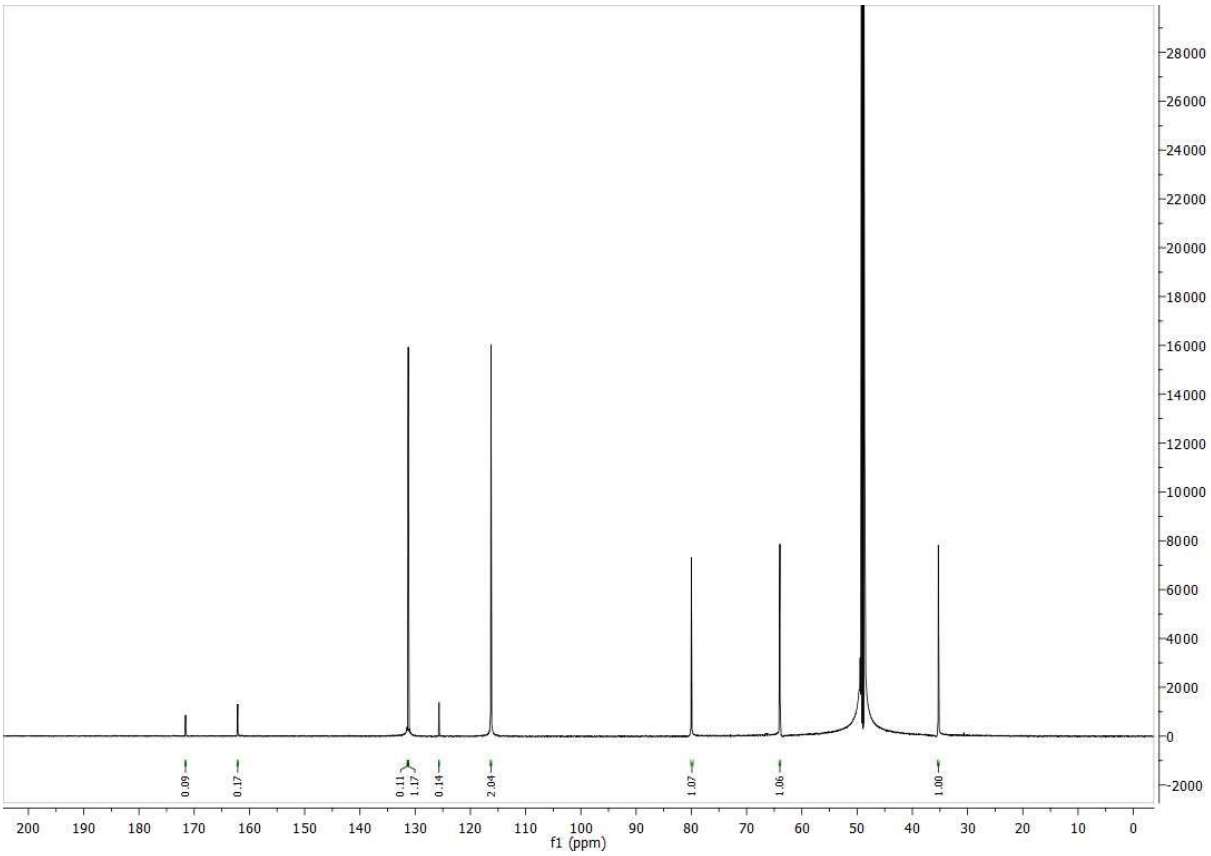

Supplementary Figure 17 ^{13}C-NMR of 4-[4-(hydroxymethyl)-4,5-dihydro-1,3-thiazol-2-yl]phenol **(**Compound **8**).

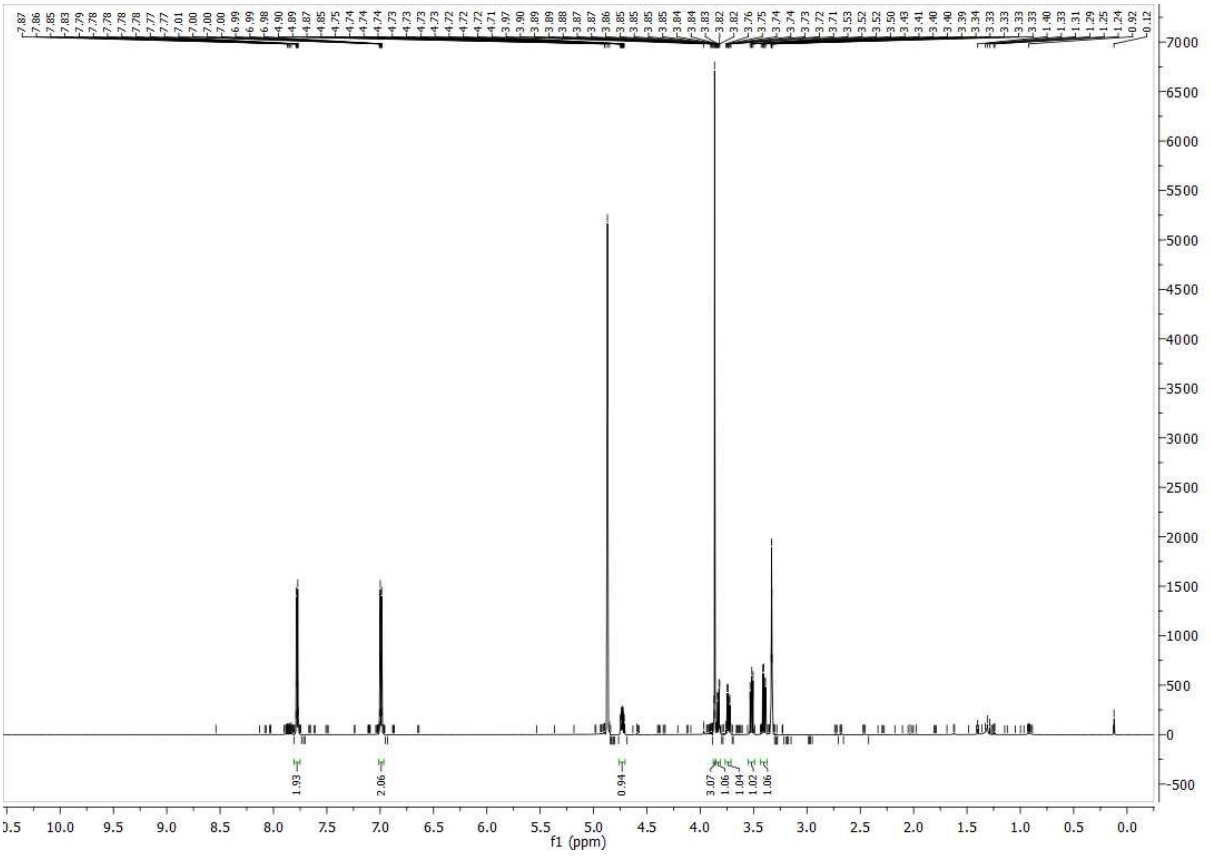

Supplementary Figure 18 ^{1}H-NMR of 4-[4-(hydroxymethyl)-4,5-dihydro-1,3-thiazol-2-yl]methoxybenzol (Compound **10)**.

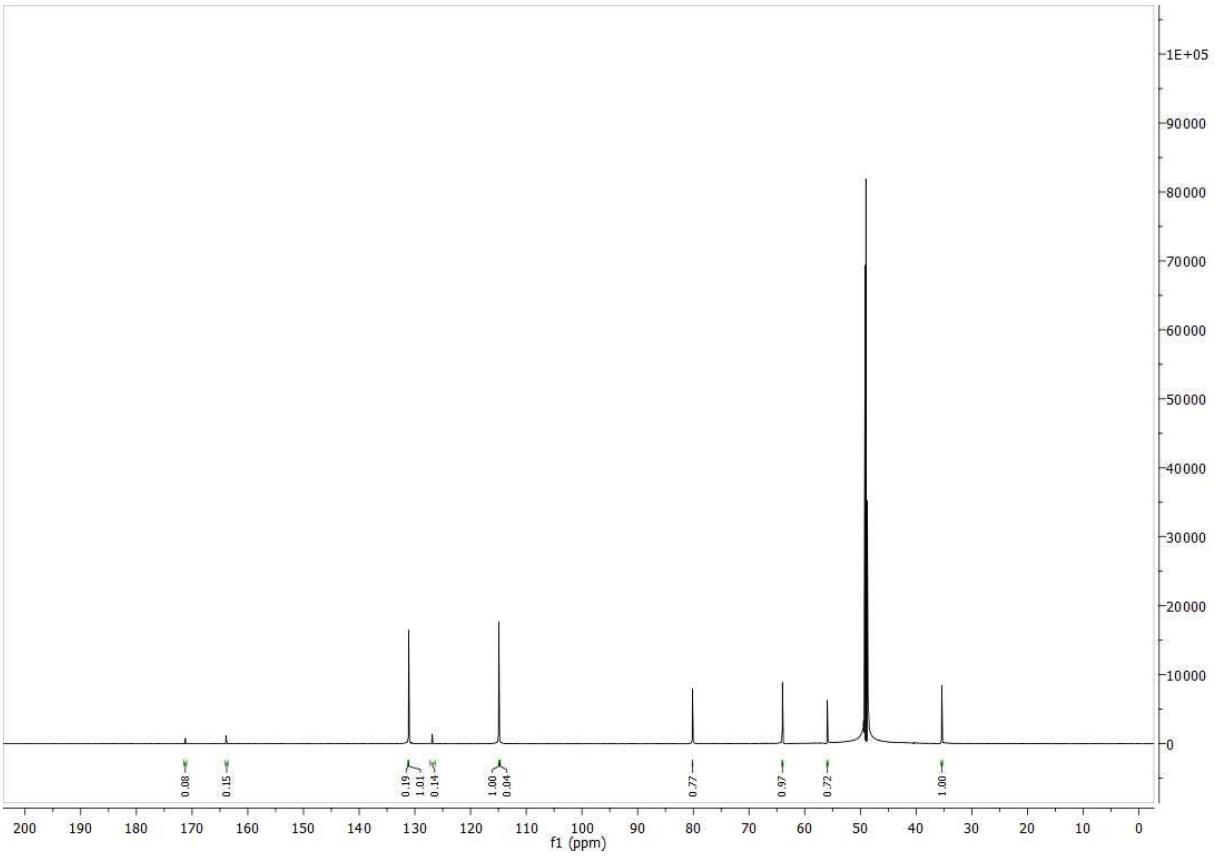

Supplementary Figure 19 ^{13}C-NMR of 4-[4-(hydroxymethyl)-4,5-dihydro-1,3-thiazol-2-yl]methoxybenzol (Compound **10)**.

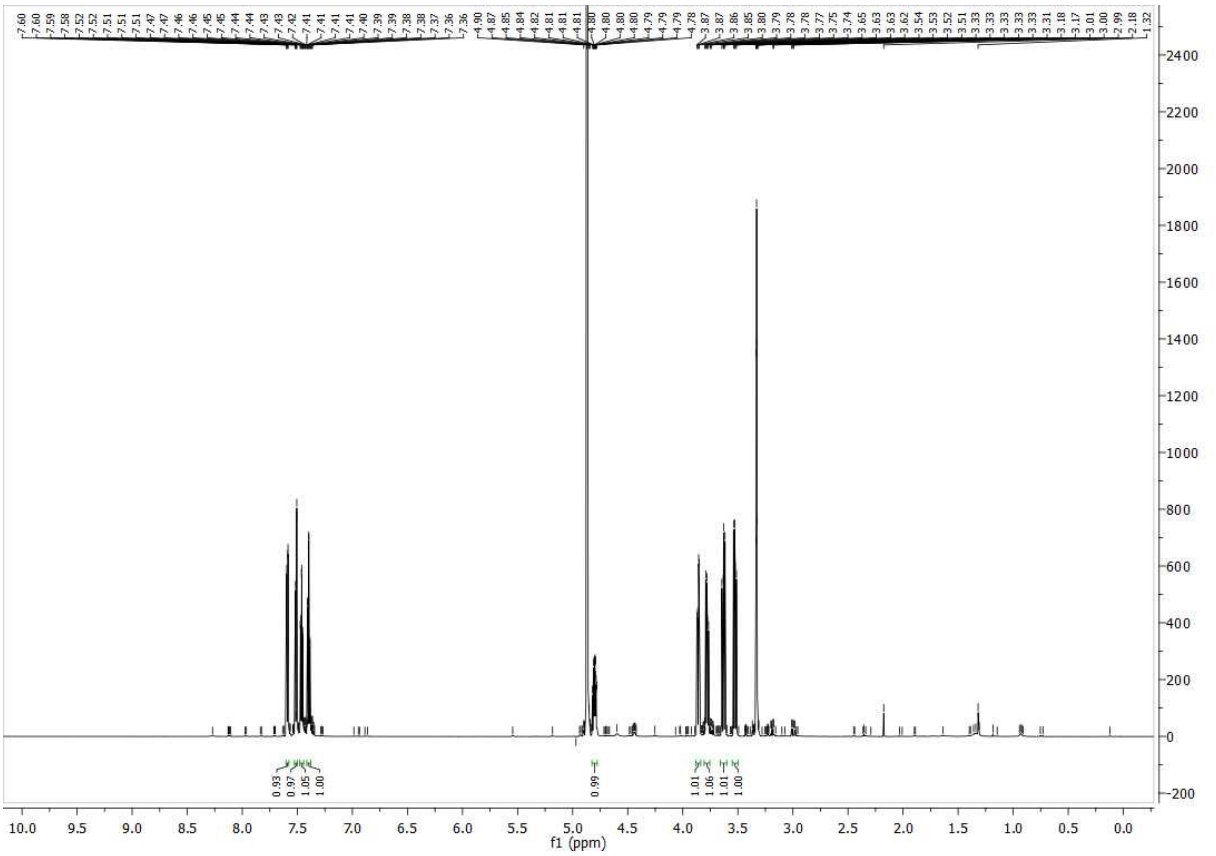

Supplementary Figure 20 ^{1}H-NMR of 2-[4-(hydroxymethyl)-4,5-dihydro-1,3-thiazol-2-yl]chlorophenol (Compound **11**).

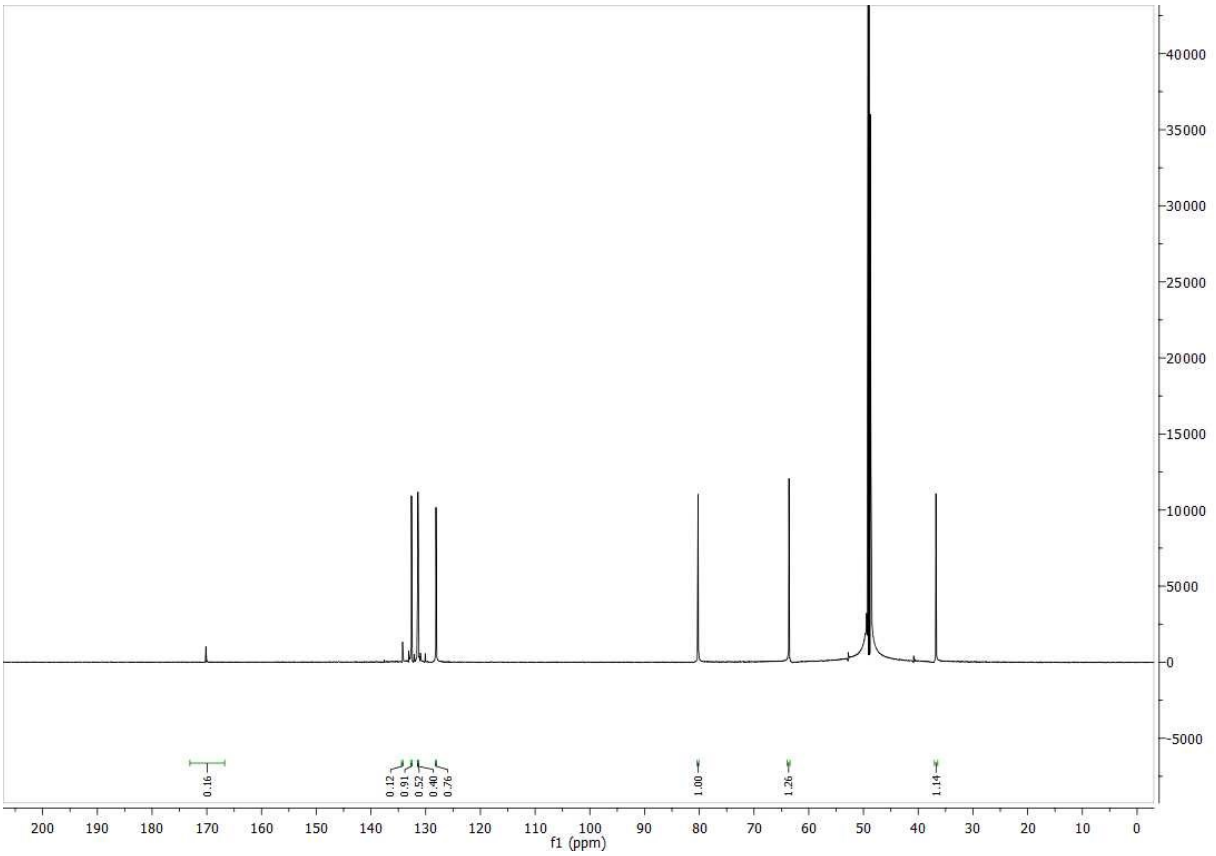

Supplementary Figure 21 ^{13}C-NMR of 2-[4-(hydroxymethyl)-4,5-dihydro-1,3-thiazol-2-yl]chlorophenol (Compound **11**).

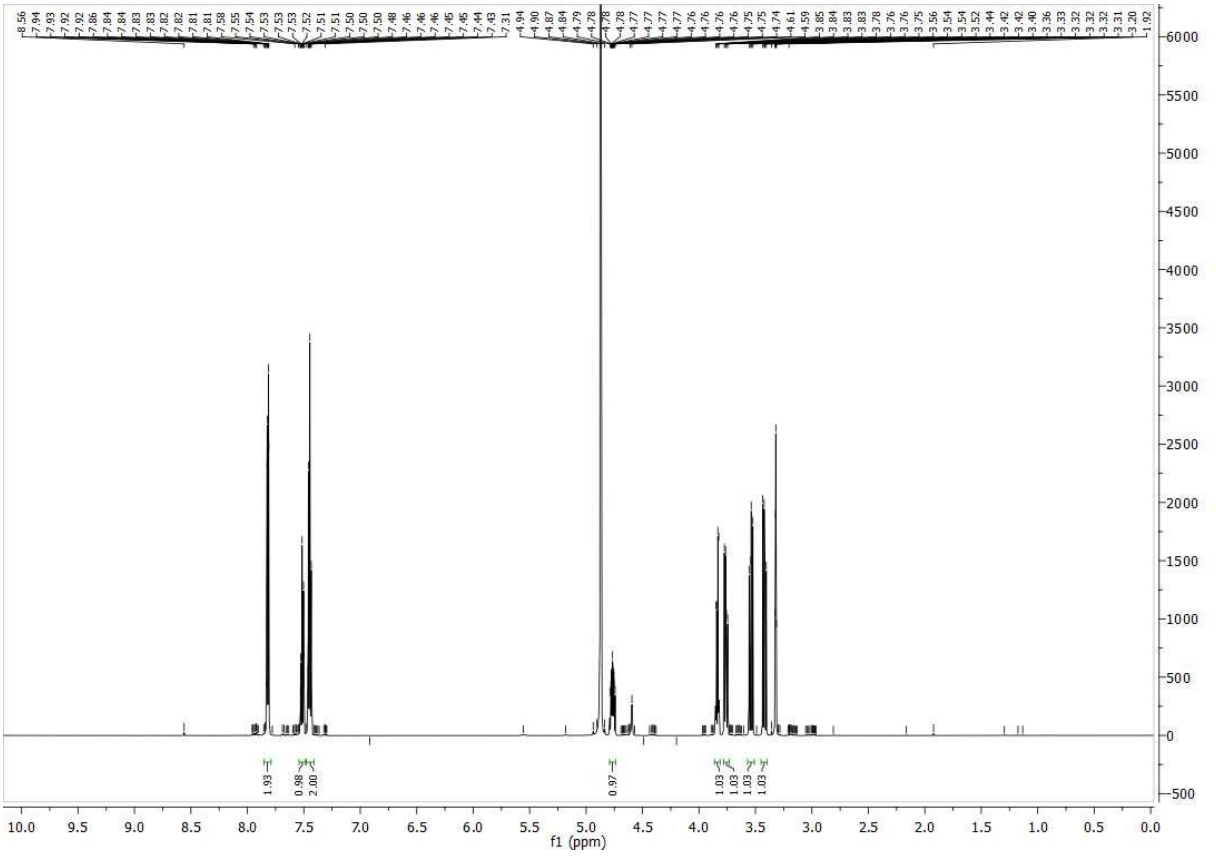

Supplementary Figure 22 ^{1}H-NMR of [4-(hydroxymethyl)-4,5-dihydro-1,3-thiazol-2-yl]benzol (Compound **12)**.

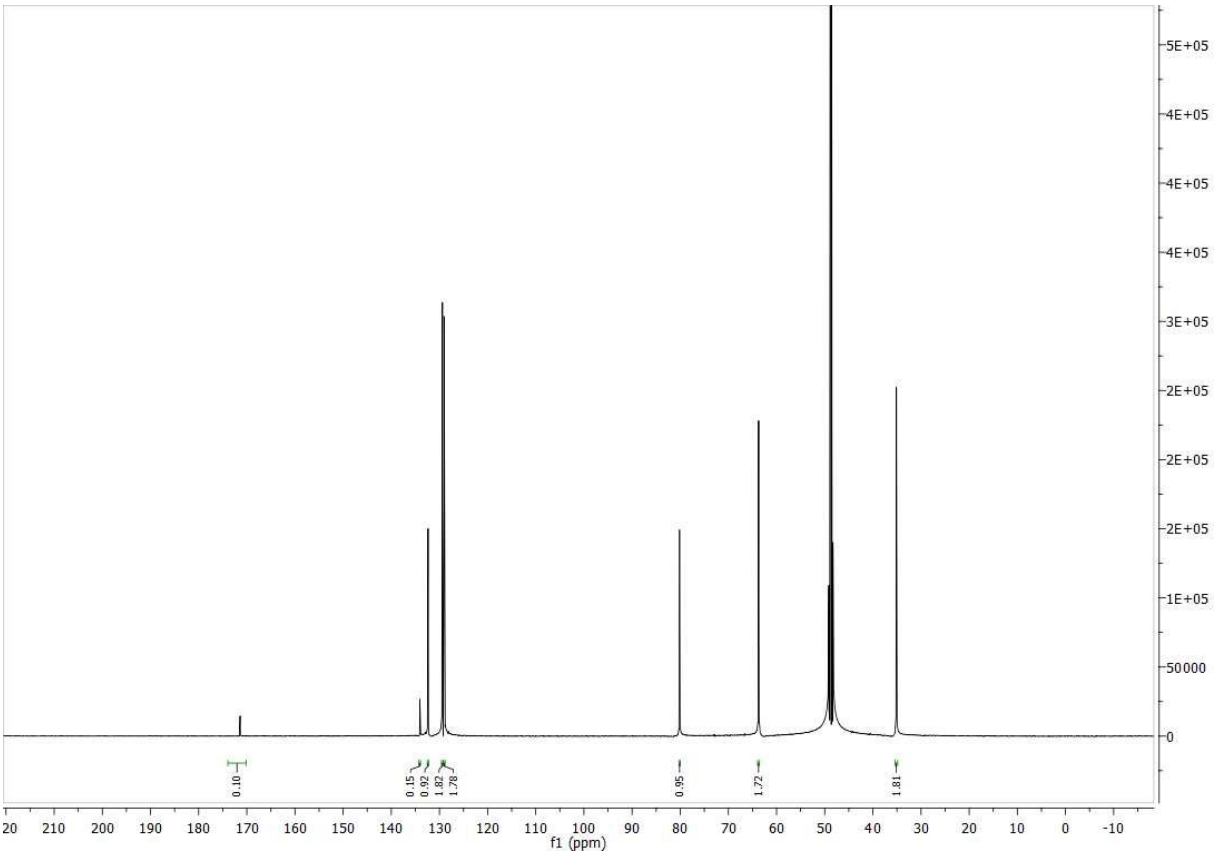

Supplementary Figure 23 ^{13}C-NMR of [4-(hydroxymethyl)-4,5-dihydro-1,3-thiazol-2-yl]benzol (Compound **12)**.

8.6 HPLC - chromatograms

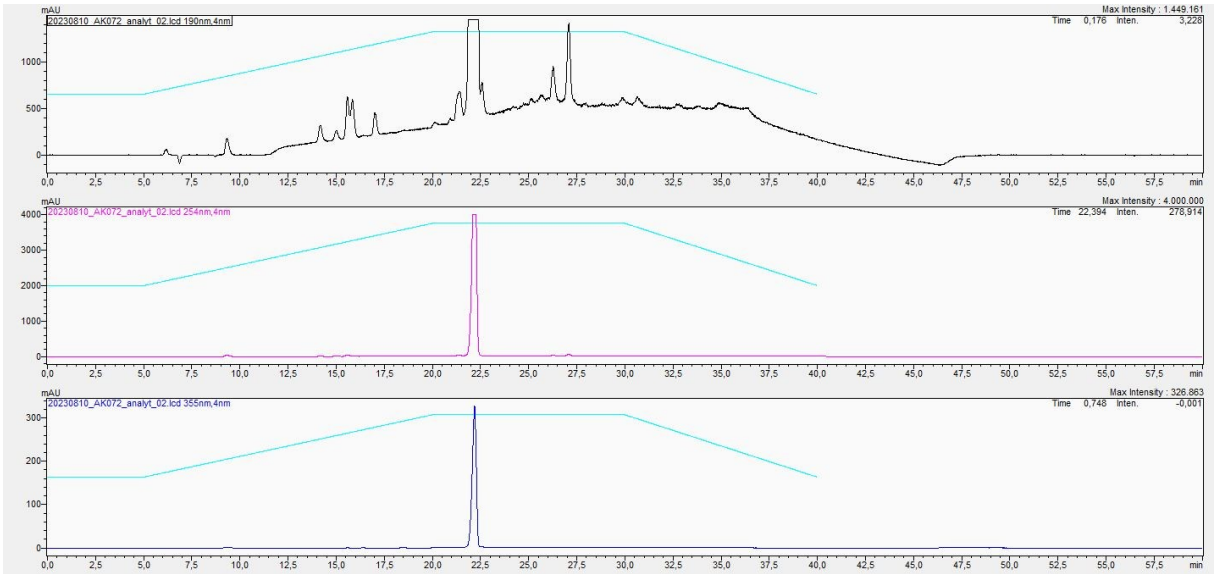

Supplementary Figure 24 Analytical HPLC of *(R)*-aerugine-d$_4$ (Compound 1-d). Chromatogram.

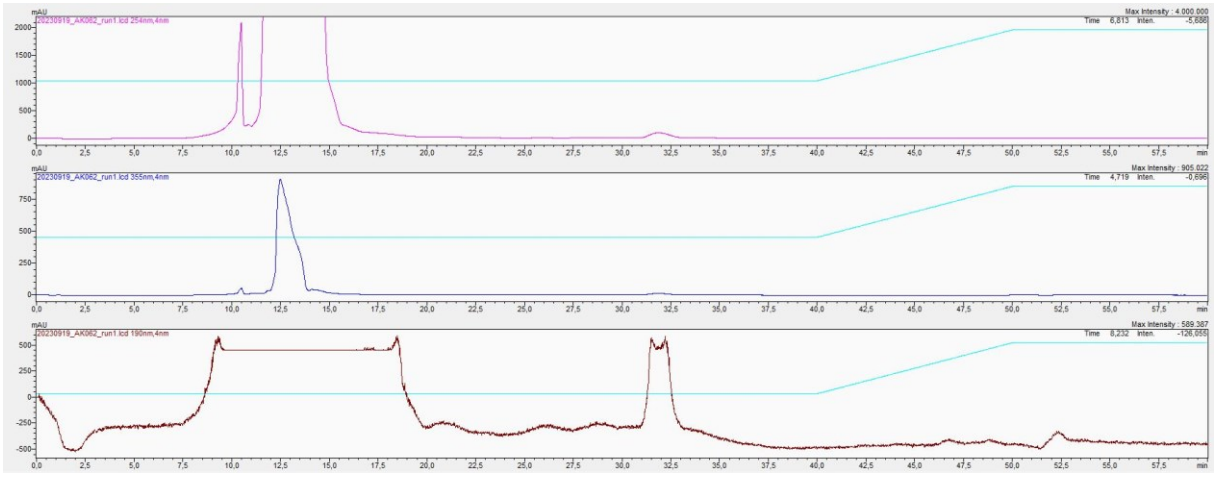

Supplementary Figure 25 Purification of Compound 8. Chromatogram.

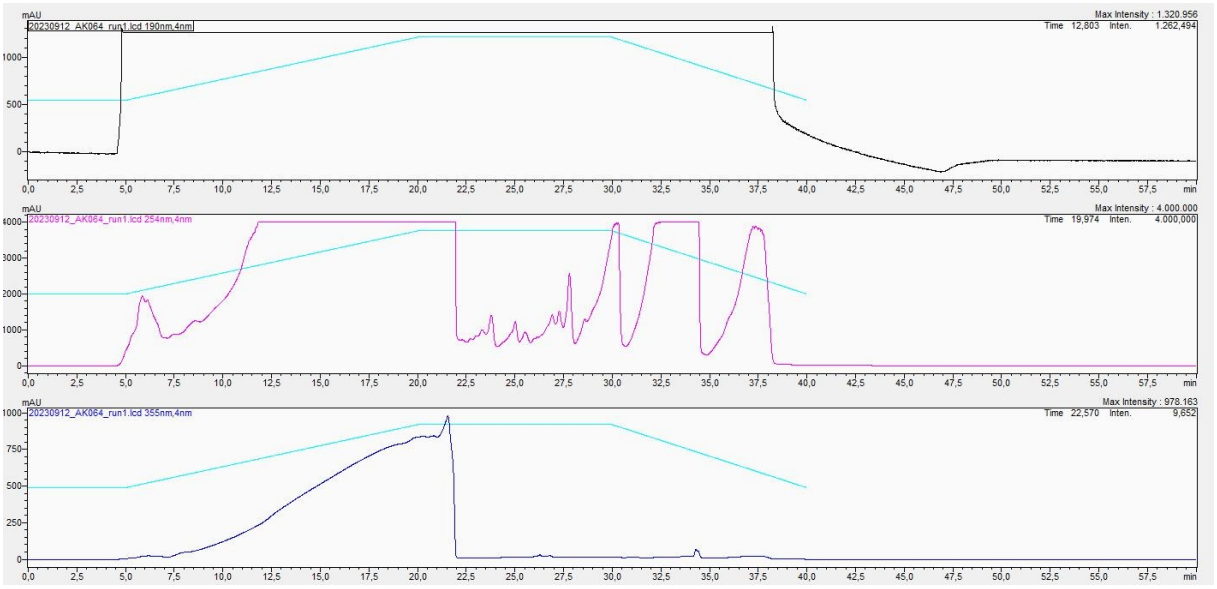

Supplementary Figure 26 Purification of Compound 10. Chromatogram.

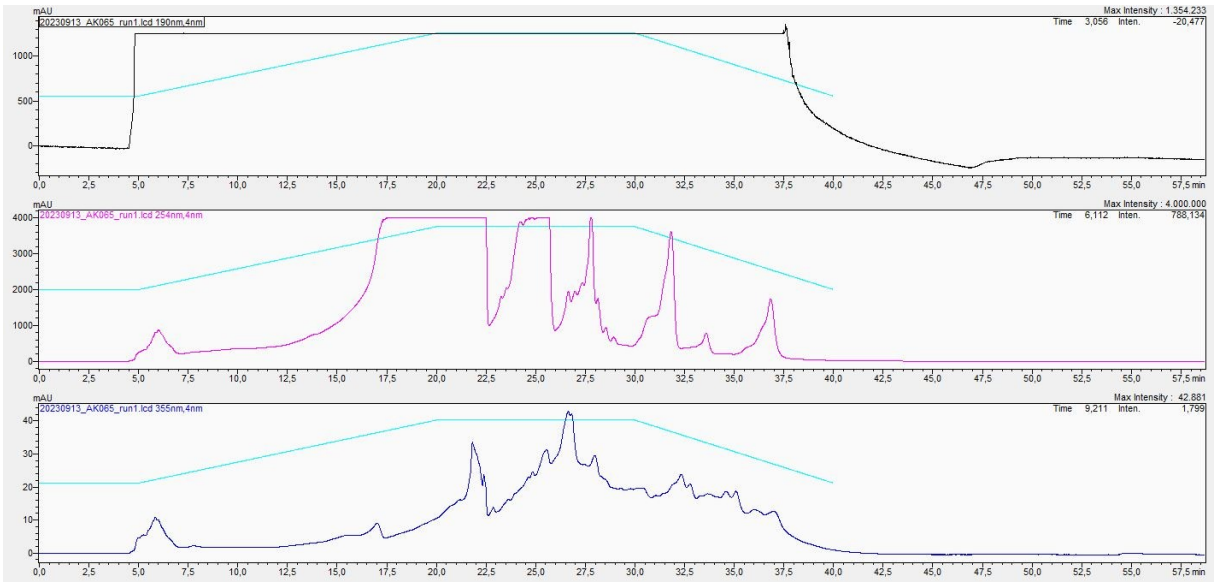

Supplementary Figure 27 Purification of Compound 11. Chromatogram.

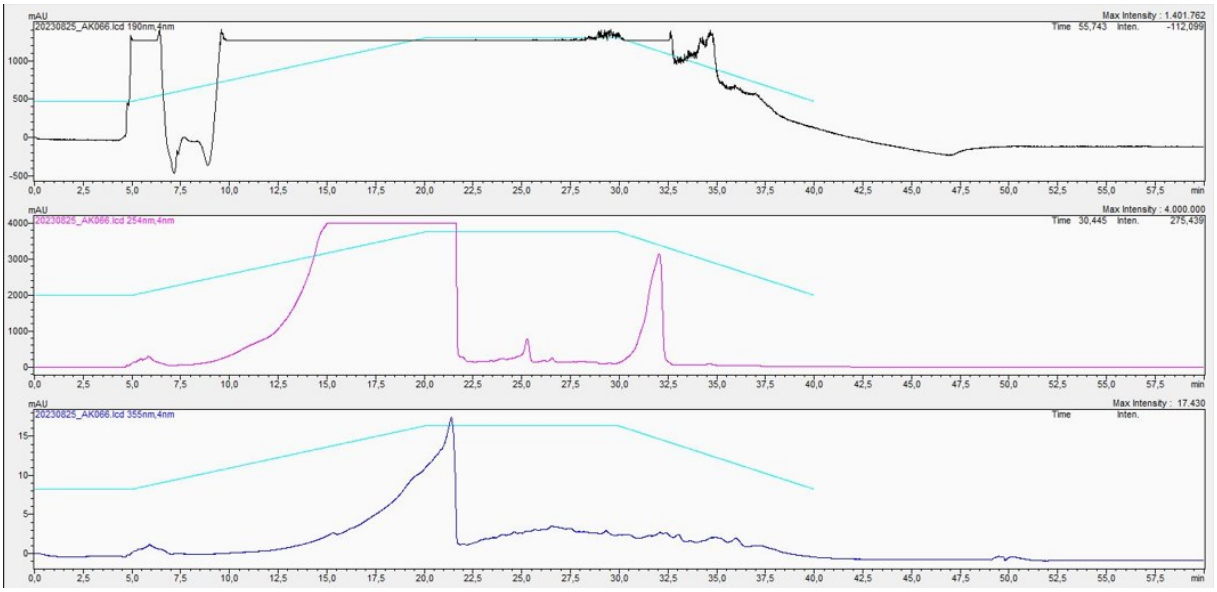

Supplementary Figure 28 Purification of Compound 12. Chromatogram.

8.7 LC-MS/MS - ms^2 spectra

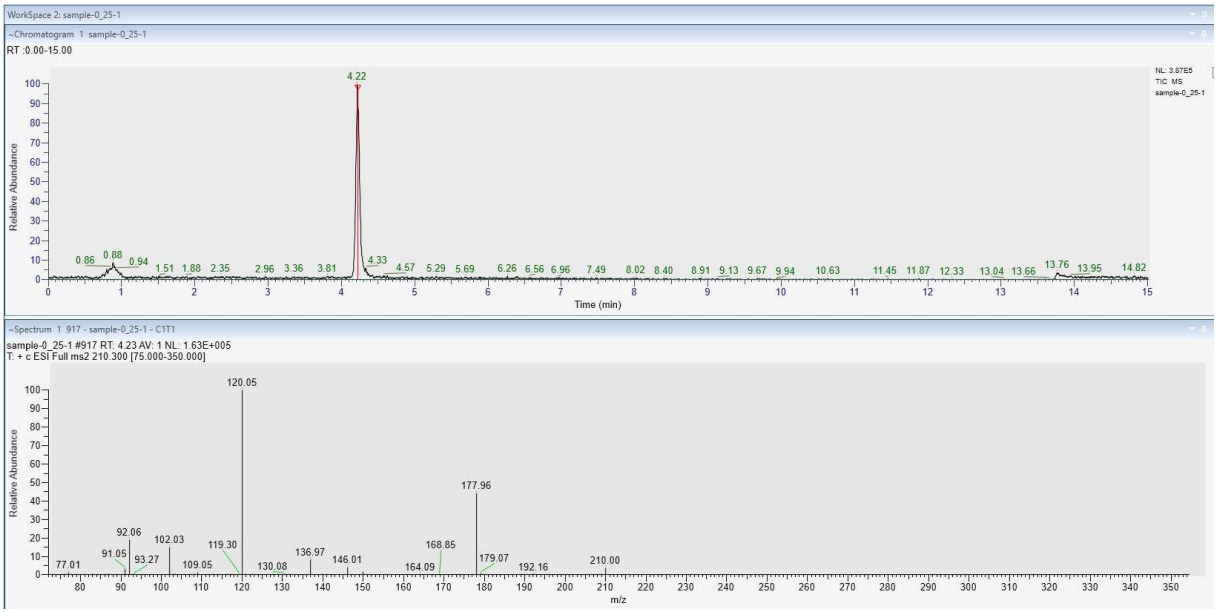

Supplementary Figure 29 Product Ion Scan of synthetic aerugine. Selected ion chromatogram and ms^2 spectrum.

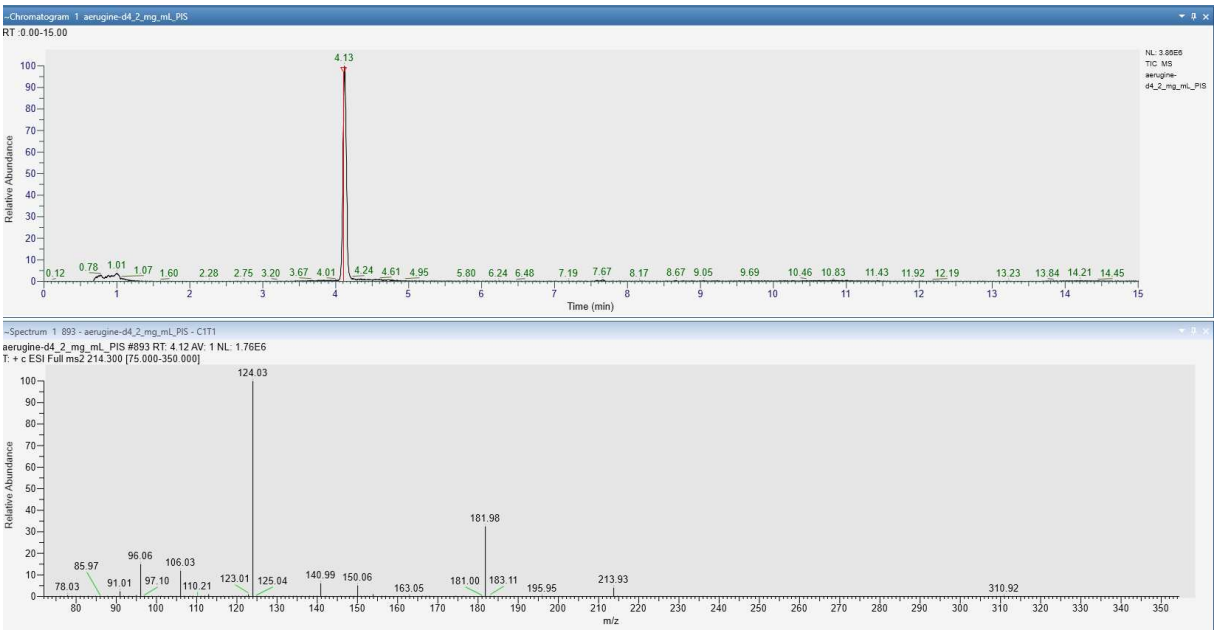

Supplementary Figure 30 Product Ion Scan of aerugine-d$_4$. Selected ion chromatogram and ms^2 spectrum.

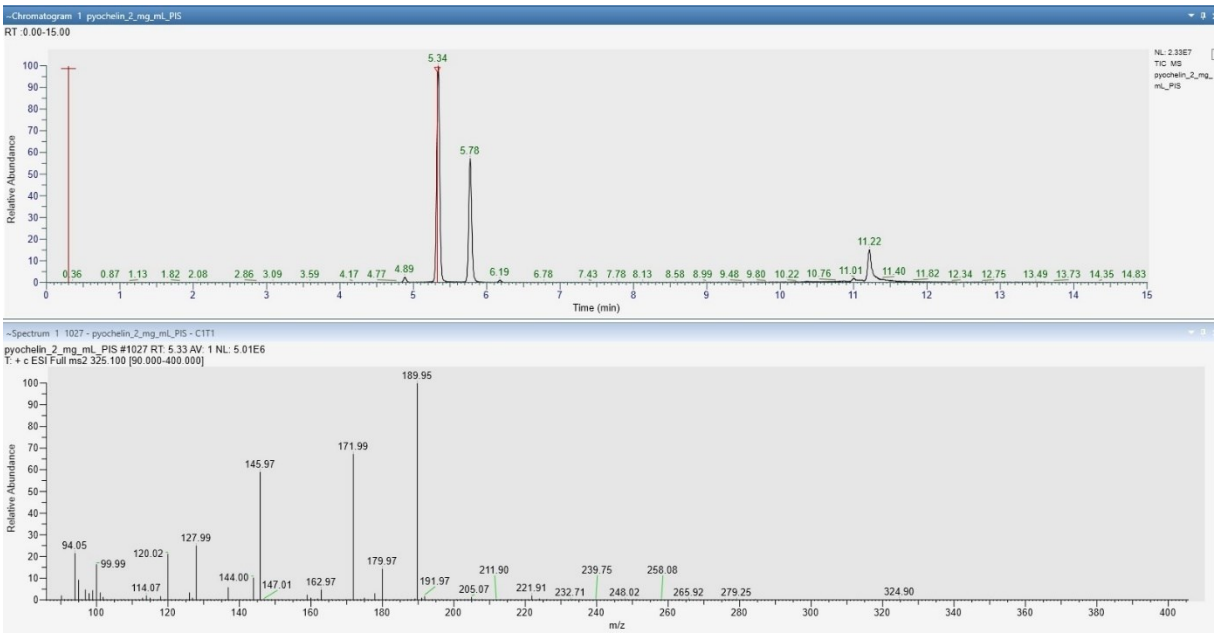

Supplementary Figure 31 Product Ion Scan of pyochelin I. Selected ion chromatogram and ms^2 spectrum (R_t = 5.34 min).

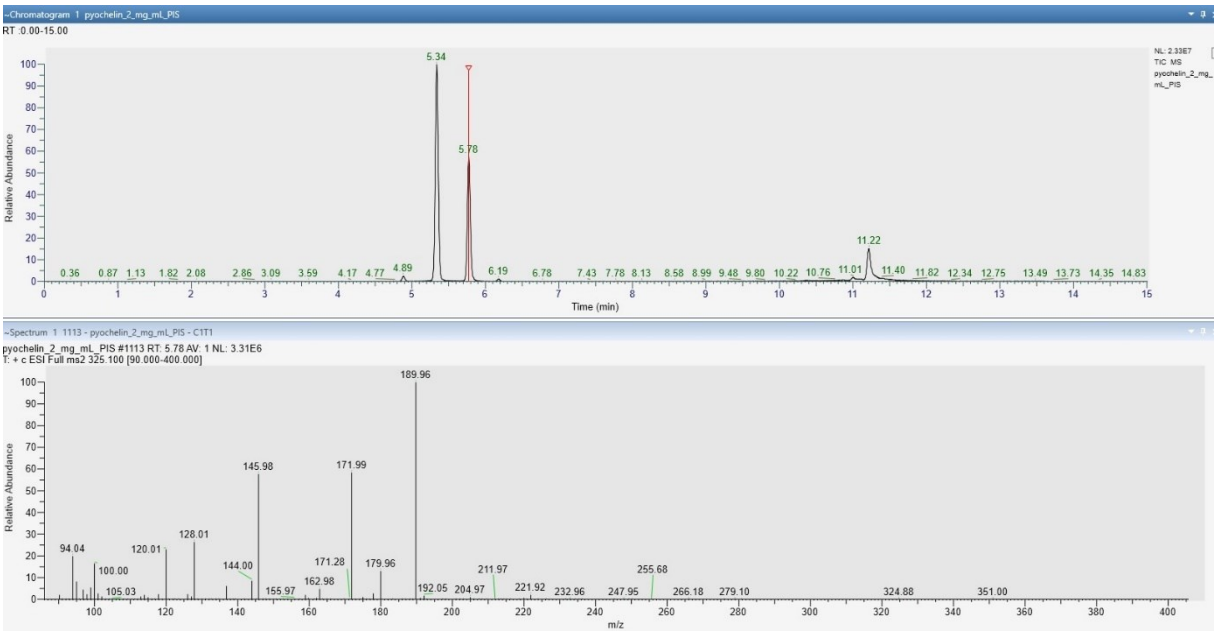

Supplementary Figure 32 Product Ion Scan of pyochelin II. Selected ion chromatogram and ms^2 spectrum (R_t = 5.78 min).

8.8 LC-MS/MS calibration curves

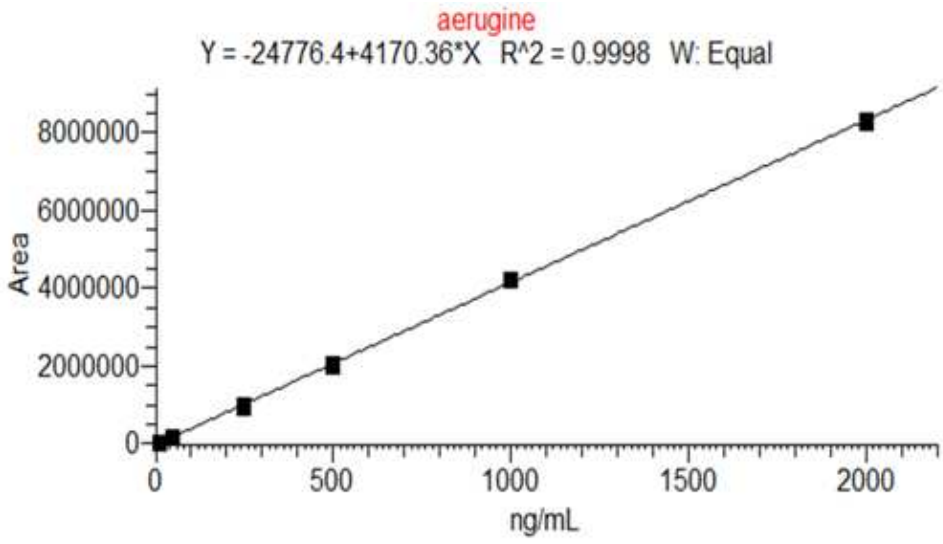

Supplementary Figure 33 Calibration aerugine in 50% MeOH in H_2O.

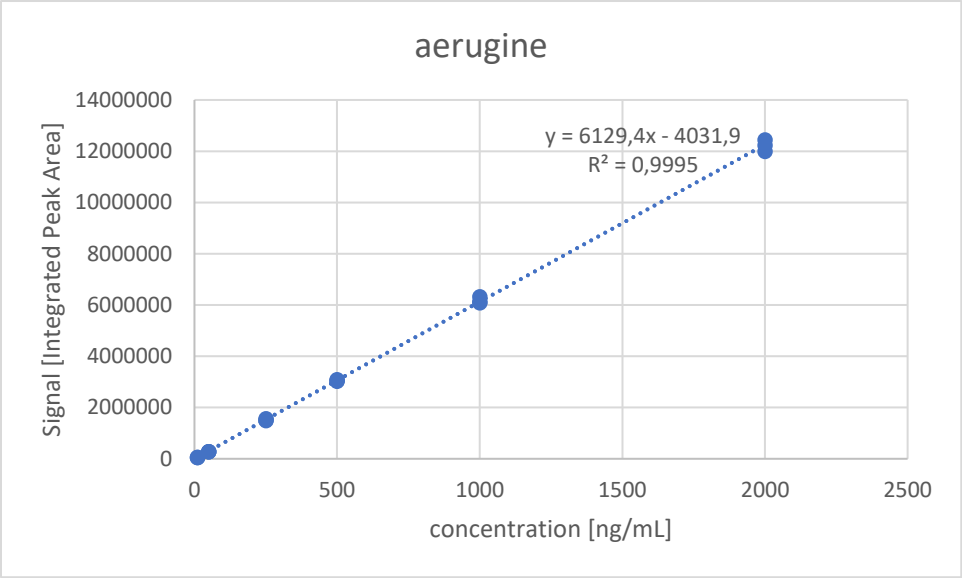

Supplementary Figure 34 Calibration aerugine in 100% MeOH.

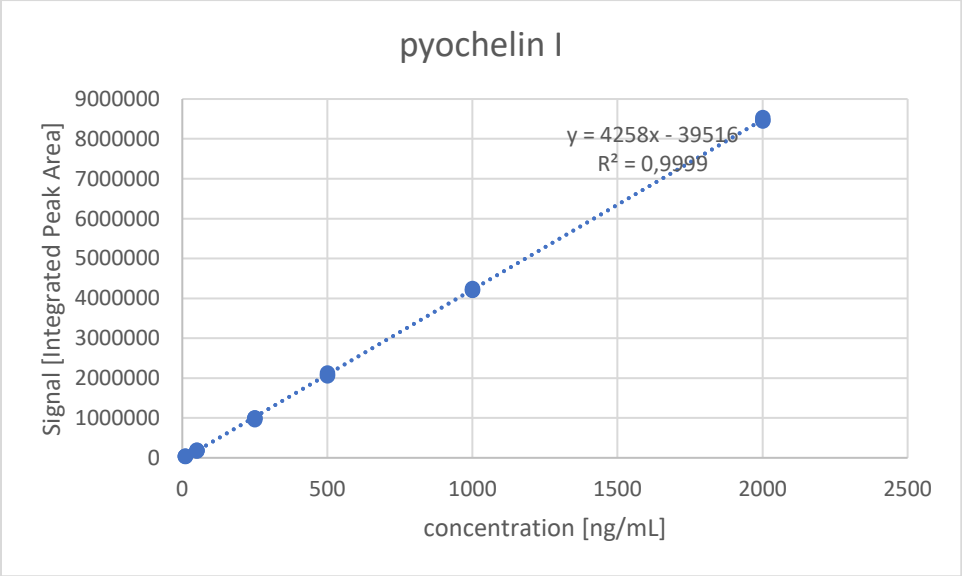

Supplementary Figure 35 Calibration pyochelin I.

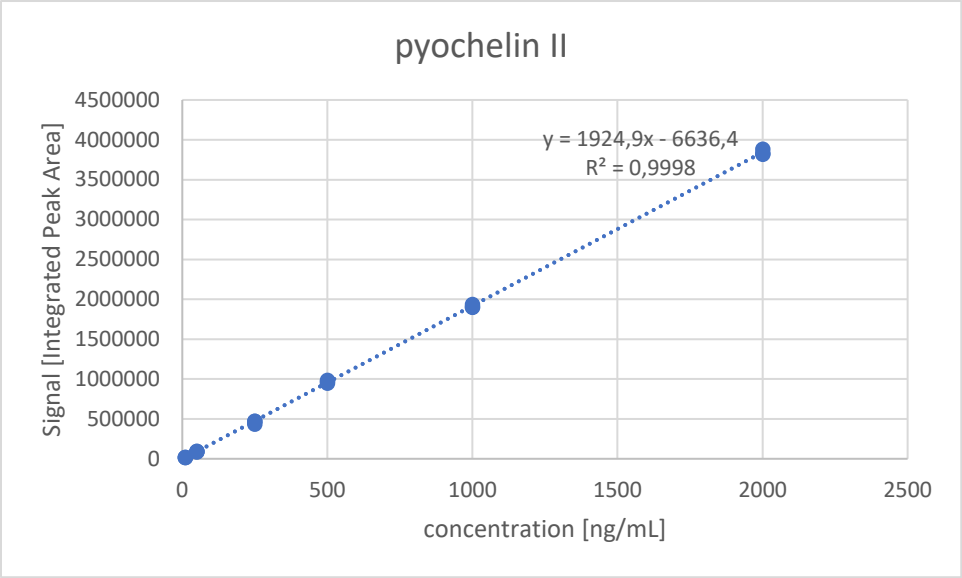

Supplementary Figure 36 Calibration pyochelin II.

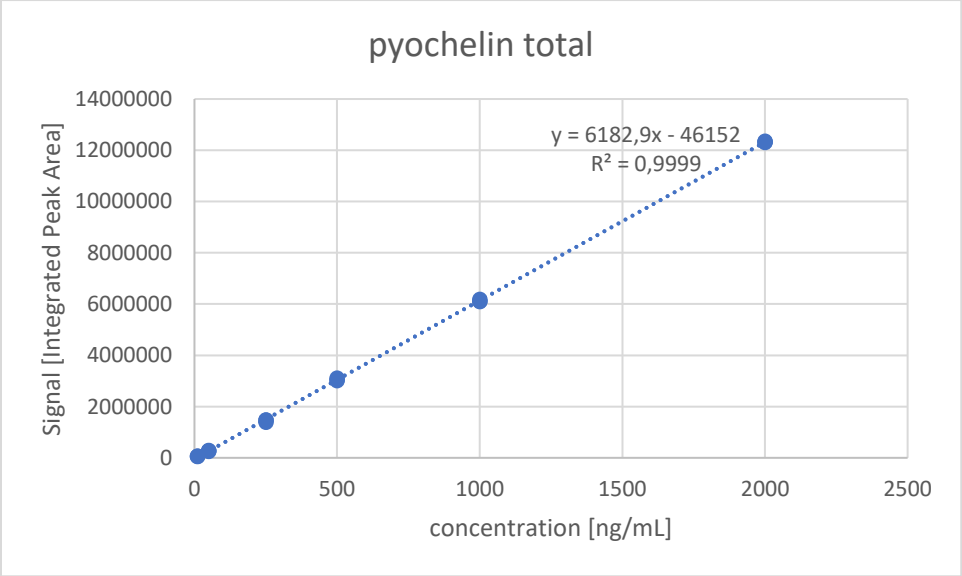

Supplementary Figure 37 Calibration pyochelin total.

8.9 LC-MS/MS quantification raw data

Supplementary Table 1 Aerugine quantification over time in PAO1 and *Y. enterocolitica*. (Y.ent.: *Y. enterocolitica* DSM4780, **(!)** indicates error in sample preparation, in grey: relative standard deviation of technical triplicates >30%)

Sample	Integrated Area	sample	Integrated Area
PAO1-6h-1-1	16405	Y.ent.-6h-1-1 **(!)**	2005558
PAO1-6h-1-2	15440	Y.ent.-6h-1-2 **(!)**	788515
PAO1-6h-1-3	11116	Y.ent.-6h-1-3 **(!)**	758697
PAO1-6h-2-1	12111	Y.ent.-6h-2-1 **(!)**	60320
PAO1-6h-2-2	15940	Y.ent.-6h-2-2 **(!)**	49445
		Y.ent.-6h-2-3 **(!)**	52326
PAO1-6h-3-1	20109	Y.ent.-6h-3-1 **(!)**	119807
PAO1-6h-3-2	17914	Y.ent.-6h-3-2 **(!)**	122666
PAO1-6h-3-3	15940	Y.ent.-6h-3-3 **(!)**	109648
PAO1-24h-1-1	9105272	Y.ent.-24h-1-1 **(!)**	6215765
PAO1-24h-1-2	9029267	Y.ent.-24h-1-2 **(!)**	6312732
PAO1-24h-1-3	8980243	Y.ent.-24h-1-3 **(!)**	4951288
PAO1-24h-2-1	6610632	Y.ent.-24h-2-1 **(!)**	1417316
PAO1-24h-2-2	5959105	Y.ent.-24h-2-2 **(!)**	1367904
PAO1-24h-2-3	6061972	Y.ent.-24h-2-3 **(!)**	1437684
PAO1-24h-3-1	8966599	Y.ent.-24h-3-1 **(!)**	1490379
PAO1-24h-3-2	8676910	Y.ent.-24h-3-2 **(!)**	1510058
PAO1-24h-3-3	8327019	Y.ent.-24h-3-3 **(!)**	1517237

Supplementary Table 2 Aerugine quantification upon iron addition in PAO1 and *Y. enterocolitica*. (Y.ent.: *Y. enterocolitica* DSM4780, "**!**" indicates error in sample preparation; "-" excluded due to insufficient extraction, in grey: relative standard deviation of technical triplicates >30%)

Sample	Integrated Area	sample	Integrated Area
PAO1-Fe0.1-1-1	7521221	Y.ent.-Fe0.1-1-1 **(!)**	-
PAO1-Fe0.1-1-2	6515054	Y.ent.-Fe0.1-1-2 **(!)**	-
PAO1-Fe0.1-1-3	4775591	Y.ent.-Fe0.1-1-3 **(!)**	-
PAO1-Fe0.1-2-1	10185345	Y.ent.-Fe0.1-2-1 **(!)**	-
PAO1-Fe0.1-2-2	9083347	Y.ent.-Fe0.1-2-2 **(!)**	1714200
PAO1-Fe0.1-2-3	9742652	Y.ent.-Fe0.1-2-3 **(!)**	1502189
PAO1-Fe0.1-3-1 **(!)**	2296588	Y.ent.-Fe0.1-3-1 **(!)**	819470
PAO1-Fe0.1-3-2 **(!)**	2273816	Y.ent.-Fe0.1-3-2 **(!)**	606807
PAO1-Fe0.1-3-3 **(!)**	2305816	Y.ent.-Fe0.1-3-3 **(!)**	557080
PAO1-Fe1-1-1	12807183	Y.ent.-Fe1-1-1 **(!)**	-
PAO1-Fe1-1-2	11645244	Y.ent.-Fe1-1-2 **(!)**	595805
PAO1-Fe1-1-3	10283356	Y.ent.-Fe1-1-3 **(!)**	579446
PAO1-Fe1-2-1	9375178	Y.ent.-Fe1-2-1 **(!)**	3336162
PAO1-Fe1-2-2	8598984	Y.ent.-Fe1-2-2 **(!)**	2360124
PAO1-Fe1-2-3	8291202	Y.ent.-Fe1-2-3 **(!)**	1955367
PAO1-Fe1-3-1 **(!)**	2852010	Y.ent.-Fe1-3-1 **(!)**	1085225
PAO1-Fe1-3-2 **(!)**	2684886	Y.ent.-Fe1-3-2 **(!)**	1170889
PAO1-Fe1-3-3 **(!)**	2833409	Y.ent.-Fe1-3-3 **(!)**	788817
PAO1-Fe10-1-1	4383528	Y.ent.-Fe10-1-1 **(!)**	773853
PAO1-Fe10-1-2	4377226	Y.ent.-Fe10-1-2 **(!)**	3387622
PAO1-Fe10-1-3	4618705	Y.ent.-Fe10-1-3 **(!)**	744164
PAO1-Fe10-2-1	186216	Y.ent.-Fe10-2-1 **(!)**	2953913
PAO1-Fe10-2-2	197427	Y.ent.-Fe10-2-2 **(!)**	2613894
PAO1-Fe10-2-3	194361	Y.ent.-Fe10-2-3 **(!)**	2480013
PAO1-Fe10-3-1 **(!)**	1738035	Y.ent.-Fe10-3-1 **(!)**	756428
PAO1-Fe10-3-2 **(!)**	1853227	Y.ent.-Fe10-3-2 **(!)**	773518
PAO1-Fe10-3-3 **(!)**	1641178	Y.ent.-Fe10-3-3 **(!)**	581599
PAO1-Fe100-1-1	253385	Y.ent.-Fe100-1-1 **(!)**	93227
PAO1-Fe100-1-2	225771	Y.ent.-Fe100-1-2 **(!)**	93362
PAO1-Fe100-1-3	244510	Y.ent.-Fe100-1-3 **(!)**	95221
PAO1-Fe100-2-1	1641767	Y.ent.-Fe100-2-1 **(!)**	211173
PAO1-Fe100-2-2	1513766	Y.ent.-Fe100-2-2 **(!)**	231763
PAO1-Fe100-2-3	1288570	Y.ent.-Fe100-2-3 **(!)**	85854
PAO1-Fe100-3-1 **(!)**	198470	Y.ent.-Fe100-3-1 **(!)**	145090
PAO1-Fe100-3-2 **(!)**	182849	Y.ent.-Fe100-3-2 **(!)**	136575
PAO1-Fe100-3-3 **(!)**	187298	Y.ent.-Fe100-3-3 **(!)**	123614

Supplementary Table 3 Screening for aerugine in PAO1, *K. pneumoniae* and *Y. enterocolitica*. (!) indicates error in sample preparation.

Organism	Medium, incubation temperature	Integrated Area
K. pneumoniae	M8; 37 °C	NF
Y. enterocolitica	M8; 37 °C	NF
PAO1	PGM; 37 °C	305806
K. pneumoniae	PGM; 37 °C	NF
Y. enterocolitica	PGM; 37 °C	NF
PAO1	PMH; 37 °C	376562
K. pneumoniae	PMH; 37 °C	NF
Y. enterocolitica	PMH; 37 °C	NF
K. pneumoniae	TSYM; 37 °C	NF
Y. enterocolitica	TSYM; 37 °C	NF
K. pneumoniae	Marine broth; 37 °C	NF
Y. enterocolitica	Marine broth; 37 °C	NF
K. pneumoniae	M8 (100 µM salicylic acid; 100 µM L-cysteine)	NF
Y. enterocolitica	M8 (100 µM salicylic acid; 100 µM L-cysteine)	NF
K. pneumoniae	PMH (100 µM salicylic acid; 100 µM L-cysteine)	NF
Y. enterocolitica	PMH (100 µM salicylic acid; 100 µM L-cysteine)	2170259
K. pneumoniae	PMH (100 µM salicylic acid; 100 µM L-cysteine; 0.1 µM $FeCl_3$)	NF
Y. enterocolitica	PMH (100 µM salicylic acid; 100 µM L-cysteine; 0.1 µM $FeCl_3$)	2154867
K. pneumoniae	M9 (0.5% Casamino acids; 100 µM salicylic acid; 100 µM L-cysteine); 37 °C	NF
K. pneumoniae	M9 (0.5% Casamino acids; 1 mM $CaCl_2$; 100 µM salicylic acid; 100 µM L-cysteine); 37 °C	NF
K. pneumoniae	PGM (100 µM salicylic acid; 100 µM L-cysteine); 37 °C	NF
K. pneumoniae	TSYM (100 µM salicylic acid; 100 µM L-cysteine); 37 °C	NF
K. pneumoniae	M9 (0.5% Casamino acids; 200 µM salicylic acid; 200 µM L-cysteine); 37 °C	NF
K. pneumoniae	M9 (0.5% Casamino acids; 1 mM $CaCl_2$; 200 µM salicylic acid; 200 µM L-cysteine); 37 °C	NF
K. pneumoniae	PGM (200 µM salicylic acid; 200 µM L-cysteine); 37 °C	NF
K. pneumoniae	TSYM (200 µM salicylic acid; 200 µM L-cysteine); 37 °C	NF
***K. pneumoniae* (!)**	PGM (deferrated, 100 µM salicylic acid; 100 µM L-cysteine); 25 °C	806034
***K. pneumoniae* (!)**	PGM (deferrated); 25 °C	722838
***K. pneumoniae* (!)**	PGM (deferrated, 100 µM salicylic acid; 100 µM L-cysteine); 37 °C	731518
***K. pneumoniae* (!)**	PGM (deferrated); 37 °C	670821

Supplementary Table 4 Detected pyochelin concentrations. (IA = Integrated Area)

sample	pyochelin I [IA]	pyochelin II [IA]	pyochelin I + II [IA]
PAO1-Fe0.1-1-1	136377648	87101850	223479498
PAO1-Fe0.1-1-2	124177688	79456292	203633980
PAO1-Fe0.1-1-3	98054044	61348147	159402191
PAO1-Fe0.1-2-1	208123379	125277880	333401259
PAO1-Fe0.1-2-2	191077627	115765212	306842838
PAO1-Fe0.1-2-3	203850264	122139235	325989499
PAO1-Fe0.1-3-1	70587202	39692320	110279522
PAO1-Fe0.1-3-2	69286388	38555717	107842105
PAO1-Fe0.1-3-3	72773984	40146966	112920950
PAO1-Fe1-1-1	207226046	129572448	336798495
PAO1-Fe1-1-2	200771280	127499824	328271105
PAO1-Fe1-1-3	0	110548115	110548115
PAO1-Fe1-2-1	198463541	117730761	316194303
PAO1-Fe1-2-2	194376256	113704294	308080549
PAO1-Fe1-2-3	180374122	105142698	285516820
PAO1-Fe1-3-1	0	40677520	40677520
PAO1-Fe1-3-2	73821033	41795434	115616468
PAO1-Fe1-3-3	70099520	39051741	109151262
PAO1-Fe10-1-1	81861482	47996967	129858449
PAO1-Fe10-1-2	81691103	47725741	129416844
PAO1-Fe10-1-3	0	52310719	52310719
PAO1-Fe10-2-1	6470077	2051549	8521626
PAO1-Fe10-2-2	7196514	2230462	9426975
PAO1-Fe10-2-3	7043355	2139363	9182718
PAO1-Fe10-3-1	42580887	24780071	67360957
PAO1-Fe10-3-2	41741914	23905084	65646998
PAO1-Fe10-3-3	36891145	20741439	57632585
PAO1-Fe100-1-1	610286	279091	889377
PAO1-Fe100-1-2	559141	261932	821073
PAO1-Fe100-1-3	1031182	432283	1463465
PAO1-Fe100-2-1	36951580	17544812	54496392
PAO1-Fe100-2-2	32234579	15086814	47321394
PAO1-Fe100-2-3	33443896	15868396	49312292
PAO1-Fe100-3-1	3501678	1132597	4634275
PAO1-Fe100-3-2	3396652	1115767	4512419
PAO1-Fe100-3-3	3238469	1112685	4351155